REPROGRAMMING OF THE MOUSE NANOG GENE IN AMPHIBIAN OOCYTE EXTRACTS

by

Sidar Bereketoğlu

BSc, MSc

Thesis submitted to the University of Nottingham for the degree of Doctor of Philosophy

January 2016

School of Life Sciences
University of Nottingham
United Kingdom

DECLARATION

I declare that this thesis is my own work and contains nothing which is the outcome of work done in collaboration with others, except as specified in the acknowledgment and that has not previously been presented as part of any other degree.

ABSTRACT

To induce pluripotency in differentiated cells, it is necessary to remodel the epigenetic marks on the regulatory regions of pluripotency genes to enable their expression. The induction of Nanog expression is crucial for establishing pluripotency. However, the epigenetic mechanisms associated with the reprogramming of Nanog expression are not fully understood. In mammalian chromatin, epigenetic control of gene expression includes DNA methylation and histone modifications. In undifferentiated cells, regulatory regions of the pluripotency genes Nanog and Oct4 are demethylated and enriched with activating histone marks while being relatively depleted of repressive marks.

One route to investigate mechanisms of cellular reprogramming is through treatment of cells with oocyte extracts from amphibians, such as *Xenopus* and axolotl. Previously, our lab demonstrated that a major difference between these extracts is that the axolotl oocyte can reprogram expression of the mammalian Nanog, while Xenopus oocyte cannot. In this study, I used extracts from oocytes of axolotl (AOE) and *Xenopus* (XOE), and focused on the mechanisms underlying the reversal of epigenetic marks in regulatory regions of the mouse Nanog gene during its reactivation. I demonstrated that AOE remodels the mouse somatic chromatin by increasing the level of 5hmC on both mouse Nanog enhancer and promoter sequences as well as adding the activating histone marks H3K27ac and H3K4me1 specifically to the Nanog enhancer. XOE was unable to induce these modifications. The expression of Nanog ortholog axNanog and histone variant H2A.Z in axolotl oocytes, but not in Xenopus oocyte, is likely to be one of the reasons for the differences. Indeed, I demonstrated the binding of axNanog and H2A.Z on the mouse Nanog gene in response to AOE, but not XOE treatment. Furthermore, my experiments have elucidated the sequence of chromatin remodelling events during oocyte extract reprogramming that begins with H2A.Z deposition at the Nanog enhancer which allows axNanog binding, followed by epigenetic alterations such as 5hmC, H3K27ac.

Taken together, this study refines our understanding of the step-wise events necessary for remodelling of somatic cell chromatin and underlies the difference in the reprogramming capacity of different Amphibian oocytes.

ACKNOWLEDGMENT

First, I would like to thank my supervisor Dr. Andrew Johnson for giving me the opportunity to take part in this project and my second supervisor Dr. Ramiro Alberio for helping me to refine my experimental approach and giving me a space in his lab in Sutton Bonington.

I am very grateful to Dr. Ian Macdonald and Dr. Ian Kerr for their support and help in completion of my PhD. I appreciate the great help from Dr. Martin Gering and Dr. Reinhard Stöger as well as their patience.

I am appreciated to all the members of the AJ, Alberio, Gering, Loose and Allegrucci labs. Thanks to Zoltan, Darren and Choulia Mola (Thanks for providing the axNanog antibody) for the helpful discussion of my work and being great lab mates. I want to particularly thank all the Axolotl and Xenopus females for sacrificing their oocytes for my project. Very special thanks to Kazhal, Maryam, and, of course, Deniz; thanks a lot for sharing lunch times, accommodation and basically the life in D Floor/QMC.

Thanks a lot guys for making Nottingham nicer for me: Meryem, Melek, Majeet, Al, Paul, Stacey, Iszara, Paco and Hamid. And thanks to my great friends in Turkey: Minnoşum, Özden, Zeynep, Aslı, Fırat, Furkan, Sri, Bilgehan and Fulya Gökalp (Thanks for the contribution on the statistical analysis). And Chris, I am appreciated for your transatlantic support and love, you were always with me.

Very special thanks go to my family as my mother for being the teacher of all my life, my father for being a serious chess-mate even when I was five years-old, and my brother for being a big brother even though he is much younger than me. I would not have been brave enough without your trust in me. And thanks to my late grandmother for teaching me how to be a strong woman.

I would also like to thank the University of Nottingham and its facilities as well as the academic and administrative staff in the School of Life Sciences and the Postgraduate Office at the QMC.

Finally, I would like to thank the Ministry of National Education Republic of Turkey and the Education Counsellor of the Turkish Embassy in London for the funding and the supportive staff who gave me guidance in conducting this PhD.

TABLE OF CONTENTS

LIST OF FIGURES

LIST OF TABLES

LIST OF ABBREVIATIONS

5caC	5 carboxylcytosine
5fC	5 formylcytonsine
5hmC	5 hydroxymethylcytosine
5mC	5 methylcytosine
AID	Activation-induced cytidine deaminase
APS	Ammonium persulfate
ATP	Adenosine Tri-Phosphate
β-MG	B-mercaptoethanol
BSA	Bovine serum albumin
Bsx	Brain specific homeobox protein
cenH3	Histone variant specific for centrometres
ChIP	Chromatin immunoprecipitation
CORF	Candidate oocyte reprogramming factors
CpG	Cytosine-guanine dinucleotides
DAPI	Fluorochrome 4’6’-diamino-2 phenylindole
DMEM	Dulbecco’s modified eagle’s medium
DMRs	Differentially methylated regions
DMSO	Dimethyl sulfoxide
DNA	Deoxyribonucleic acid
DNMT	DNA methyltransferase
DTT	Dithiothreitol
EGTA	Ethyleneglycol-bis (2-aminoethyl-ether) tetraacetic acid
EMSA	Electrophoretic mobility shift assay
EpiSCs	Epiblast stem cells
ES	Embryonic stem cells
FBS	Foetal bovine serum
FCS	Foetal calf serum
Fgf	Fibroblast growth factor
GV	Germinal vesicle
H3	Histone H3

H3K4me1	Histone H3 lysine 4 mono-methylation
H3K4me3	Histone H3 lysine 4 tri-methylation
H3K9me3	Histone H3 lysine 9 tri-methylation
H3K27ac	Histone H3 lysine 27 acetylation
H4	Histone H4
H4K16	Histone H4 lysine 16
HATs	Histone acetyltransferases
HCl	Hydrochloric acid
HDACs	Histone deacetyltransferases
HEK293T	Human Embryonic Kidney 293 cells
HP1	Heterochromatin protein 1
ICM	Inner cell mass
iPS	Induced Pluripotent Stem Cells
JmjC	Jumonji C
K	Lysine
KAT	Lysine acetyltransferases
KCl	Potassium chloride
KDAC	Lysine deactylase
KDM	Lysine demethylase
KH_2PO_4	Potassium di-hydrogen orthophosphate
Klf4	Kruppel-like factor 4
KMT	Lysine methyltransferase
LIF	Leukemia Inhibitory Factor
MEF	Mouse embryonic fibroblasts
MET	Mesenchylmal-to-epithelial transition
MiR145	Single microRNA
$MgCl_2$	Magnesium chloride
MYST	Moz/Ybf2/Sas2/Tip60 family
NaCl	Sodium chloride
NT	Nuclear transfer
NDR	Nucleosome depleted regions

OSKM	Oct4, Sox2, Klf4, c-Myc
PBS	Phosphate buffer saline
PBS-T	Phosphate buffer saline with 0.1% Tween 20
PCR	Polymerase chain reaction
PGCs	Primordial germ cells
PMSF	Phenylmethylsulfonyl fluoride
PRC2	Polycomb repressive complex 2
PRMT	Protein arginine N-methyltransferases
PVDF	Polyvinylidene difluoride
PWS	Prader-Willi syndrome
qPCR	Quantitative polymerase chain reaction
RNA	Ribonucleic acid
RT	Room temperature
SCNT	Somatic cell nuclear transfer
SD	Standard deviation
SDS	Sodium dodecyl sulphate
SDS-PAGE	SDS-polyacrylamide gel electrophoresis
TDG	Thymine DNA glycosylase
T-DMR	Tissue dependent and differentially methylated region
TEMED	N,N,N’,N’-tetramethylethylenediamine
TET	Ten-eleven translocation
Utf1	Undifferentiated embryonic cell transcription factor 1

CHAPTER 1

INTRODUCTION

The field of stem cell biology has flourished in recent years with the advent of technologies to reprogram somatic cells to pluripotency, such as induced pluripotent stem (iPS) cells (Takahashi and Yamanaka, 2006). Methods for inducing pluripotency, and refinement of culture conditions for embryonic stem (ES) cells, have facilitated the investigation of many issues in biology. Developmental biology, for example, has benefited immensely from the study of reprogrammed stem cells as these new methods have paved the way for new models and ways to study differentiation and reprogramming.

The nature of the stem cell state has been mysterious, owing to the relative rarity of adult stem cells and the difficulty of culturing such cells. Adult stem cells are undifferentiated and have a capacity to self-renew, adjacent to the somatic cells in a tissue or an organ, and are multipotent in that they can give rise only to the cell types of that specific tissue. For instance, hematopoietic stem cells and neural stem cells are lineage restricted multipotent stem cells. On the other hand, ES cells can differentiate to any cell type, a condition typically referred to as pluripotency. Effective protocols for the production and culture of ES and iPS cells have recently been defined (Olmer et al., 2010). However, many reprogramming methods are still highly inefficient. This lack of efficiency has

been attributed to weak reprogramming methods such as the inability to reverse epigenetic marks as well as the low viability of privileged cell populations. Therefore the stem cell field should improve the relatively well-defined techniques which show high efficiency such as somatic cell nuclear transfer and oocyte extract reprogramming. While the mechanisms of action of these techniques are not completely understood, they reliably generate reprogrammed cells at a higher efficiency than transcription factor-based reprogramming. Therefore understanding oocyte reprogramming might improve existing methods for stem cell reprogramming.

In this thesis, I focus on the reacquisition of pluripotency using amphibian oocyte extracts, which have the ability to modify the epigenome of somatic cells, such as fibroblasts, to an epigenetic state compatible with pluripotency (Bian et al., 2009). Molecules, such as chromatin modifiers, transcription factors, histones, and chaperons, within oocyte extracts can remodel somatic chromatin and change the gene expression profile of somatic nuclei. Furthermore, the application of oocyte extract is effective even when reprogramming cells from distantly related species, owing to the high conservation of pluripotency transcription factors.

In this thesis, I report the timing and kinetics of chromatin remodelling at key genetic loci using chromatin immunoprecipitation (ChIP) and qPCR techniques. This approach has led to the discovery that chromatin remodelling events can happen as early as three hours after the cytosol of somatic cells is exposed to axolotl oocyte extract. Knowing the sequence of events can further increase our

understanding of reprogramming, which is a highly complex multifactorial process, but can also underscore the rank and importance of specific chromatin marks in transcriptional regulation.

1.1 LITERATURE REVIEW

1.1.1 Epigenetics and Chromatin

1.1.1.1 DNA Methylation

Methylation of cytosine residues acts as a stable and effective mechanism for regulating gene expression as it directly affects transcription of DNA and is necessary for murine embryo development (Messerschmidt et al., 2014, Li et al., 1992). Methylation of CpG dinucleotides is a heritable epigenetic modification in vertebrates (Holliday and Pugh, 1975, Riggs, 1975). It occurs at the 5' position of cytosines, generally in the context of CpG dinucleotides and is an epigenetic change which prevents rearrangements of chromatin thus favouring chromosomal stability (Chen et al., 1998). DNA methylation plays important roles in embryonic development besides genomic imprinting, X chromosome inactivation (Ruzov et al., 2011, Cotton et al., 2015). This enzymatically-catalysed modification mostly inhibits transcriptional activity and is recognised by DNA-binding repressor proteins that silence genes directly (Medvedeva et al., 2014). Regions enriched with CpG sequences, called CpG islands, are mainly located within transcription start sites and/or regulatory elements of genes, such as promoters (Takai and Jones, 2002, Smallwood et al., 2011), wherein methylation

is related to the silencing of genes. However, the location of methylated CpGs is linked to the regulation of the transcriptional unit. For instance, methylation does not have a repressive role in transcription if it is located in active gene bodies; evidence suggests that it might even facilitate elongation of transcription (Takai and Jones, 2002) and/or might affect splicing (Laurent et al., 2010). On the contrary, increased methylation on the repeat regions, e.g. centromeres, leads to chromosomal stability to supress transposable elements' expression (Moarefi and Chedin, 2011). Although the function of methylation on promoters is well-studied, less has been published about the role of CpG methylation on enhancer regions; nevertheless, it is also known as a mark for gene silencing and chromosomal stability on enhancers, similar to its function in promoters (Hon et al., 2013).

There are several methods of measuring DNA methylation (5mC) that use the restriction enzymes which are sensitive to methylation, methylated DNA-binding proteins, or immunoprecipitation of methylated DNA (MeDIP). Also it is possible to detect the level of DNA methylation by using combined bisulfite restriction analysis (COBRA) which provides quantification of the percentage of methylation on a region of interest as well as pyrosequencing. However, in the approaches using bisulfite conversion such as genome-wide bisulfite sequencing, COBRA or pyrosequencing, cannot distinguish methylated (5mC) and hydroxymethylated cytosine (5hmC) since 5hmC acts similar to 5mC upon bisulfite conversion; while unmethylated cytosines are converted to thymine, 5hmCs and 5mCs remain as cytosines in the sequence. To be able to use these approaches, 5hmC can be

converted to 5-formylcytosine (5fC) which is detected as unmethylated cytosine (converted to thymine); an approach which was achieved with the use of Tet enzymes in a manner identical to oxidative demethylation (Booth et al., 2013). In another study an efficient quantification of oxidation products, 5fC and 5caC, was shown by using the methylation assisted bisulfite (MAB) assay. This method was used to map 5fC and 5caC in mouse ES cells and demonstrated that the level of 5fC and 5caC was increased on active promoters and enhancers which are hypomethylated (Neri et al., 2015). A similar strategy can be used for pyrosequencing; DNA is converted by oxidation followed by bisulfite treatment can be used as a substrate in pyrosequencing to obtain a quantitative analysis of the methylation level. Using methylation and hydroxymethylation enrichments in parallel, another study was able to compare sequencing datasets to determine signal from these modifications. Enrichment of hydroxymethylation was performed by immunoprecipitation and enrichment of methylated cytosine was conducted using a commercial kit that uses immobilized CpG-binding proteins to purify the DNA. Using both of these methods together, the group was able to refine traditional bisulfite sequencing data (Piyasena et al., 2015). Moreover, immunoprecipitation of the hydroxymethylated cytosine can be analysed by a 5hmC specific antibody.

Although studies on DNA methylation in animals mainly concern methylation of CpG sequences, it was reported that non-CpG sequences (C might be followed by A, C or T) are also methylated throughout the genome in plants and fungi, and in mouse and human ES cells (Ramsahoye et al., 2000, Lister et al., 2009),

preventing elongation of transcription (Cokus et al., 2008, Rountree and Selker, 1997). Even though differentially methylated non-CpG sequences were detected in mammals, their function in transcriptional regulation remains mostly unclear. However, it was recently shown that methylation on non-CpG sequences has a role in supressing transcription in adult mouse neurons (Barres et al., 2012, Guo et al., 2014).

The enzymes, DNMT1, DNMT3A and DNMT3B are responsible for catalysing DNA methylation and maintaining its stability. DNMT3A and DNMT3B are the enzymes which initially catalyse *de novo* DNA methylation (Okano et al., 1998, Okano et al., 1999, Chen et al., 2003), while DNMT1 is recruited to hemi-methylated DNA (Tsumura et al., 2006, Bostick et al., 2007) to maintain the inherited methylation pattern during cell divisions.

These enzymes are required for survival of somatic cells, and also cancer cells (Rhee et al., 2002, Chen et al., 2007), but they are not required for ES cell viability (Tsumura et al., 2006). However, methyltransferase activity has been reported to be necessary for homeostasis of particular stem cell types. For instance, DNMT3A is required for the differentiation of haematopoietic stem cells (Challen et al., 2011). Moreover, DNMTs are crucial for early embryonic development in mammals, so that their depletion causes lethality in embryogenesis (Li et al., 1992, Okano et al., 1999, Stancheva et al., 2001). Mutation of these enzymes leads to abnormal DNA methylation and inheritance of genetic diseases, such as immunodeficiency, centromeric instability, facial anomalies (ICF) syndrome, Prader-Willi/Agelman syndrome (PWS/AS) and

several cancer types in human (Okano et al., 1999, Xu et al., 1999, Chen et al., 2007, Robertson, 2005). These studies indicate that the balance between DNA methylation and demethylation is essential to properly orchestrate gene regulation in mammalian development.

Active DNA demethylation

DNA demethylation is associated with active transcription, as methyl groups on cytosines are removed passively or actively to allow for a more amenable state for subsequent gene expression. Active demethylation describes the removal of methyl groups from DNA directly in a replication-independent manner. This often includes DNA repair mechanisms (Barreto et al., 2007), such as base excision repair, which carries out the active genome-wide DNA demethylation in primordial germ cells (PGCs) (Hajkova et al., 2010). Active demethylation of DNA can be carried out by Ten-eleven translocation (TET) methylcytosine dioxygenases, activation-induced cytidine deaminase (AID), and thymine DNA glycosylase (TDG) enzymes (Inoue and Zhang, 2011, Iqbal et al., 2011, Cortazar et al., 2011), and the Tet family of enzymes have recently been linked to the formation of another epigenetic modification, 5-hydroxymethylation.

Tet family enzymes and 5-Hydroxymethylation

The discovery of the Tet family of enzymes showed that the DNA demethylation machinery also includes oxidation of methylated DNA as an intermediate, rather than direct removal of the methyl group. Rao's group demonstrated that 5mC can be hydroxymethylated by human Tet1 to generate 5hmC (Tahiliani et al.,

2009). Later, this function was also attributed to the Tet protein family members Tet 1-3, in murine (Ito et al., 2010).

TET family proteins are part of a superfamily comprising the iron Fe (II) and 2-oxoglutarate (2OG)-dependent dioxygenases. They contain conserved domains in mouse and human, such as a catalytic domain including iron-binding sites and a CXXC domain (except Tet2) which has an affinity to bind unmethylated CpG sequences (Tahiliani et al., 2009). These biochemical properties provide Tet proteins with the ability to recognize the hemi-methylated and fully-methylated forms of cytosine with their iron-binding domain, and unmethylated cytosine with their CXXC domain (Tahiliani et al., 2009, Ficz et al., 2011, Pastor et al., 2011).

It was shown that Tet1 interacts with the polycomb repressive complex 2 (PRC2) and binds to CpG-rich promoters to silence genes with which this complex is associated (Wu et al., 2011a). This indicated that Tet family proteins have repressive roles in transcription regulation. However, Tet1 can also recognize methylated and hemimethylated CpG or non-CpG sequences as a substrate to initiate active demethylation (Tahiliani et al., 2009, Ficz et al., 2011).

The oxidizing ability of Tet family proteins may go further to generate 5-formylcytosine (5fC) and 5-carboxylcytosine (5caC) from 5hmC (Wu and Zhang, 2011); these forms of cytosine exist in the murine ES cell genome (Ito et al., 2011, He et al., 2011, Pfaffeneder et al., 2011). It was shown that overexpression of Tet proteins resulted in 5fC and 5caC over-production in HEK293 cells, and also depletion of Tets caused a reduction in the levels of 5fC and 5caC in mouse

ES cells (Ito et al., 2011). These findings indicate that there is a dynamic regulation of DNA methylation which is initiated by Tet family proteins (Figure 1.1).

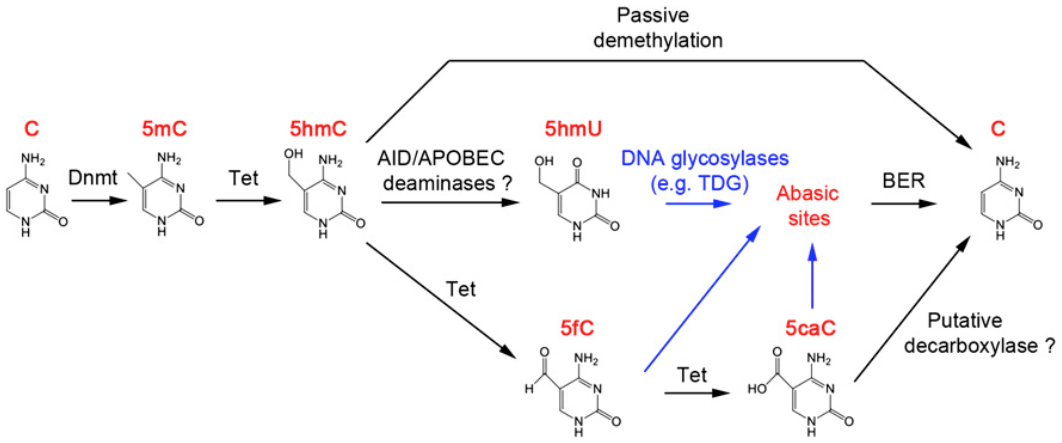

Figure 1.1 Model for the DNA demethylation process initiated by Tet proteins. Methylation of cytosines is carried out by DNMTs. Methylated DNA is hydroxylated by Tet family proteins to generate 5hmC. Hydroxymethylated DNA can be demethylated by replication-independent mechanisms; a) recognised by Tets for further oxidation to 5fC and 5caC, finally to C by decarboxylases, b) recognised by AID/APOBEC deaminases then subjected to DNA repair, by DNA glycosylases to produce Cytosine, c) or 5hmC can be recognised by DNMTs and lead to replication-dependent demethylation mechanisms. Cytosine (C) and its derivatives are marked in red. The reactions by DNA glycosylases are marked in blue (Adapted from Wu and Zhang, 2011).

1.1.1.2 Histone Modifications

1.1.1.2.1 Nucleosomes

DNA exists as a highly ordered series of 'beads on a string' (Kornberg, 1974). This packaging into units known as nucleosomes serves many roles in cells. Firstly, this packaging serves to create order. Secondly, nucleosomes allow for the direct allosteric inhibition of the transcriptional machinery, such as RNA polymerases

and transcription factors, with DNA (Schweikhard et al., 2014). Lastly, nucleosomes allow for the formation of chromatin microenvironments where loci transcribed at similar levels can associate with one another (Pombo and Dillon, 2015). Indeed, the most important role of the histones with regard to development is the regulation of transcriptional activity within a locus (Lorch et al., 1987, Li et al., 2007).

A canonical nucleosome is comprised of a core octamer around which 147 bp of DNA are coiled. The octamer is further comprised of two tetramers, each consisting of an H3, an H4, an H2A and an H2B histone variant. Bringing further order to the chromatin is the H1 linker histone that binds to the internucleosomal regions and stabilizes chromatin structure (Luger et al., 1997). The presence of each nucleosome is inhibitory to transcription, which is highlighted by the existence of chromatin remodelling complexes that move histones along the DNA.

Histone tails on the N-terminus provide an added level of complexity. These largely unordered peptide sequences exist apart from the core octamer and provide a platform for histone modifications that recruit transcription factors, transcription inhibitors, polymerases, etc. These modifications include phosphorylation, methylation, acetylation, ubiquitination. Also the specific modified residue informs the transcriptional activity of the loci (Iwasaki et al., 2013).

Another modification of the nucleosome occurs through the exchange of canonical histone subunits for so-called histone variants. These histone variants, such as H2A.Z, macroH2A, H2A.B and H3.3 vary by several amino acids from their

canonical counterparts. H2A.Z has specifically been shown to have activating and repressive roles within specific structural contexts (Subramanian et al., 2015). The incorporation of these variants is accomplished by nucleosome remodelling complexes in a tightly regulated process which allow for another level of transcriptional regulation (Kamakaka and Biggins, 2005, Weber and Henikoff, 2014).

Taken together, the nucleosome is a key player in transcriptional regulation. Specific loci can contain, in theory, an infinitely complex chromatin landscape from which transcriptional activity is governed. There exist multiple levels of complexity at the amino acid, monomer, tetramer, and octamer levels in the nucleosome.

1.1.1.2.2 Histone Modifications

DNA is wrapped around histone proteins to form nucleosomes to generate a physical barrier to the transcription machinery factors to prevent inappropriate transcriptional activity. However, this system is not stable and nucleosomes move throughout transcription regulatory regions depending on lineage-specific transcriptional activity. Histone modifications are important characters that establish the dynamic structure of the chromatin (Bannister and Kouzarides, 2011).

As a result of post-translational histone modifications, chemically unstable histone residues (such as lysine, arginine, and serine) become more stable for

the transcription status in a poised or active manner. These covalent modifications of histones are reversible and change according to the gene expression profile and lineage commitment. Enrichment of specific histone marks provides information about the transcriptional activity. For instance, tri-methylation of lysine 4 on histone 3 (H3K4me3) marks active promoters, while tri-methylation of lysine 27 on histone 3 (H3K27me3) marks repressed promoters (Lee et al., 2010).

Even though each histone modification has an individual effect on gene expression, they typically act synergistically or antagonistically within individual nucleosomes within an individual cell; this creates a complex histone code that provides information about the epigenetic status of the gene's transcription (Rothbart and Strahl, 2014). For instance, H3K4me3 and H3K27me3 appear together on many promoters in mouse embryonic stem cells and confer a poised transcriptional activity to developmental genes (Akkers et al., 2009, De Gobbi et al., 2011). The poised (bivalent) promoters, which are transcriptionally active only during differentiation, are marked by bivalent histone modifications. This is because the histone modifying enzymes are mostly in a multi-subunit complex and residues modified by one of the components of this complex can create a binding site for another histone modifier enzyme. For instance, COMPASS-like histone-modifying complexes include: UTX (to demethylate H3K27me3), MLL3/4 (to methylate H3K4), and WDR (to acetylate H3K9 and H4K16) (Schuettengruber et al., 2011).

Histone methylation and acetylation regulation

Covalent histone modifications are added or removed by specific protein complexes. These proteins can be identified according to their enzymatic activities, such as histone/lysine acetyltransferase (HAT/KAT), histone/lysine deacetylase (HDAC/KDAC), lysine methyltransferase (KMT) or lysine demethylase (KDM). The marks generated by these proteins are recognised by other protein complexes to alter gene expression status. For instance, bromodomain proteins bind acetylated lysine residues and chromodomain proteins bind methylated lysine residues (Lalonde et al., 2014).

There are three essential enzyme classes that add methyl groups on lysine residues (KMTs) which are: the SET-domain-containing proteins, DOT1-like proteins and protein arginine N-methyltransferases (PRMT) (Greer and Shi, 2012). Two essential enzyme families remove the methyl groups from lysine residues (KDMs): amine oxidases and jumonji C (JmjC)-domain-containing, iron dependent dioxygenases (Greer and Shi, 2012). Lysine residues are acetylated by lysine acetyltransferases (KATs), also known as histone acetyltransferases (HATs). Two main families of HATs are known: the GNAT (Gcn5) family and the MYST (Moz/Ybf2/Sas2/Tip60) family. Four acetyl groups that are removed from lysine residues by four classes of histone deacetylases (HDACs): Class I-IV (Dreveny et al., 2014). It was reported that these HATs and HDACs are not only responsible for the regulation of acetylation/deacetylation on histones, but also other proteins in the nucleus and cytosol, implicating the importance of their enzymatic activities in a wide range of biochemical processes (Choudhary et al., 2014).

1.1.1.2.3 Histone Variants

Histone variants can be considered as expanded histone modifications since they are incorporated into chromatin in exchange with core histones. Histone variant proteins have homology to their corresponding histone family amino acid sequence and similar protein fold structures. Deposition of histone variants remodels the chromatin to a less-condensed state in eukaryotes, thereby tailoring the chromatin organisation to allow for active transcription. Histone exchange with variants is carried out in a replication-independent manner by chromatin remodelling complexes which are ATP-dependent. The purpose of histone exchange is related to regulating the nuclear mechanisms such as DNA repair, genomic stability, chromosome segregation, and gene expression (Weber and Henikoff, 2014).

H3.3: Histone variant H3.3 differs with histone H3 by only five amino acids (Filipescu et al., 2013). Even though H3.3 enrichment was mostly reported at the regions of transcriptionally active genes, such as active gene promoters, cis-regulatory regions and bodies (Mito et al., 2007, Schneiderman et al., 2012) to establish euchromatin, it is also enriched at repressed regions of mouse ES cell chromatin, such as pericentric heterochromatin and telomeres (van der Heijden et al., 2007, Goldberg et al., 2010). It is not understood how the substitution of four to five amino acids in H3.3 impacts nucleosome instability. However, co-enrichment of H2A.Z and H3.3 on/near nucleosome-depleted regions (NDRs) of active genes regulatory regions suggests a role for these histone variants in increasing chromatin accessibility (Jin and Felsenfeld, 2007). Indeed, it was

shown that nucleosomes have similar stability when they include histone H3 and histone H2A or its variant H2A.Z; however, stability is decreased when H3.3 and H2A.Z are included in the nucleosomes on or around transcriptionally active regulatory regions (Jin and Felsenfeld, 2007).

*cenH3: cenH3*is a H3 histone variant which is specific for centromeres; it is also known as centromeric histone. It contains 60% amino acid similarity with histone H3 (Malik and Henikoff, 2003).

macroH2A: This variant has a non-histone globular domain which is a C-terminal macro domain, and it exists in vertebrates (Talbert et al., 2004). The macroH2A variant is around three times larger by amino acid length than histone H2A with a 65% similarity in amino acid sequence. It was reported that macroH2A is more stable in high salt concentrations than H2A (Chakravarthy et al., 2005). These differences result in higher stability of macroH2A-containing nucleosomes than those containing H2A. Indeed, enrichment of macroH2A was observed on the inactive X chromosome and contributes to its heterochromatic structure (Costanzi and Pehrson, 1998, Zhang et al., 2005). Moreover, macroH2A is enriched in the transcriptionally silenced pluripotency gene loci, accompanied by the repressive histone mark H2K27me3, in differentiated cells. Also, macroH2A decreases the activity of chromatin remodelers SWI/SNF and ISWI, and these chromatin remodelers manage the exchange of macroH2A (Angelov et al., 2003, Chang et al., 2008).

H2A.B: It is also referred to as H2A.Bbd (Barr body-deficient). H2A.B is a variant which exists only in mammals and has a 50% sequence similarity to histone H2A

(Ishibashi et al., 2010). It is also known as H2A.Lap1 (lacks acidic patch 1) because it lacks an acidic patch present on the surface of histone H2A. Moreover, H2A.B has a shorter C-terminus compared to H2A (Soboleva et al., 2012). Therefore, nucleosomes including H2A.B are physically different than those including histone H2A; around 30 bp less DNA is required to wrap around H2A.B nucleosomes by making these nucleosome less stable and more easily digested by micrococcal nuclease (Gautier et al., 2004, Bonisch and Hake, 2012). It was reported that H2A.B deposition in nucleosomes might be maintained by the general chaperon NAP-1 in vitro (Okuwaki et al., 2005). Enrichment of H2A.B was demonstrated on transcriptionally active gene bodies in mouse ES cells (Chen et al., 2014).

H2A.Z: H2A.Z is one of the major histone variants. It is a highly conserved protein found in all metazoans and shows around 60% similarity to the amino acid sequence of H2A (Zlatanova and Thakar, 2008). Although the structure of nucleosomes including H2A or H2A.Z is similar, their functions in chromatin structure are quite different since the presence of H2A.Z results in a unique expanded acidic patch on the nucleosomes (Suto et al., 2000). Studies showed that this acidic patch, which is provided by H2A.Z, is required for bivalent gene promoters to initiate transcriptional activity during ESC differentiation (Subramanian et al., 2013). Three amino acid substitutions in the C-terminal are primarily responsible for this expanded acidic patch: Glycine92 (Gly92), Aspartic acid97 (Asp97), and Serine98 (Ser98). These substitutions create hydrogen bonds

favouring interactions with chromatin remodelers (Suto et al., 2000, Goldman et al., 2010).

H2A.Z deposition is a genome-wide modification; however, it is mostly enriched at regulatory regions and transcriptional start sites (TSSs). Moreover, it has variable roles in the regulation of gene transcription (Ku et al., 2012, Hu et al., 2013). Studies on H2A.Z showed that it has an essential role in the regulation of ESC differentiation (Creyghton et al., 2008, Hu et al., 2013), and the regulation of lineage commitment, for instance T-cell activation (Sutcliffe et al., 2009), and muscle differentiation (Cuadrado et al., 2010). Moreover, it was shown that H2A.Z has a crucial role in maintaining pluripotency by physically interacting with pluripotency factors, such as Nanog (Wang et al., 2015). However, the question of how H2A.Z can be such an effective regulator in many diverse mechanisms, like a “rheostat”, remains unanswered.

H2A.Z deposition is regulated by the proteins which remodel chromatin. It is targeted to chromatin regions by the SWR1 complex in all eukaryotes (SRCAP, in mouse and human) (Ruhl et al., 2006). The p400/Tip60 proteins in all higher eukaryotes are ATP-dependent enzymes which are responsible for the deposition of H2A.Z (Choi et al., 2009). Moreover, in yeast, it was reported that INO80, which functions in DNA repair, has a role in transcription-dependent removal of H2A.Z from nucleosomes (Papamichos-Chronakis et al., 2011); a counterpart for INO80 has not been identified in higher eukaryotes. Histone chaperons also have roles in the exchange of histone variants (Burgess and Zhang, 2013). For example, ANP32 was shown to remove H2A.Z from promoter and enhancer

regions that might substitute for the function of INO80 in higher eukaryotes (Obri et al., 2014).

Besides the biochemical differences between H2A.Z and H2A that chromatin remodelers can recognise, the post-translational histone modifications also have a significant role in H2A.Z deposition. For instance, enrichment of H3K56ac on active or inactive genes leads to H2A.Z removal from chromatin (Watanabe et al., 2013). Additionally, the DNA methylation level can affect H2A.Z exchange. 5-aza-2'-deoxycytidine, an inducer of DNA demethylation, stimulates SRCAP, a chromatin remodeler, to enhance H2A.Z deposition leading to nucleosome depletion. This suggests that DNA methylation and H2A.Z are mutually antagonistic (Yang et al., 2012). On the other hand, studies showed that incorporation of H2A.Z might be random, but at low levels, throughout the genome, and the level of H2A.Z is regulated by its removal (Hardy et al., 2009); therefore, to understand the dynamics of H2A.Z exchange all these factors should be taken into consideration.

1.1.1.3 Chromatin Structure

Emil Heitz discovered that chromatin exists in two different structures, heterochromatin and euchromatin, by their staining profile: Heterochromatin was more intensely-stained, while euchromatin was less intense, indicating heterochromatin has a more compacted structure (Heitz, 1928). Euchromatin is described as having hyperacetylated and hypomethylated nucleosome regions,

thus, it is transcriptionally active in interphase. In contrast, heterochromatin is condensed, and has hypoacetylated and hypermethylated nucleosome regions; thus it is more compact and transcriptionally silenced (Hoskins et al., 2007).

However, additional terms are required to explain the differential states of chromatin due to its cell-specific and dynamic nature. For instance, the ratio of heterochromatin which is organised in a more 'closed' or compact state is higher in somatic cells, but there is a higher ratio of the euchromatin in undifferentiated pluripotent cells which is organised in a more 'open' state. In other words, the euchromatin/heterochromatin ratio is higher in pluripotent cells (Gaspar-Maia et al., 2011).

Furthermore, using electron microscopy, it was shown that ES cells have primarily an open chromatin structure, while differentiated cells have greater heterochromatin content (Park et al., 2004); this suggests that an open chromatin structure acts in the maintenance of pluripotency. Indeed, the chromatin composition of core histones, linker histones and heterochromatin protein (HP1) is more relaxed in ES cells (Bhattacharya et al., 2009, Meshorer et al., 2006). It is thought that ES cell chromatin has a de-condensed structure to permit the deposition of transcription factors, and therefore more robust transcriptional activity is possible to ensure the maintenance of pluripotency (Mattout and Meshorer, 2010).

Epigenetics of Open and Closed Chromatin

In ES cell chromatin, small genomic regions containing lineage-specific genes are locally condensed into heterochromatin prior to differentiation. Condensation of these regions is dynamically carried out by epigenetic alterations (Bannister and Kouzarides, 2011). For instance, while repressive histone marks are found at a low level, only covering silenced genes, activating histone marks are enriched more globally in chromatin. For instance, tri-methylation of Lys9 in histone H3 (H3K9me3) is highly enriched in heterochromatin. Using ChIP-seq, it was shown that H3K9me3 is enriched in only 4% of the genome of ES cells, while it is found in 12% of the chromatin in somatic cells. This suggests that closed chromatin exists in ES cells and it expands during differentiation (Hawkins et al., 2010). The opposite is true for acetylation of H3K9 (H3K9ac). H3K9ac, which is an open chromatin mark, is highly enriched in ES chromatin and it is diminished in differentiated chromatin (Krejci et al., 2009).

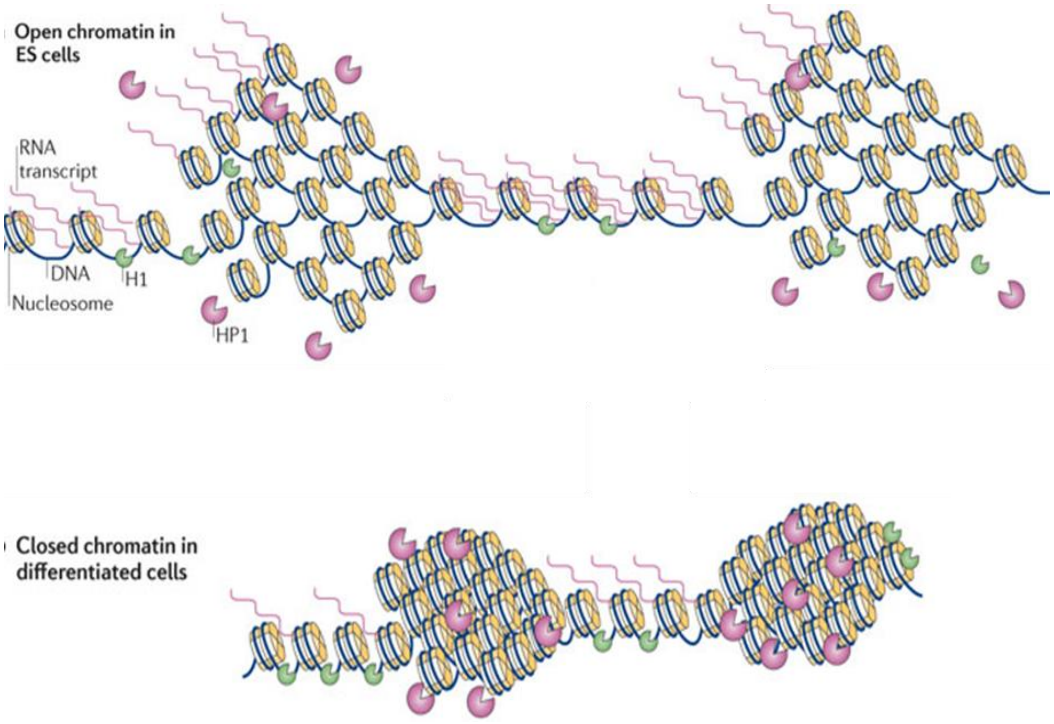

Figure 1.2 Chromatin structures in pluripotent cells and differentiated cells. Undifferentiated cells possess an open chromatin structure which is transcriptionally more active, while differentiated cell chromatin is in a more condensed form with lower transcriptional activity (Adapted from Gaspar-Maia, 2011).

1.1.2 Pluripotency Network Early Development

Pluripotency defines the ability of a cell to differentiate into the forerunners of any adult cell type (Smith, 2005). Following the morula stage of mouse development, the inner cell mass (ICM) forms in the blastocyst and it contains pluripotent cells. ES cells were derived from the ICM of mouse embryos (Evans and Kaufman, 1981, Martin, 1981), and from human embryos (Thomson et al., 1998) for *in vitro* experiments. The ICM of the mature blastocyst contains cells in the ground state of naïve pluripotency, which gives rise to the epiblast, associated with a transition to primed pluripotency after implantation. Primed

epiblasts are committed to receiving signals intrinsically as well as from extraembryonic tissues to initiate lineage specification.

In vitro studies showed that exposing ES cells to activin and Fgf can drive naïve ground state ES cells to differentiate into primed pluripotent EpiSCs. The reprogramming of EpiSCs to ES cells requires the introduction of specific reprogramming transcription factors (Batlle-Morera et al., 2008, Guo et al., 2009).

1.1.2.1 Core Transcriptional Network in Pluripotency

Oct4/Sox2

Sox2 and Oct4 are crucial transcription factors for the establishment and maintenance of pluripotency in development (Nichols et al., 1998, Avilion et al., 2003). Oct4 contains a POU domain and is also known as POUf51 (Pesce and Scholer, 2001). Sox2 contains an SRY-related high-mobility group (HMG) domain (Avilion et al., 2003). Within stem cells, Oct4 and Sox2 form a heterodimer and bind to specific genetic targets, such as undifferentiated embryonic cell transcription factor 1 (Utf1), F-box protein 15 (Fbx15), Nanog, and also Pou5f1 (Oct4) and Sox2 which regulate pluripotency and are associated with maintaining ES cell self-renewal (Nishimoto et al., 1999, Tokuzawa et al., 2003, Tomioka et al., 2002, Chew et al., 2005, Okumura-Nakanishi et al., 2005). Oct4 and Sox2 heterodimers bind to a site within the cis-regulatory element of these targets. Oct4 and Sox2 have both been shown to directly regulate the pluripotency

transcription factor Zfp206 which is an upregulator of Oct4 and Nanog expression in ES cells (Wang et al., 2007). Although these factors are mostly known by their roles in pluripotent cells, their functions in other cell types may vary (Niwa et al., 2000).

It has been shown that Oct4 and Sox2 cooperate to promote their own expression (Chew et al., 2005, Catena et al., 2004, Okumura-Nakanishi et al., 2005). Klf4 has also been shown to regulate the expression of both Oct4 and Sox2 (Wei et al., 2009). Intriguingly, a single microRNA, MiR145 has been shown to inhibit Oct4, Sox2, and Klf4 (Xu et al., 2009). This co-regulation underscores the complex regulatory machinery that drives the pluripotent stem cell state. Furthermore, Oct4 and Sox2 have recently been found to be up-regulated by Yap1 in pre-cancerous cells in lung tissue (Bora-Singhal et al., 2015). Similarly, Lin28 has been found to promote the upregulation of Oct4 and Sox2 in oral squamous carcinoma cells to a stem-like state (Chien et al., 2015), indicating the importance of interactions with Oct4 and Sox2 in cancer stem cells.

Nanog

Nanog is a homeobox containing transcription factor which is necessary for the establishment of pluripotency in the developing inner cell mass (Mitsui et al., 2003, Chambers et al., 2003). Expression of Nanog mRNA begins within the inner cells of the morula during mouse development (before blastocyst formation) (Wang et al., 2003). Nanog is expressed at a high level in the inner cell mass (ICM) until the mid-blastocyst; it is then downregulated in the epiblast during the late blastocyst stage and finally lost by pre-implantation stage (Mitsui et al.,

2003, Chambers et al., 2003). Nanog expression is also detected during the post-implantation development in migrating PGCs (Yamaguchi et al., 2005) until they reach the gonads (Resnick et al., 1992). Thus, the Nanog expression pattern indicates that it functions in pluripotent cells of the pre- and post-implantation stages of embryonic development where nuclear reprogramming occurs (Chambers et al., 2003, Hatano et al., 2005, Yamaguchi et al., 2005).

Nanog-deficient blastocysts do not produce an inner cell mass (Silva et al., 2009). Although Oct4 has been described as a master of stem cell fate regulation, Oct4 and Nanog interact and co-function in establishing pluripotency in ES cells, and in the silencing/suppression of differentiation mechanisms (Wang et al., 2006, Liang et al., 2008). ES cells express Oct4 and Oct4-deficient ES cells differentiate into trophoblast cells (Tanaka et al., 1998). Therefore, Nanog and Oct4 are two fundamental transcription factors, which are stage- and tissue-specific, in the development of pluripotency (Loh et al., 2006, Lavial et al., 2007). It was reported that Sox2 competes with PSBP (pluripotential cell-specific Sox element binding protein) to form a complex with Oct4 protein and to bind to a sox-oct element; this suggests that Sox2 may be dispensable in ES cells (Kuroda et al., 2005).

Silva et al. (2009) showed that Nanog protein has the capability of enhancing somatic cell reprogramming (Silva et al., 2009) and this ability is conserved in Nanog genes from other vertebrates (Theunissen et al., 2011a). Mouse Nanog has 85% similarity to Nanog from rat, 54% to human, 24% to chicken and 13% to zebrafish. Although Nanog is conserved across vertebrate species, the most

highly conserved region is the homeodomain (55% in Zebrafish). Nanog orthologs in non-eutherian vertebrates do not contain the tryptophan repeat (WR) domain which is required for dimerization of Nanog monomers (Mullin et al., 2008, Wang et al., 2008, Dixon et al., 2010). Although Nanog monomers cannot rescue LIF-independent self-renewal, their ability to participate in the maintenance of pluripotency is conserved in vertebrates (Dixon et al., 2010). Nanog is thought to have evolved from brain specific homeobox protein (Bsx) which has the highest homeodomain identity to Nanog in invertebrates. It is the homeodomain that has been identified as the functional part of Nanog, yet none of the invertebrate homeodomains, such as Bsx, function in reprogramming assays (Theunissen and Silva, 2011). There exists a Nanog-like orthologue in teleost fish which regulates the formation of extraembryonic tissue, but does not play a role in the acquisition of pluripotency in the embryo (Camp et al., 2009, Sanchez-Sanchez et al., 2011, Xu et al., 2012).

Nanog regulation by transcriptional factors Oct4 and Sox2

In mouse embryos, the expression of Oct4 and Sox2 begins before compaction of the blastomeres, but expression of Nanog is initiated after compaction, hinting that Nanog might be regulated by Oct4/Sox2 heterodimers (Avilion et al., 2003, Palmieri et al., 1994). Indeed, this is further supported by data showing that the Oct4/Sox2 heterodimer binds to the Nanog promoter and regulates its expression in mouse and human (ES) cells, as shown by chromatin immunoprecipitation (Chew et al., 2005) electrophoretic mobility shift assay (EMSA), fluorescent reporter assays, and also by mutagenesis techniques (Rodda

et al., 2005). Also, the Nanog locus in several mammals, such as mouse, rat, human, cow and elephant were found to have an oct-sox binding element located in the proximal upstream (promoter) regions (Rodda et al., 2005). Moreover, Oct4 and Sox2 binding to the Nanog promoter was demonstrated by ChIP in mouse and human embryonic stem cells (Rodda et al., 2005, Kuroda et al., 2005).

Epigenetic regulation of Nanog

Epigenetic regulation of Oct4 and Nanog is dependent on canonical mechanisms such as DNA methylation and histone post-translational modification; however, there are some locus-specific variations. The Nanog gene is expressed in ES cells but not in trophoblast stem (TS) cells or NIH3T3 cells, showing a tissue specific expression of Nanog (Hattori et al., 2007). Hattori et al. (2007) showed that the Nanog gene promoter is repressed by hypermethylation. Sequences encoding so-called tissue-dependent and differentially methylated region (T-DMR), upstream of the Nanog gene, undergo tissue-specific epigenetic modifications and have a role in Nanog regulation.

Transcription-activating modifications such as demethylation of DNA and histone H3K4 methylation are enriched in T-DMRs of ES cells compared with TS cells. Conversely, in the T-DMRs of ES cells, repressive epigenetic modifications, methylation of DNA and histone H3K9 and H3K27 methylation, are not detected or are at very low levels, while these regions are hypermethylated and histone H3K9 and H3K27 are deacetylated in TS cells. Therefore, it is clear that Nanog gene regulation is under control of epigenetic dynamics (Hattori et al., 2007).

Nanog Interactome

The three-dimentional organisation of chromatin is important for transcriptional regulation. The association of promoters with enhancers or insulators brought about by the looping of chromatin can lead to transcriptional activation or repression. This interaction can occur in cis, along the same chromosome, and in trans, between different chromosomes. The reorganisation of chromatin into higher-order structures has also been found to be important in the control of pluripotency and differentiation. For instance, the loss of interaction between the enhancer and promoter regions of pluripotency genes such as Nanog and Oct4 lead to the silencing of these genes (Kagey et al., 2010, Levasseur et al., 2008). Proteins such as Mediator, cohesin and CTCF (CCCTC-binding factor), involved in chromatin looping, have been found to interact with pluripotency factors and were shown to bind the target sites of these factors, implying that they may play an important role in rearranging the chromatin to establish and maintain pluripotency (Donohoe et al., 2009, Tutter et al., 2009, Kagey et al., 2011, Nitzsche et al., 2011). Consistent with this, in Mediator and cohesin depleted ES cells, interaction between the promoter and enhancer of pluripotency factors is abolished, leading to the premature differentiation of ES cells (Levasseur et al., 2008; Kagey et al., 2010).

A recent study using a modified 4C-seq assay showed that in the pluripotent state, the promoter and enhancer of Nanog interacts with each other as well as the regulatory regions of various other pluripotency genes, in cis- and trans-. During reprogramming of somatic cells, Nanog mostly regains these pluripotency

specific interactions, constituting an interactome. Consistently, this interactome is lost during differentiation (Apostolou et al., 2013). Proteins such as Mediator, cohesin and CTCF are important for establishing this Nanog specific interactome. In support of this, when components of Mediator and cohesin, Med1 and Smc1a, were knocked down in ES cells, interactions between pluripotency genes were abolished, leading to the downregulation of these genes. This was accompanied by the establishment of new interactions between differentiation-related genes leading to their upregulation (Apostolou et al., 2013). Another study using a 3C assay showed that differentiated cell-specific interactions are reduced and undifferentiated cell-specific interactions are increased prior to Nanog transcriptional activation. This is established by the interaction between the Nanog enhancer and promoter regions with the regulatory regions of pluripotency-related genes such as Oct4, Lefty1 and Phc1 (Kagey et al., 2010; Apostolou et al., 2013). These studies showed that chromatin looping is essential for the maintenance of pluripotency however it is not sufficient to initiate transcriptional activity. The loci in ES and iPS cells which were found to interact with Nanog have features specific to open chromatin that is not found in MEFs. For instance these loci are enriched with the activating histone marks H3K27ac, H3K4me1, H3K4me2, and H3K4me3 and bound by pluripotency transcription factors Oct4, Sox2, Nanog, Esrrb, and Klf4 (Apostolou et al. 2013). These results indicate that the features of undifferentiated cells such as open chromatin structure and pluripotency transcriptional network can be regained by reprogramming process.

Active enhancers in mouse ES cells are co-occupied by the transcription factors Oct4, Sox2, Nanog (Chen et al., 2008, Whyte et al., 2013) and components of Mediator and cohesin (Kagey et al., 2010). Indeed, this feature of active enhancers was confirmed using ChIP-seq data that identified more than 8000 enhancers to which these transcription factors are bound in ES cells (Whyte et al., 2013). It was found that a small number of these enhancers (231 of more than 8000) play important roles in maintaining ES cell identity. These enhancers are enriched with the active enhancer-specific histone modifications, H3K27ac and H3K4me1, and are occupied by Med1, suggesting these active enhancers interact to generate large multi-enhancer groups, known as super-enhancers (Whyte et al., 2013). Super-enhancers in ES cells are bound by pluripotency factors at a greater level than typical enhancers. Moreover, these active enhancer clusters are associated with essential pluripotency genes, Oct4, Sox2, Nanog, as well as the genes encoding DNA-modifying factors, Tet1 and Tet2 (Whyte et al., 2013). Therefore, super-enhancers function on broad promoter domains for transcriptional activity and have a role in the Nanog-specific interactome.

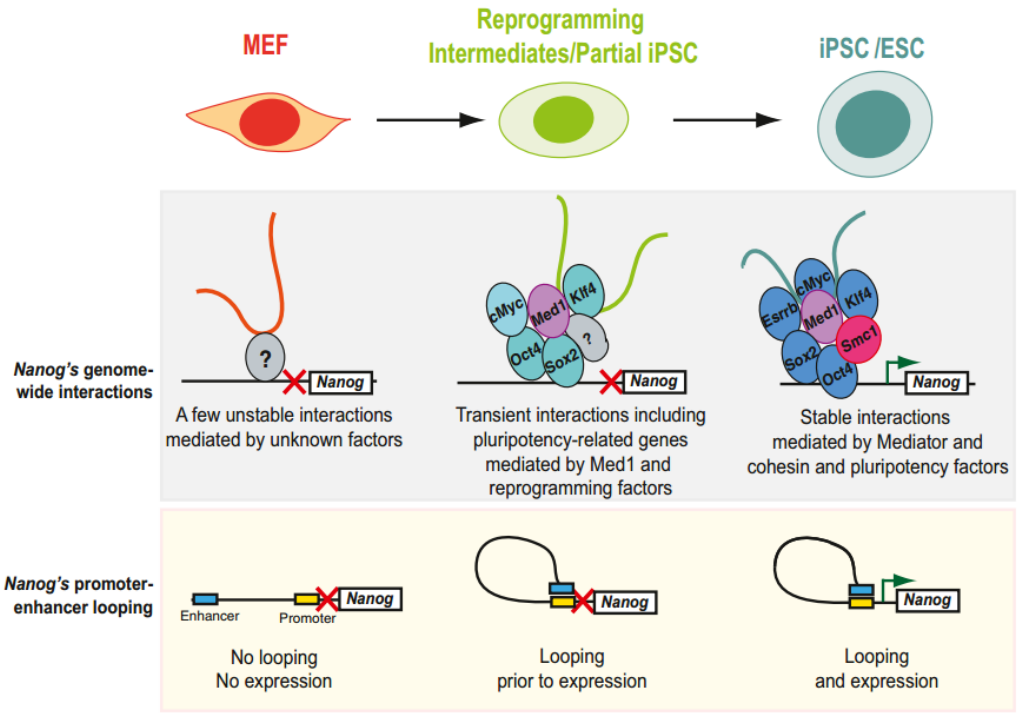

Figure 1.3: Model presenting forming Nanog gene interactome during differentiation and reprogramming. Nanog locus is in cis- and trans- interactions with other pluripotency-related loci in undifferentiated state by a multiprotein complex which includes other pluripotency factors, Mediator (Med1) and cohesin (Smc1). This interaction is more random and less stable in the differentiated state and becomes maintained in undifferentiated chromatin with the help of Mediator and cohesin (Apostolou et al., 2013).

1.1.3 Reprogramming of Somatic Cells to Pluripotency

1.1.3.1 Phases of Reprogramming

There are two phases in reprogramming, a 'stochastic phase', which is the initiation of reprogramming, and a 'deterministic' phase, which is the maturation of reprogramming. In addition, an intermediate step is thought to exist which is 'rate-limiting' (Mikkelsen et al., 2008, Buganim et al., 2012).

Stochastic Initiation Phase

In the early stages of reprogramming, defined as between 0 and 3 days, the surface markers of somatic cells should disappear and pluripotent cell-specific markers should emerge. It was reported that after transfection of somatic cells by the Yamanaka factors; Oct4, Sox2, Klf4, cMYC (OSKM), defined as the minimal combination of transcription factors required to induce pluripotency (Takahashi and Yamanaka, 2006), downregulation of the surface marker Thy1 occurs before upregulation of SSEA1, a marker of pluripotent cells (Stadtfeld et al., 2008). Cells which still express Thy1 after 9 days indicate the failure to downregulate mesenchymal genes, suggesting that cells remain refractory to reprogramming after OSKM induction (Polo et al., 2012). The events observed in the early phase of reprogramming following ectopic expression of reprogramming factors (OSKM) in the differentiated cells include: an increase in cell proliferation, MET (mesenchymal-to-epithelial transition) initiation (Li et al., 2010), activation of DNA repair mechanisms, alteration of metabolic activities and changes in the epigenetic status, such as histone modification at differentiation genes. These events can cause a variety of effects in the cells such as apoptosis, senescence or reprogramming, leading to heterogeneity among cell cultures (Hansson et al., 2012, Buganim et al., 2012).

Intermediate Phase

Between days 3 and 9, before the transition from the stochastic phase to the deterministic phase, there is an intermediate phase ('rate-limiting' step) which delays transition to the pluripotent state. Here, pluripotency genes are

stochastically activated, developmental regulators are temporarily inactivated, and metabolic activities are switched to glycolysis. In this decision step, several genes can be activated which would lead the cells to pluripotency, such as Utf1, Esrrb, Dppa2, Lin28 and Nanog. Activation of these genes precedes the deterministic phase of reprogramming by activating endogenous Sox2 expression. Following Sox2 activation hierarchical events begin, leading to iPS cells. The rate-limiting step is also seen as stochastic (Hansson et al., 2012, Polo et al., 2012, Buganim et al., 2012). According to this model, reactivation of Nanog expression sits at a later stage in this phase, reducing heterogeneity among the cells and leading to the deterministic phase of reprogramming, and therefore the acquisition of ground state pluripotency (Silva et al., 2009).

Deterministic Terminal Phase

The final, deterministic, phase of reprogramming includes activation of the endogenous pluripotency network. In the deterministic phase, the cytoskeleton and the metabolism of the cells are switched to an ES cell-like state, differentiation genes are silenced, and also the epigenetic and transcriptional features of the cells are altered to resemble ES cells. This phase is relatively shorter and more predictable than the stochastic phase because it includes less probabilistic events (Polo et al., 2012, Sancho-Martinez and Izpisua Belmonte, 2013). There are several pluripotency-associated genes that are hierarchically activated in this phase including LIN28, ESRRB, SALL4, DNMT3B, Nanog, OCT4, and FGF4 (Golipour et al., 2012, Hansson et al., 2012).

Epigenetic Memory interferes with reprogramming

'Epigenetic memory' refers to retention of the somatic gene transcription pattern in donor cell nuclei following the induction of gene activation by reprogramming. It is among the major impediments to reprogramming efficiency. It is caused by the retention of epigenetic marks which are not completely remodelled. It was reported that chromatin reprogrammed by somatic cell nuclei transfer (SCNT), a method of reprogramming where the nucleus of a somatic cell is transplanted into an enucleated oocyte, has less propensity to retain epigenetic memory than chromatin reprogrammed by transcription factors (iPSCs). The epigenetic marks, which are not erased by reprogramming, cause retention of similar epigenetic pattern in the neighbouring sites (Ng and Gurdon, 2008a, Halley-Stott and Gurdon, 2013).

1.1.3.2 Approaches to Reprogramming

1.1.3.2.1 Reprogramming by inducing specific factors

The Yamanaka era of reprogramming

Yamanaka and colleagues showed that expression of a combination of four transcription factors could induce pluripotency in somatic cells, to generate iPS cells. These genes, octamer-binding transcription factor 3/4 (Oct3/4), sex determining region Y-box 2 (Sox2), Krueppel-like factor 4 (Klf4) and c-Myc induced pluripotency in a small subset of cultured cells (OSKM) (Takahashi and

Yamanaka, 2006). Compared to the other Yamanaka factors, overexpression of Oct3/4 is essential for efficient iPS cell generation (Carey et al., 2011, Wu et al., 2011b). This reprogramming technique allows for the generation of patient matched pluripotent cells for research and opened the door for autologous stem cell transplant therapies. iPS cells can be transplanted into mouse blastocysts to give rise to all three germ layers (Takahashi and Yamanaka, 2006). Furthermore, these cells have the capacity to differentiate into a multitude of cell types under defined conditions, similar to ES cells.

The potential for using these cell lines for clinical purposes is compromised by the ectopic expression of the reprogramming factors. For instance, the oncogene c-Myc can initiate p53 signalling which causes cell arrest or apoptosis (Mah et al., 2011). Recently, non-integrating methods of reprogramming have been devised to introduce pluripotency factors, such as episomal vectors, mRNA transfection and Sendai-viral systems which reduce the possibility of mutations that would occur during integration to the host genome (Schlaeger et al., 2015). Although introducing these specific factors into differentiated cells induces pluripotency, the efficiency of Yamanaka reprogramming is low. Moreover, previous studies showed that epigenetic memory persists as DNA methylation and histone modifications (as a result of transcriptional and metabolic activities) in early passage iPS cells, favouring in vitro differentiation more representative of the donor cell (Bar-Nur et al., 2011, Panopoulos et al., 2012).

Thomson factors in reprogramming

The group of James Thomson introduced an alternative set of four factors, introduced with a lentiviral expression system, which could also reprogram human somatic cells to pluripotency (Yu et al., 2007). These factors were Oct4, Sox2, Nanog and Lin28 (OSNL), thus emphasizing the importance of the gene Nanog in reprogramming. Furthermore, this report bolstered the importance of the gene Lin28, which is involved in both miRNA regulation and insulin-like growth factor signalling (Yu et al., 2007). The importance of Oct4 and Sox2 are also underscored here.

1.1.3.2.2 Reprogramming using chemicals

Recently, reprogramming of somatic cells with small molecule compounds was reported (Hou et al., 2013). A combination of six compounds consisting of valproic acid, CHIR99021, 61642, tranylcypromine, forskolin and DZNep was sufficient to reprogram cells to pluripotency. These compounds act by inhibiting histone deacetylase with valproic acid (Phiel et al., 2001), inhibiting GSK3b and thus activating the WNT pathway by CHIR99021 (Li et al., 2011, Ying et al., 2008), inhibiting TGFβR1 signaling (616452) and histone lysine demethylation (tranylcypromine), inhibiting cAMP production (forskolin) and specific histone methylation (DZnep). Prior work to this end had included the discovery of 616452, also known as RepSox, a small molecule capable of replacing Sox2

activity and inducing Nanog, which also leads to successful reprogramming (Ichida et al., 2009).

The discovery of a small molecule cocktail addressed many clinical concerns about the potential therapeutic capacity of iPS cell technology. Namely, the use of genome-integrating viruses to overexpress Yamanaka factors has a high potential for inducing oncogenic mutations. By using small molecules, theoretically, mutations are not introduced and therefore patient-derived iPS cells will maintain genome integrity, ploidy, and sequence.

1.1.3.2.3 Somatic cell nuclear transfer

Somatic cell nuclear transfer (SCNT) refers to the transfer of nuclei from differentiated cells into oocytes for the purpose of reprogramming the donor cell nuclei. This procedure involves direct injection of somatic cells into oocyte cytoplasm. By transferring the porous somatic nuclei into the cytoplasm of an enucleated mature oocyte, oocyte factors are able to act on the somatic chromatin and reconfigure the epigenetic landscape.

SCNT experiments were first carried out using amphibian cells (Briggs and King, 1952), which culminated in the production of phenotypically normal swimming tadpoles after transferring nuclei from embryonic cells or fully differentiated cells into enucleated eggs (Gurdon, 1962, Gurdon and Uehlinger, 1966). These findings were later extended to mammals (Wilmut et al., 1997) and later still ES cells were produced from SCNT embryos (Wakayama et al., 2001). Recently,

human ES cells were cultured from human embryos derived by transplanting the nuclei of human fibroblast cells by SCNT into human oocytes, and the differentiation ability of these cells was similar to embryo-derived ES cells, indicating the efficient reprogramming of somatic nuclei to pluripotency (Tachibana et al., 2013).

1.1.3.2.4 Oocyte Reprogramming

Another derivation of SCNT, and the focus of this thesis, is the treatment of mammalian somatic cells with extracts from the oocytes of amphibians. Results from SCNT indicate that amphibian oocytes contain factors that can reprogram differentiated mammalian cells to pluripotency. Gurdon's group has demonstrated the reprogramming potential of Xenopus oocytes (Simonsson and Gurdon, 2004, Murata et al., 2010). For instance, endogenous Oct4 expression in mammalian somatic cells was re-established by injection of cells into the germinal vesicle (GV) of Xenopus oocytes. In addition, the Thy-1 gene, used as a marker for differentiation, was inhibited (Byrne et al., 2003). The same group also showed that the Oct4 promoter in somatic nuclei was demethylated in a DNA replication-independent manner, suggesting an enzymatic activity for DNA demethylation (Simonsson and Gurdon, 2004) is present in oocytes.

Injecting cells into the GV of oocytes has significant limitations, however, such as inefficient recovery of viable cells. Therefore, *ex ovo* experiments using cells incubated in extracts from oocytes and eggs was developed as an alternative. By this approach, it was also shown that Oct4 was reactivated following one week in

culture, of human leukocytes incubated in extracts from *Xenopus* eggs (Hansis et al., 2004). Deacetylation of histone H3K9 was observed under these conditions. In addition reactivated expression of Oct4 and Sox2 was observed in porcine fibroblasts incubated in Xenopus egg extract (Miyamoto et al., 2007). Our lab further showed that Xenopus oocyte and egg extracts can remodel the nuclear lamina of mammalian differentiated cells by removing nuclear Lamin A/C (Alberio et al., 2005). Later, it was shown that extracts from the oocytes of axolotls, a urodele amphibian, have the ability to reprogram the epigenetic modifications on mammalian cells. These modifications included reduction in the levels of the transcription repressing histone mark H3K9me3, and DNA methylation, as well as the addition of the activating histone mark H3K9ac (Bian et al., 2009). Indeed, oocyte extract from axolotl can reprogram the epigenetic profile of breast cancer cells more efficiently than extract from Xenopus oocytes (Allegrucci et al., 2011).

More recent studies have demonstrated that there are hierarchical events following nuclear transfer into amphibian oocytes (Jullien et al., 2014). RNA-seq analysis detected both the down- and up-regulation of many genes in mouse fibroblasts, with the selective transcription of mammalian reprogramming genes indicating that oocyte reprogramming is a targeted transcriptional process without stochastic global gene activation (Jullien et al., 2014). This study negates previous assertions that somatic cell-specific genes are activated in addition to pluripotent-specific genes (Biddle et al., 2009).

1.1.4 Differences between axolotl and Xenopus

Two suborders of amphibians, anurans (frogs) and urodeles (salamaders) are represented by model organisms, Xenopus and axolotl, respectively, and studies have identified major differences in their development mechanisms (Houston and King, 2000, Johnson et al., 2001, Nieuwkoop, 1996). Among the most profound differences in their development is the mode of primordial germ cell (PGC) specification. PGCs are the cells which establish the germ line in embryogenesis. Specification of PGCs is programmed by maternally inherited germ plasm in *Xenopus laevis*, an anuran species. Germ plasm forms which includes germ line determinants that inhibit transcription and translation, thus inhibiting the response of PGCs to extracellular signals (Houston and King, 2000, Taguchi et al., 2012, Lai and King, 2013). Germ plasm evolved independently in multiple different species throughout evolution; teleost fish, anurans, and birds. However, PGC specification is different in urodeles. Axolotls do not have a germ plasm and they program PGC formation by induction from extracellular signals (Johnson et al., 2003, Chatfield et al., 2014). Therefore, the mode of PGC specification in Xenopus is preformation, while it is a regulative mode in the axolotl (Johnson et al., 2001). As germ plasm is maternally inherited, cells are set aside early in the development of the organism to become germ cells, as opposed to the conserved mode of PGC induction, and this frees the soma to evolve at a much higher rate, and allowing for the development of novel traits (Johnson et al., 2003, Johnson et al., 2011, Evans et al., 2014). But as the regulative mode of PGC specification is conserved from Axolotls to higher mammals, the gene regulatory networks that govern these mechanisms are also

conserved, making Axolotl a more appropriate model to study the mechanisms that establish pluripotency.

The regulative mode of PGCs suggests an established pluripotency whereas in preformation pluripotency mechanisms only apply to the somatic cell lineages but exclude the PGC line as it is preformed. In support to this divergent mechanisms in PGC specification, core pluripotency factors, like Nanog and Oct4, are absent in Xenopus (Dixon et al., 2010). On the other hand, germ plasm was not identified in mouse (Eddy, 1981), and conservation of Nanog confirmed the need for ground state pluripotency in early development, which is conserved from urodeles to mammals (Dixon et al., 2010, Johnson et al., 2011). In other words, transcription factors such as Oct4 and Nanog, which are crucial regulators for both pluripotency and the specification of the germ line in mammals, exist in axolotl, suggesting a conserved mechanism of germ cell specification is shared from urodeles to mammals (Bachvarova et al., 2004, Johnson et al., 2003, Dixon et al., 2010). However, the Xenopus genome does not contain an ortholog of Nanog or Oct4 but it has three genes related to Oct4, XlPou91, XlPou25 and XlPou60, which can maintain the self-renewal capacity of murine embryonic stem cells (Morrison and Brickman, 2006).

It was recently showed in our lab that the gene expression profile of axolotl oocytes resembles that of mouse ES cells, while Xenopus oocytes have a more different gene expression profile (Johnson, unpublished data). For instance, while Nanog, Oct4, H2A.Z, Klf4, and Lin28 are highly expressed in both axolotl oocytes and mouse ES cells, expression of these factors is not detected or is

found at a very low level. On the other hand, while Sall4 and Stat3 factors are expressed in Xenopus oocytes, they are not expressed in axolotl oocytes or mouse ES cells (Johnson, unpublished data). These findings support the idea that axolotls and mammals have a common ancestor.

In this thesis, the reprogramming capacity of axolotl oocyte was tested and compared to that of Xenopus oocytes. The results indicate that the absence of a Nanog ortholog limits the reprogramming capacity of Xenopus oocytes in comparison to axolotl oocytes. It was previously shown in our lab that axolotl oocytes can reactivate expression of the endogenous Nanog in mammalian somatic cells, suggesting that urodeles represent the amphibious ancestor to mammals (Johnson et al., 2011).

1.2 AIMS AND OBJECTIVES OF THIS STUDY

To achieve reprogramming, the somatic chromatin environment must be remodelled to that of a stem cell-like state. This involves reversal of epigenetic marks on somatic chromatin and reactivation of the transcriptional machinery that reprograms the somatic chromatin. In this study, I aimed to evaluate the step-wise hierarchical sequence of modifications at key genetic loci using the reprogramming efficiency of axolotl oocyte extracts.

Previously in our lab, it was shown that axolotl oocyte extract can rapidly reprogram differentiated mammalian cells by altering the epigenetic status of somatic chromatin and inducing re-expression of the endogenous mammalian Nanog gene. *I hypothesised that AOE provides the microenvironment to facilitate the reactivation of the inactive Nanog in somatic cells.* Nanog is a rate-limiting factor in the reprogramming of pluripotency, and axolotl oocytes express a conserved Nanog ortholog. In this study, I focused on the epigenetic regulation of the regulatory regions of the mouse Nanog gene.

CHAPTER 2

GENERAL MATERIALS AND METHODS

In this study, all reagents and chemicals were purchased from Sigma-Aldrich, Dorset, United Kingdom, unless otherwise stated.

2.1 MATERIALS

NIH3T3 mouse (*Mus musculus*) fibroblasts (ATCC, CRL-1658) were the somatic cells reprogrammed in this study; they are hypertriploid and the chromosome number is 68. Mouse embryonic fibroblasts (MEFs) were the control cells in reprogramming experiments. Human embryonic kidney (HEK 293T) cells were used to produce lentiviral vectors. Amphibian oocyte extracts were prepared from mature females' ovaries from frog (*Xenopus laevis*) and axolotl (*Ambystoma mexicanum*) and were used to incubate the cells to be reprogrammed.

2.2 METHODS

2.2.1 Cell culture

2.2.1.1 Mammalian somatic cell culture

NIH3T3 cells, MEFs, and HEK 293T cells were cultured at 37 °C in 5% CO_2 in complete culture media containing the following, the β-Mercaptoethanol was

excluded from the HEK 293T media: DMEM with 2 mM non-essential amino acids (Sigma), 0.1mM β-Mercaptoethanol (Sigma, M6250), 100 IU/ml penicillin and 100 µg/ml streptomycin, 10% foetal bovine serum (FBS) (Sigma), and 2mM L-Glutamine (Sigma, G7513).

2.2.1.2 Mouse embryonic stem cell culture

Wild-type mouse ES cells of CGR8 (ECACC 07032901) line were cultured on flasks that were previously treated with 1% gelatine in culture media containing the following: DMEM with 2mM non-essential amino acids (Sigma), 0.1mM β-Mercaptoethanol, 100 IU/ml penicillin and 100 µg/ml streptomycin, 15% foetal calf serum (FCS) (Sigma), 2mM L-Glutamine (Sigma), and 100ng/ml cytokine leukaemia inhibitory factor (LIF) (Chemicon).

2.2.1.3 Passaging cells

Mammalian cell lines were passaged when they reached about 80-90% confluency. NIH3T3 cells, MEFs, and HEK 293T cells growing in culture flasks were washed twice with 1% PBS. All cells were collected by 0.05% Trypsin (Sigma) incubation for 2-3 minutes at 37 °C to detach the cells before pipetting into a 20 ml Sterilin tube containing between 10 ml of culture medium and centrifuged at 300 x g for 10 minutes. Following centrifugation, the supernatant was aspirated; pelleted cells were resuspended in culture media and counted using a haemocytometer. Then, cells were transferred into a new cell culture flask, splitting the passaged flask in a 1:3 ratio.

2.2.1.4 Cryopreservation of cell lines

Following Trypsin incubation and counting, cells were centrifuged at 300 x g for 10 minutes. Then, pelleted cells were quickly resuspended in freeze media which contains regular complete culture media plus 10 % DMSO (Dimethyl sulfoxide). Cells were resuspended at concentration of 0.5-3.0 x 10^6 and 1 ml aliquots of cells transferred into cryoprotective ampules then placed inside a passive freezer (Nalgene Mr. Frosty, product no. C1562) filled with isopropyl alcohol and incubated at –80 °C overnight before being transferred into liquid nitrogen.

2.2.2 Histone extraction

In order to test by Western blot, histone proteins were extracted from NIH3T3 and mouse ES cells. 2 x 10^5 number of cells were harvested, washed with ice-cold PBS, and centrifuged at 800 x g for 10 minutes. The pellet was resuspended in Triton extraction buffer (TEB: 0.5% Triton X 100, 2 mM phenylmethylsulfonyl fluoride (PMSF), 0.02% NaN_3) to lyse the cells at a density of 10^7 cells per ml and incubated on ice for 10 minutes. Lysate was centrifuged at 6,500 x g for 10 minutes at 4 °C to precipitate the nuclei. The nuclei were washed in TEB and centrifuged again at 6,500 x g for 10 minutes. The pellet was resuspended in 0.2 N HCl at a cell density of 4 x 10^7 nuclei per ml and finally histones were extracted by incubating overnight in the acid solution at 4 °C. The next day, samples were centrifuged at 6,500 x g for 10 minutes at 4 °C. The quantity of histone protein in the resulting supernatant was determined using a BIO-RAD protein assay.

2.2.3 BIO-RAD Protein Assay

This is a derivative of the Bradford assay which allows colorimetric measurement of protein concentration. Using a concentration gradient of BSA (2-14 µg/ml) and BIO-RAD dye absorbance was measured at 595nm on a spectrophotometer. A standard curve was generated. Then, the histone protein concentration was measured by comparing 1 µl of the sample in the mixture with the standard curve.

2.2.4 Western Blot

2.2.4.1 SDS-PAGE

Samples were boiled for 5 minutes in Laemmli loading buffer and then loaded onto SDS-PAGE (1D-mini gels) which has 10% resolving gel and 5% stacking gel. The gels were run in the Bio-Rad Mini-protean III electrophoresis chamber with 1 liter of 1 X TGS buffer for about 1 hour at 100 V. Bio-Rad protein markers were used to determine relative molecular weight.

2.2.4.2 Immunoblotting

After SDS-PAGE, the proteins were transferred onto PVDF membrane (Bio Rad) through the application of electric current. Before the transfer, the membrane was submerged in ethanol for 1 minute and then equilibrated in transfer buffer along with the components of the transfer apparatus (2x sponges, 2x blotting paper, SDS-PAGE gel). The protein transfer was run at 70 V for 2 hours. After the transfer, the membrane was washed with PBS-Tween20 0.1% thrice for 10 minutes each, and incubated in primary antibody solution overnight at 4 °C

agitating gently on rocker. Following the primary antibody incubation, the membrane was washed in 0.1% PBS-Tween20 four times for 10 minutes each. Incubation in the secondary antibody (Horseradish Peroxidase labelled rabbit IgG diluted in PBS-Tween20 0.1% at 1:10000) lasted 1 hour at room temperature with gentle rocking. The membrane was again washed four times for 10 minutes each with PBS-Tween20 0.1%. The resulting signal was viewed with the Amersham ECL plus Western Blotting detection kit in a Bio-ChemiDoc System for 20 minutes exposures.

2.2.5 Lentiviral vector production and cell transduction

2.2.5.1 DNA plasmids used for creation of cell lines

The plasmids TetO-FUW-oct4 (Addgene, plasmid no. 20323) and TetO-FUW-sox2 (Addgene, plasmid no. 20326) were purchased from ADDGENE. To prepare plasmid stocks suitable for cell transfection the plasmid DNA was transformed into competent *E. coli* cells.

2.2.5.2 Plasmid transformation

100 µl of *E. coli* cells were transfected with 2 µl of plasmid by incubation on ice for 30 minutes, then, treated for 'heat-shock' at 42 °C for 45 seconds. Following 5 minutes incubation on ice, 750 µl of SOC media was added. The cells were incubated at 37 °C for 1 hour. 70-100 µl of cell solution was spread on bacterial culture plates which contain 100 µl of Ampicillin (100 mg/ml) per 100 ml of agar. AMP^+ agar plates were incubated overnight at 37 °C.

2.2.5.3 Plasmid mini preparation

A single white colony was picked from the plates and incubated in 3ml of LB media containing Ampicillin overnight at 37 °C in a shaker. Following centrifugation of the cells at 300 x g for 10 minutes, the supernatant was removed. The Qiagen Mini Prep kit was used to prepare the plasmid DNA by following the recommended guidelines. The cell pellet was resuspended in 200 µl of NaOH/SDS lysis solution. 150 µl of 5 M potassium acetate was added and the mix was centrifuged at maximum speed for 1 minute. Nucleic acids were precipitated with isopropanol on ice for 10 minutes and then centrifuged for 1 minute. Supernatant was removed and pellet was resuspended in 0.4 ml buffer before an RNase treatment for 25 minutes at 37 °C. 100 µl of 7.5 M ammonium acetate solution and 1 ml of 100% ethanol were used to precipitate the plasmid DNA on ice for 10 minutes, and the mix was then spun for 5 minutes at 10,000 rpm. Qiagen columns were used for purification. Finally, plasmids were eluted with 50 µl of nuclease free water.

2.2.5.4 Nanodrop quantification of DNA

DNA samples were stored at -20 °C following quantification by Nanodrop spectrophotometer (ND-1000) and the 260:280 ratio of 1.8 was considered pure.

2.2.5.5 Lentivirus production

A lentivirus stock was produced for the two Tet-system plasmid DNA samples to incorporate the desired genes into the NIH3T3 cell–genome. This transduction

resulted in inducible expression of Oct4 and Sox2, and zeocin resistance in the murine fibroblasts.

Day 1: HEK 293T cells were plated on flasks at a density of 8 x 10^6. Transfection reagent mixture was firstly prepared in an Eppendorf tube as: 30µl of FuGene6 transfection reagent (Roche) and 500 µl of serum free DMEM and incubated for 5 minutes at room temperature. Then, backbone vector DNA (10 µg), psPAX2 packing DNA (7.5 µg), and pMD2-G envelope DNA (2.5 µg) were added into the reagent mixture. Following the incubation for 15 minutes at room temperature, the entire transfection mixture was added to the flasks containing HEK 293T cells in 6 ml of culture media.

Day2: The transfection media was replaced with regular HEK 293T media.

Day3: NIH3T3 cells to be transduced were plated onto a six well plate, two wells for each of the two constructs.

2.2.5.6 Lentiviral Transduction of NIH3T3 cells

Day4: The virus media from the HEK 293T cells was collected and filtered with a 0.45 µm filter (7ml from each flask). Fresh culture media was placed on HEK 293T cells to obtain more virus media. To generate a cell line with combined expression of both Oct4 and Sox2 factors, 2 ml of virus media including both Oct4 and Sox2 constructs was added onto NIH3T3 cells in a six-well plate. 4 µg/ml of Polybrene (Santa Cruz, sc-134220) was added into virus media to increase transduction efficiency of the virus.

Day5: After overnight transduction, virus media was replaced with fresh virus media.

Day6: Virus media was replaced with fresh culture media for NIH3T3 cells.

Day7: Following overnight incubation with regular media, the transduced cells were selected by zeocin antibiotic treatment. Zeocin (Invitrogen, R250-01) was added to the NIH3T3 culture at a final concentration of 400 µg/ml which was previously determined by the kill curve. The cells were then cultured for 1 week in zeocin containing selection media.

2.2.6 Immunofluorescence

In order to test for Oct4 expression in the transduced NIH3T3 cell line, an immuno-cytochemistry procedure was used. The transduced Oc4/Sox2 cell line was induced in the 24 hours-presence of 2 µg/ml doxycycline (Sigma Aldrich) which is the tetracycline analogue. In this assay, doxycycline-induced cells (+ dox) were tested in parallel to uninduced (- dox) NIH3T3 cells as negative control. Mouse ES cells were used as positive control due to the fact that Oct4 is constitutively expressed in these cells. Cells were grown on glass cover slips and were stained for the expression of Oct4. Fixation of cells was carried out by 20 minutes incubation in 2% paraformaldehyde. Fixed cells were permeabilized using a solution of 0.2% Triton X100 for 30 minutes. Next, samples were blocked for 1 hour in 5%-BSA-PBS-T (PBS-T consisted of 1xPBS with 0.05% Tween20) at 37 °C, with three 5 minute-washes in 1%-BSA-PBS-T washing buffer. Then the cells were incubated in blocking buffer containing the appropriate concentration of Oct4 antibody (Santa Cruz, sc-5279) (1:100) overnight at 4 °C. The next day, the

samples were washed four times for 5 minutes in washing buffer, and incubated in the dark for 1 hour with Jackson FITC-conjugated donkey anti-rabbit secondary antibody (1:200) in washing solution.

At the end of secondary antibody incubation, samples were washed four times for 5 minutes and then mounted on microscope slides using Vectashield mounting medium. Nuclear staining was carried out with DAPI (4',6-diamidino-2-phenylindole). Slides were sealed with nail varnish before being stored at 4 °C in the dark to preserve fluorescence. Slides were examined under a compound microscope (Nicon Eclipse 80i) and imaged (Nicon Digital Camera DXM1200F).

2.2.7 Cell permeabilization

Cell membranes must be permeabilized to expose the somatic cell nuclei to the reprogramming factors present in oocyte extracts. To optimize the permeabilization conditions, a curve using varying concentrations of digitonin and different additional treatment times was performed. Protease inhibitor cocktail (PIC) (Sigma) was added to the permeabilization buffer (PB) right before the experiment (5 µl of 10 mg/ml solution per 20 ml PB). Digitonin (Sigma) was freshly prepared at a concentration of 40 mg/ml in DMSO.

Cells were collected when they were at 80-85% confluence. Trypsinized cells were resuspended in a small volume of media, counted, and for every 4 x 10^6 cells were incubated in 2 ml of PB including 2 µl of digitonin (40 mg/ml). The samples were quickly placed on ice for 45-60 seconds to prevent over heating of the cells due to the exothermic reaction of digitonin permeabilization. Permeabilization was terminated by adding 8 ml of ice-cold PB buffer, and the samples were centrifuged

at 1500 rpm to pellet the permeabilized cells. To examine the permeabilization efficiency, the cells were visualized under a fluorescent microscope to assess the rate of permeabilization by staining with Dextran and PI. For that purpose, 10 µl aliquots of the cells were added to a 5 µl of a 1:20 dilution of green fluorescent Dextran dye and 1 µl of Propidium iodide (PI) (0.1 µg/ml). They were stained for 10 minutes under a cover of aluminium foil.

2.2.8 Incubation of cells in Amphibian oocyte extracts

After permeabilization, the cells were counted and incubated in oocyte extracts containing with an energy-regenerating system, which was provided by 150 µg/ml Creatine Phosphokinase (CPK) (Sigma, C-3755), 60 mM Phosphocreatine (PK) (P-7936) and 1:100 dilution of 100 mM stock solution of ATP (Sigma, A7699). 2 x 10^6 cells were incubated at 17 °C for 3 and 6 hours in 200 µl of oocyte extracts which includes CPK, PK, ATP and also PIC.

After the treatment, 1 ml of PB buffer containing 1% Penicillin/streptomycin and PIC was added to each tube and centrifuged at 1500rpm for 5 minutes. The supernatant was removed and cell pellet was saved at -80 °C for use in ChIP experiments.

2.2.9 Chromatin Immunoprecipitation

Chromatin Immunoprecipitation (ChIP) can be used to study the mechanisms that regulate gene expression, histone conversion and transcription. To increase the confidence of the results, I used at least three biological replicates for each

experiment. The numbers of biological replicates were indicated in the relevant figure legends.

2.2.9.1 In vivo cross-linking

To start cross-linking the chromatin protein to DNA, each group of 2 x 10^6 cells was re-suspended gently with 1 ml of fixative (1% of formaldehyde in PBS) and incubated at room temperature for 10 minutes. To terminate cross-linking, 100 µl of Glycine was added to each tube, to neutralize un-reacted formaldehyde, and then incubated a further 5 minutes at room temperature. Cross-linked cells were pelleted by centrifuging for 5 minutes at 800 x g at room temperature. As much medium as possible was aspirated and care was paid to avoid damaging the cells. Pelleted cells were washed twice in 1 ml of ice-cold PBS (Magna ChIP A Kit, Millipore, catalogue no. 17-610) including 1 µl of protease inhibitor cocktail II (Magna ChIP A Kit, Millipore, catalogue no. 17-610) and pelleted by centrifuging for 5 minutes at 800 x g at 4^{o}C.

2.2.9.2 Cell and nuclear lysis

Pelleted cells were lysed in 100 µl of cell lysis buffer (Magna ChIP A Kit) including 0.5 µl of protease inhibitor cocktail II by re-suspending very gently and they were incubated on ice for 15 minutes. The cell suspension was mixed gently for a short time every 5 minutes. After the incubation, the cell suspension was homogenized 10 times with a Dounce homogenizer to assist cell lysis. The cell suspension was centrifuged at 800 x g at 4 ^{o}C for 5 minutes.

The supernatant was removed and the cell pellet was re-suspended in 100 µl of Nuclear Lysis Buffer (Magna ChIP A Kit) including 0.5 µl protease inhibitor. It is important to not make bubbles at this stage because they may interfere with the sample during sonication.

2.2.9.3 Shearing DNA (Sonication)

In this study, Diagenode Bioruptor UCD-200 was chosen as the sonicator device since it is able to shear six samples at the same time, avoiding differences between samples. To shear the cross-linked DNA to a length of about 200-800 bps it is necessary to establish optimal shearing conditions. For this purpose, the initial number of cells and number of sonication pulses must be optimized. Sonication was carried out by repeating a 30 seconds-pulse with 30 seconds-rest for 2 x 10^6 cells. Number of repeats was optimized according to the cell types: for NIH3T3 cells, 14 times; for MEFs and ESCs 12 times of pulses. The samples were kept on ice during sonication to prevent denaturation of the chromatin by heat generated by sonication.

To determine the effectiveness of sonication, 5 µl of cell lysate containing unsheared DNA or sheared DNA was separated on 1.5% agarose gel and migration was compared with a 100 bp DNA marker. To prepare these samples, they were incubated with 1 µl of 10 mg/ml RNase A at 37 ^{o}C for 30 minutes, then 1 µl of Proteinase K at 62 °C for 2 hours. The sheared DNA should be seen as a smear in the gel image.

The sheared samples were spun at 11,000 x g at 4 °C for 10 minutes to remove insoluble material before immunoprecipitation process.

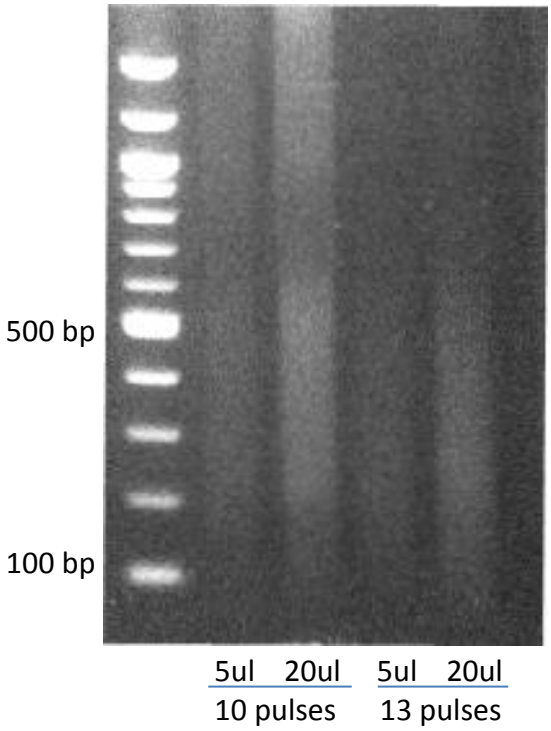

Figure 2.1 Optimisation of sonication conditions To optimise the conditions for shearing genomic DNA obtained from 2 x 10^6 cells (NIH3T3, mouse ES cells, or MEF) were used. Gel image shows the 10 and 13 (X30 seconds pulse and X30 seconds rest) pulses and the volumes of 5 and 20 µl of each sheared DNA. Smeared DNA shows the DNA size is optimised to between 200 bp to 400 bp.

2.2.9.4 Immunoprecipitation of cross-linked protein

Immunoprecipitation was started directly following sonication. 100 µl of a sonicated sample was diluted in 400 µl of ice-cold dilution buffer including 2 µl of protease inhibitor cocktail II (Magna ChIP A Kit, Millipore, catalogue no. 17-610). 5

µl (1% of the chromatin) of the diluted sample was removed and saved at 4 ^{o}C as the input before immunoprecipitation.

20 µl of suspended protein A magnetic beads (Magna ChIP A Kit) and 4 µg of the antibody of interest were added (only Nanog antibody was used 6 µg) into diluted samples, including an IgG control for each cell group. Antibody binding to the protein-bound DNA with the antibody of interest was carried out overnight at 4 ^{o}C with rotation.

Nanog	3.0 µl / 1 x 10^6
H3K27ac (Active Motif, 39133)	1.5 µl / 1 x 10^6
H3K4me1 (Active Motif, 39297)	2.5 µl / 1 x 10^6
5hmC (Active Motif, 39769)	1.0 µl / 1 x 10^6
H2A.Z (Active Motif, 39113)	1.5 µl / 1 x 10^6
Oct4 (Santa Cruz, sc-5279)	2.5 µl / 1 x 10^6
IgG (Millipore, 17-610)	1.5 µl / 1 x 10^6

Table 2.1 Antibodies used in ChIP

DNA was immunoprecipitated with Protein A magnetic beads. Complexes between Protein A magnetic beads-antibody and DNA were collected with a magnetic separator (Magna grip rack) and were washed by re-suspending the beads in 0.5 ml of each of the cold buffers (Magna ChIP A Kit) listed below. They were incubated for 3-5 minutes on a rotating top followed by magnetic clearance.

a. Low Salt Immune Complex Wash Buffer
b. High Salt Immune Complex Wash Buffer
c. LiCl Immune Complex Wash Buffer
d. TE Buffer

Following washing steps, input and immunoprecipitated samples were incubated in 100 µl ChIP elution buffer (including SDS) and 1 µl Proteinase K solution at 62 °C for 2 hours with shaking, then at 95 °C for 10 minutes. After the samples were cooled to room temperature, Protein A magnetic beads were removed from the Proteinase K treatment with the magnetic separator. DNA was purified from immunoprecipitated samples and input samples. Purified DNA was transferred into the filter tubes supplied by the Magna ChIP A Kit. DNA was eluted in 50 µl nuclease-free water and was analysed in quantitative PCR.

2.2.10 Quantitative PCR

Quantitative PCR (qPCR) was carried out with Applied Biosystems 7500 Fast Real-Time PCR System. Each sample for qPCR contained a total of 20 µl including 10 µl of SYBR®-Green Master Mix, 0.5 µl of 10 mM forward and reverse primer mixture, 6.5 µl of nuclease-free water, and 3 µl of sheared (input or immunoprecipitated) DNA sample. This was prepared as triplicates for each reaction.

The following regions of the mouse genome were amplified: Nanog enhancer, Nanog promoter, Nanog intron, MyoD1 enhancer, and MyoD1 promoter were amplified. I used the following qPCR conditions: Initial denaturation at 94 °C for 10

minutes, 42 cycles of 94 °C for 20 seconds (denaturation) and 60 °C for 1 minute (annealing and extension).

Nanog enhancer: 202 bp

Forward: 5'-CTC GAA TGT TGG GCT TAG GA-3'

Reverse: 5'-GAG AGG TAG GGG CAT CAC AG-3'

5'CTCGAATGTTGGGCTTAGGAATGGGGAGACAAGAGCCATCACAGAATGCCTATTGTCC
TTCAATATGTTAGCGATGGGCCCCGTGCTTTAGATTTTAGGCTTGTATTTTCTTTGTGTGT
GTGTGTGTTTGTTTTGTTTCTGTTTCTTTAGGCAGTCTGGAGATCAGGCTGGCTTTCAACT
CCCTGTGATGCCCCTACCTCTC 3'

Nanog promoter: 136 bp

Forward: 5'-GGA GAA TAG GGG GTG GGT AGG GTA G-3'

Reverse: 5'-CAG CCT TCC CAC AGA AAG AG-3'

5'GGAGAATAGGGGGTGGGTAGGGTAGGAGGCTTGAGGGGGGAGGAGCAGGACCTAC
CCTTTAAATCTATCGCCTTGAGCCGTTGGCCTTCAGATAGGCTGATTTGGTTGGTGTCTTG
CTCTTTCTGTGGGAAGGCTG 3'

Nanog intron 1: 142bp

Forward: 5'-TTG TTG AGA CGG GCT GAT CT-3'

Reverse: 5'-CTT CTC CCT GCT CCC TCT TC-3'

5'TTGTTGAGACGGGCTGATCTCAAATTCTCCCATCTCAGCTACTGGAGCAGGGGGGCTT
TAGATTTGTGCTACCCACTGTCAGGATCAGAGGTTTACAGTGTAGATGCGGTCACGGTTC
TAATGAAGAGGGAGCAGGGAGAAG 3'

MyoD1 enhancer: 64 bp

Forward: 5'-CAG CCA AGT ATC CTC CTC CA-3'

Reverse: 5'-AAG CTG AGC ACT CTG GGA GA-3'

5'CAGCCAAGTATCCTCCTCCAGCAGCTGGTCACAAAGCTGGTTAATCTCCCAGAGTGCTC AGCTT 3'

MyoD1 promoter: 80 bp

Forward: 5'-TCA GGC CGG ACA GGA GAG-3'

Reverse: 5'-CCC GGC TGT AGA TAG CAA A-3'

5'TCAGGCCGGACAGGAGAGGGAGGGGTGGGGGACAGTGGGTGGGCATTCAGACTGCC AGCACTTTGCTATCTACAGCCGGG 3'

Oct4 promoter: 113 bp

Forward: 5'-TTT AGG CTC TCC AGA GGA TG-3'
Reverse: 5'-GAC ACC TCA CAA ACC AGT TG-3'

5'TTTAGGCTCTCCAGAGGATGGCTGAGTGGGCTGTAAGGACAGGCCGAGAGGGTGCAG TGCCAACAGGCTTTGTGGTGCGATGGGGCATCCGAGCAACTGGTTTGTGAGGTGTC 3'

Table 2.2 Primer sets used in qPCR

2.2.11 Analysing the qPCR results

2.2.11.1 The Comparative C_T ($\Delta\Delta C_T$) Method

The comparative C_T (cycle threshold) method, also called as 'signal over background', provides a clear detection of changes, as fold difference, at certain time points of gene expression in real-time quantitative PCR experiments.

Arithmetic formulas were used to show the difference of the tested sample to an endogenous housekeeping control which is used to normalize the gene expression level to 1. In this set of experiments, the endogenous control was the C_T value of DNA derived from untreated cells. Using this comparative C_T method, 'fold difference' between time points can be calculated with no need to produce a relative standard curve since all changes are estimated according to normalized endogenous control. Input samples, 1% of initial sheared chromatin, were used as endogenous control.

Ct values show the accumulated fluorescent signal for the amplification of a specific region of DNA and define the numbers of cycle in which linear amplification starts. Therefore, a lower Ct value shows a higher amount of target region. Cycle threshold values ranging from 18 to 30 are accepted as a strong yield of target DNA in the start reaction. Between a 37-38 cycle threshold value, the amount of target DNA can be interpreted as moderate and a higher value than 38 determines a very low amount of target DNA.

In the following experiments on immunoprecipitation of chromatin, total sheared DNA, input, was used as a calibrator to show how much DNA was derived from each set of samples (getting input DNA was explained above). This calibration calculation is:

$$\mathbf{C_{T\ target} - C_{T\ input} = \Delta C_T}$$

This gives the ΔC_T value which is calculated for each of the time points. Then the relative difference of target to reference, $\Delta\Delta C_T$, is calculated using the ΔC_T value in the formula:

$$\mathbf{\Delta C_{T\ target}} - \mathbf{\Delta C_{T\ reference}} = \mathbf{\Delta\Delta C_T}$$

Using the $\Delta\Delta C_T$, finally, the fold difference is calculated with this arithmetic/logarithmic formula:

$$\mathbf{2^{-\Delta\Delta CT}}$$

2.2.11.2 Percentage of Input Method

In this method, amplification signals from immunoprecipitated DNA are divided by amplification signals from its own input (total sheared DNA) sample. The percentage of input method allows the determination of separate values for each sample without using a calibrator sample. In this way, it is possible to examine the value of untreated (0 hour) samples. First, the formula used to adjust the $\mathbf{C_T}$ value of input (1%) to 100% is:

$\mathbf{C_{T\ input}}$ - 6.644 (log2 of 100)

This result is the adjusted input which is used in the formula to calculate percentage of input:

$100 \times 2^{\text{adjusted input} - Ct_{IP}}$

The experiment in which the percent of input method used for calculation was explained above and the figure below shows the excel file for this method.

	A	B	C	D	E	F	G	H	I	J	K	L	M	N
1	samples	inp 1	inp 2	inp 3	avr Ct	st dev	adj inp		IP 1	IP 2	IP 3	avr Ct	st dev	100*2^adj inp-IP
2	Nanog 0h	24.56	24.7	24.64	24.62	0.06	17.98		30.7	30.71	30.81	30.74	0.06	0.014368756
3	Nanog 6h	24.02	24	24.01	24.01	0.004	17.37		28.89	28.84	28.97	28.9	0.062	0.033750898

2.2.12 Statistical analysis

The Friedman test is used as the nonparametric alternative of parametric repeated measures ANOVA to check the differences between two dependent groups such as before and after treatments. Since the number of observations is not enough for a parametric test to validate the assumptions, the nonparametric alternative is preferred. Differences were considered statistically significant at $p<0.05$.

CHAPTER 3

EPIGENETIC MODIFICATIONS TO THE MOUSE NANOG GENE IN RESPONSE TO AMPHIBIAN OOCYTE TREATMENT

3.1 Introduction

A major aspect of transcriptional regulation is carried out by the acquisition of epigenetic modifications, which have important roles during development. These marks must be remodelled during the reprogramming of somatic cells to pluripotency where it is crucial to reverse the epigenetic modifications which silence the pluripotent genes in somatic chromatin. In this chapter, to investigate the modification of DNA in the regulatory regions of the mouse Nanog gene, I focused on 5-hydroxymethylation, an intermediate in DNA demethylation, as well as the histone modifications H3K4me1 and H3K27ac, on the regulatory regions of the mouse Nanog gene after treatment with amphibian oocyte extracts.

3.2 Hydroxymethylation of the mouse Nanog gene regulatory regions upon amphibian oocyte extract treatment

3.2.1 Background

DNA methylation has a prominent role in mammalian development and it is a primary mode by which gene expression is stabilized (Kass et al., 1997, Smith and

Meissner, 2013, Senner, 2011, Messerschmidt et al., 2014). It has been clearly established that in early zygote formation methyl groups are removed from DNA (Santos et al., 2002). Later in development, the level of methylation on DNA changes according to cell type and stage of development. While pluripotency genes are hypomethylated in pluripotent cells, they become hypermethylated during cellular development (Borgel et al., 2010). Therefore, to achieve reprogramming of somatic chromatin, pluripotent genes must be demethylated.

Amphibian oocytes contain factors to demethylate DNA in pluripotency genes (Hansis et al., 2004, Simonsson and Gurdon, 2004, Barreto et al., 2007, Alberio et al., 2005, Bian et al., 2009). It has been shown by methyl-sensitive restriction enzyme assays and bisulphite analysis that four methyl-sensitive restriction enzyme sites located in the Oct-4 promoter were methylated in adult mouse thymus cells. However, after treating the cells in *Xenopus* oocytes for 30 hours, demethylation of these sites was initiated and in 90 hours the Oct4 promoter was totally demethylated (Simonsson and Gurdon, 2004). It was previously demonstrated in our lab that both axolotl and Xenopus oocytes can remove methyl groups from the promoters of the pluripotency genes Nanog and Oct4 (Bian et al., 2009). Bian et al (2009) showed in a bisulfite assay that AOE treatment of mouse embryonic fibroblasts (MEFs) resulted in a significant reduction of the methylation level on the Oct4 promoter from 85% to 62% and a slight methylation reduction on the Nanog promoter, from 31% to 25.6% upon 5 hours of AOE treatment. Moreover, different levels of Oct4 and Nanog gene transcription were detected by quantitative real-time PCR in cultured MEFs after AOE treatment after

two weeks of incubation (Bian et al., 2009). Increasing level of Nanog expression in contrast to slight demethylation on its promoter might indicate the presence of undetected 5hmCs in classic bisulfite sequencing.

Methylation of DNA occupies an important place in the regulation of tumour suppression in many cancer types, such as breast cancer, alongside other genetic regulation. Therefore, reprogramming the methylation status of tumour supressing genes is an effective way of pausing or regressing tumour growth. Allegrucci et al. (2011) analysed the competence of amphibian oocyte extracts to reverse DNA demethylation on the regulatory elements of tumour suppressor genes by bisulfite sequencing. Their results demonstrated that extracts of oocytes from axolotl and Xenopus, as well as extract from ES cells, had the ability to demethylate cytosine residues in the regulatory regions of these genes. However, among the cell types tested, extracts from axolotl oocytes were the most efficient (Allegrucci et al., 2011), because epigenetic factors in amphibian oocytes can remodel mammalian somatic chromatin in DNA replication-independent manner (Simonsson and Gurdon, 2004, Alberio et al., 2005, Bian et al., 2009). This suggests that replication-independent DNA demethylation is carried out via enzymatic mechanisms, which are ATP-dependent (Hansis et al., 2004, Bian et al., 2009, Alberio et al., 2005).

DNA demethylation is known to exert cell type-specific regulation of gene expression. Using base-resolution methylome maps, more than 300,000 tissue-specific differentially methylated regions (tsDMRs) were identified in adult mouse tissues. These were mostly located at distal cis-regulatory regions, suggesting a

role in the regulation of gene expression. Moreover, some of the tsDMRs at cis-regulatory regions were found within inactive enhancers in adult tissues, which were active during embryo development (Hon et al., 2013), suggesting an active role for methylation in gene silencing.

Hydroxylation of methyl groups on the cytosine residues of CpG islands is an intermediate step in active demethylation. 5-hydroxymethlcytosine was discovered as a novel sixth base in the DNA sequence. Its production is catalysed by oxidation of methylated cytosine by the Tet family of proteins (Kriaucionis and Heintz, 2009, Tahiliani et al., 2009, Ito et al., 2010). Hydroxymethylation of cytosine takes place as an intermediate reaction in the pathway leading to active DNA demethylation (Kriaucionis and Heintz, 2009, Tahiliani et al., 2009, Globisch et al., 2010). Moreover, 5-hmC is enriched on LINE-1 elements, which are repetitive elements in heterochromatin that are reprogrammed before implantation, suggesting a role for 5-hmC production in the demethylation process (Booth et al., 2012).

However, the abundance of 5-hmC in several tissue types in mammals indicates that 5-hydroxymethylation is not only a demethylation intermediate; it is also a cell type-specific epigenetic alteration that functions in the opening of compact chromatin, enabling access of transcription factors to chromatin and the subsequent initiation of transcriptional activity. For instance, pluripotency genes are enriched with 5-hydroxymethylation in mouse embryonic stem (ES) cells and neuronal stem cells; moreover, an increased level of hydroxymethylation in euchromatin implies a role for 5hmC in transcriptional activity (Kriaucionis and

Heintz, 2009, Tahiliani et al., 2009, Globisch et al., 2010, Szwagierczak et al., 2010).

Ito et al. (2010) showed that mouse ES cells overexpress Tet1, a principle member of the Tet family, whose deletion causes a deficiency in the ability of mouse ES cell to self-renew. Moreover, regulatory regions of pluripotency genes are occupied by Tet1 (Wu and Zhang, 2011), suggesting a role for Tet1 in their regulation by epigenetic mechanisms. Depletion of Tet1 and 2 caused downregulation of several genes functioning in the maintenance of the ES cell environment, such as Esrrb, Klf2, Dppa3, Zfp42 and Prdm14 genes, suggesting that Tet proteins play roles in the regulation of these transcriptional network elements. It has been shown that Tet proteins can interact with the core pluripotency factors Nanog and Oct4, and it is recruited to their target genes (Costa et al., 2013).

Although it is known that 5-hydroxymethylation of cytosine residues is prominent within the regulatory regions of active pluripotent genes in mouse ES cells (Wu and Zhang, 2011), it is unclear how the emergence of this mark is regulated during reprogramming. It was recently demonstrated that Tet1 and Tet2 are two of the proteins identified as interacting with Nanog protein in mouse embryonic stem cells and this interaction accelerates reprogramming efficiency (Costa et al., 2013). Therefore, it is important to analyse Tet-catalysed hydroxymethylation of regulatory regions within the Nanog gene upon AOE treatment. Unpublished transcriptome data from our lab shows that axolotl oocytes express Tet family enzymes. Exploiting the epigenetic remodelling capacity of amphibian oocyte

extracts, I analysed the level of hydroxymethylation of regulatory regions of the mouse Nanog gene after incubation in amphibian oocyte extracts.

3.2.2 RESULTS

3.2.2.1 Comparing the levels of 5hmC and 5mC after AOE treatment

To assess the effects of AOE treatment on the levels of methylation (5mC) and hydroxymethylation (5hmC) in the mouse Nanog enhancer, chromatin immunoprecipitation (ChIP) assay and quantitative (q) PCR were used. 2 x 10^6 digitonin-permeabilized NIH3T3 cells were treated with AOE for 6 hours. Following cell lysis, genomic DNA was sheared to the scale of 200-800 bp. 1% of total sheared DNA was saved as input and the rest was immunoprecipitated with antibodies specific for 5mC (Active Motif, catalog no. 61255), 5hmC (Active Motif, catalogue no. 39769) and IgG (Millipore, Magna ChIP Kit A content, catalog no. PP64B). Input and immunoprecipitated DNA was analysed by quantitative (q) PCR for the following regions: the Nanog enhancer, the MyoD1 enhancer, the MyoD1 promoter and the Nanog intron 1. Finally, the parameters from the mouse Nanog enhancer amplification at time points 0 and 6 hours from 5mC and 5hmC immunoprecipitations were compared to negative control IgG pull-down, to test antibody specificity.

Using the mean cycle threshold (C_t) values, fold differences between the time points, 0 and 6 hours, were calculated as described in detail in Chapter 2. This corresponded to about a 1.5 fold increase for the level of 5hmC on the Nanog enhancer, while it was about 0.6 fold decrease in the level of 5mC on the Nanog enhancer after 6 hours of incubation. IgG immunoprecipitation was at similar levels in untreated cells (Figure 3.1). As a negative control, I measured the level of

DNA from the MyoD1 enhancer and promoter, or the first intron of Nanog. AOE treatment did not change the level of methylation or hydroxymethylation on these sequences (Figure 3.1). These results suggest that the hydroxymethylation pathway is used in the demethylation of Nanog gene regulatory sequences by AOE.

A.

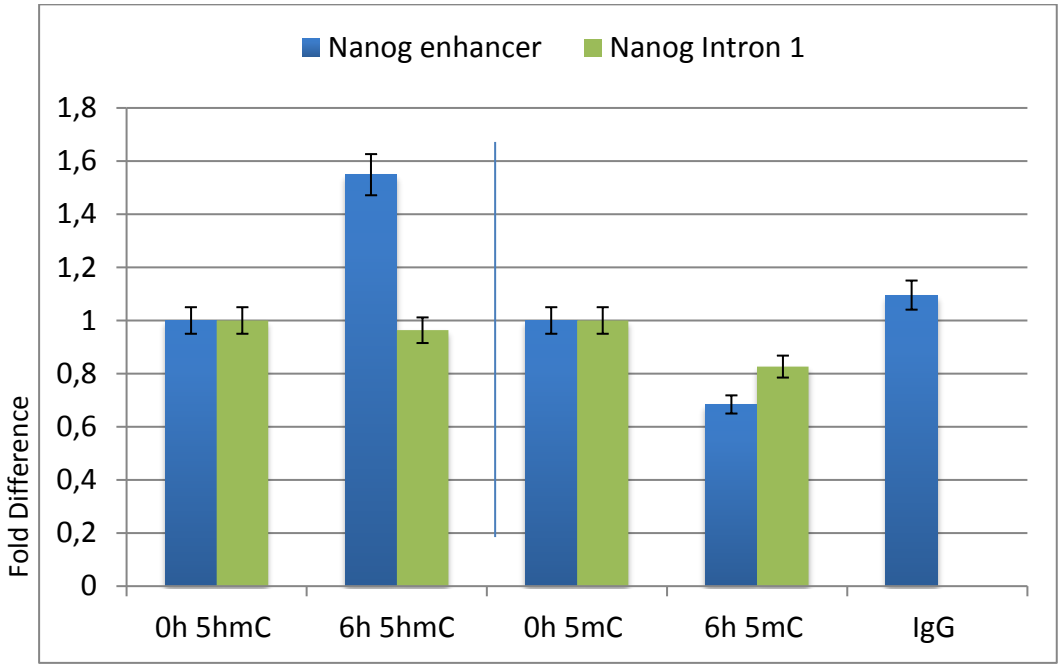

B.

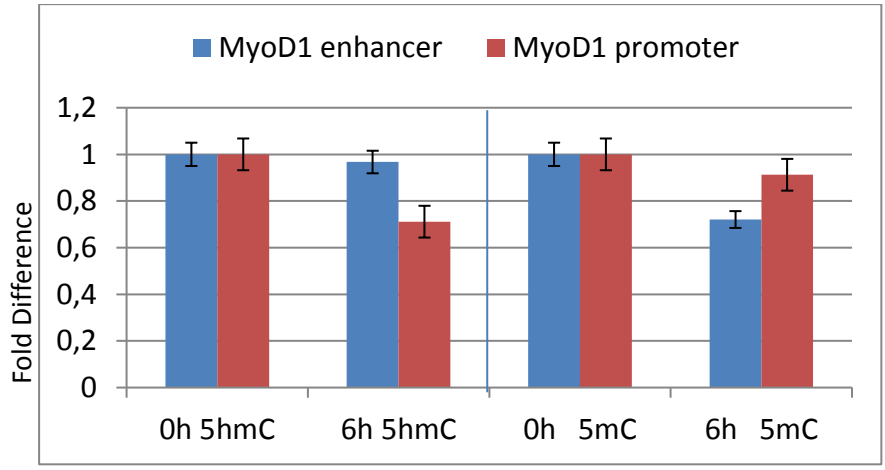

Figure 3.1 Levels of 5hmC and 5mC on the Nanog enhancer in NIH3T3 cells after AOE treatment Sheared chromatin from 2 x 10^6 cells was immunoprecipitated with 5 µg of 5hmC and 5mC antibodies and the levels of specific DNA sequences (as indicated) were quantified by qPCR. A. The graph shows the changes in fold differences of 5hmC and 5mC levels in the Nanog enhancer (blue) and the Nanog intron 1 (green) in NIH3T3 cells treated with AOE. Immunoprecipitation with IgG is a negative control. B. The graph shows the changes in fold differences in 5hmC levels on MyoD1 enhancer (blue) and MyoD1 promoter (red) in control cells and cells treated for 6 hours with AOE. Biological repeat number= 3 and error bars indicate standard deviations in technical replicates.

3.2.2.2 Level of 5hmC on the Nanog enhancer and promoter after AOE treatment

Transcriptome analysis by our lab showed that Tet is expressed in axolotl oocytes, while it is not detectable in Xenopus oocytes. Therefore, I used ChIP to assess the relative hydroxymethylation levels of selected Nanog enhancer and promoter regions in order to determine whether AOE can catalyse production of 5hMC. I performed companion experiments with XOE.

NIH3T3 cells were permeabilized with digitonin and then incubated in the oocyte extracts of axolotl or Xenopus for several time points as indicated in Figures 3.2 and 3.3. Following the extract treatment, sheared chromatin was immunoprecipitated with 5 µg of commercial antibody specific for 5hmC (Active Motif, catalogue no. 39769). IgG immunoprecipitation with a commercial antibody (Millipore, Magna ChIP Kit A content, catalog no. PP64B) was used as a negative control. Following immunoprecipitation, qPCR was performed for Nanog enhancer and promoter regions, accompanied with the negative controls: MyoD1 enhancer and promoter, and Nanog intron 1.

As the panel A of Figure 3.2 shows, 5hmC IP resulted in about a 6 fold enrichment of Nanog enhancer sequences relative to levels in untreated cells after only 3 hours of incubation in AOE. Further treatment did not increase the capture of enhancer sequences. In contrast, promoter sequences increase during the interval between 3 and 6 hours of AOE incubation, 4 fold and 12 fold relative to the untreated cells. This suggests that hydroxylation of DNA is mostly completed in 3

hours on the enhancer, while it continuously increased for 6 hours on the promoter sequence.

Figure 3.2 panel B showed the level of 5hmC on the negative controls. There was no detected signal for any change on the regulatory regions of mouse MyoD1 gene or non-coding region Nanog intron 1. This result suggested that AOE specifically remodels the chromatin of the Nanog gene.

Level of 5-hydroxymethylation of cytosine on Nanog enhancer and promoter after XOE treatment

Bian et al. (2009) showed that Xenopus oocyte extract can demethylate the promoter of the Nanog gene. To understand whether the promoter and enhancer of the Nanog gene are hydroxymethylated in XOE, I performed ChIP assay with the same approach above. Figure 3.3 shows that there was no apparent enrichment in signal corresponding to sequence from the Nanog enhancer from samples treated in XOE when compared to either untreated cells, or in control samples after IgG immunoprecipitation. This indicates that XOE is not capable of hydroxymethylating the DNA, suggesting DNA demethylation does not include a step in which the DNA is converted from a methylated to hydroxymethylated status by Tet enzyme catalysis. (For the activity of XOE, see Appendix A.)

A.

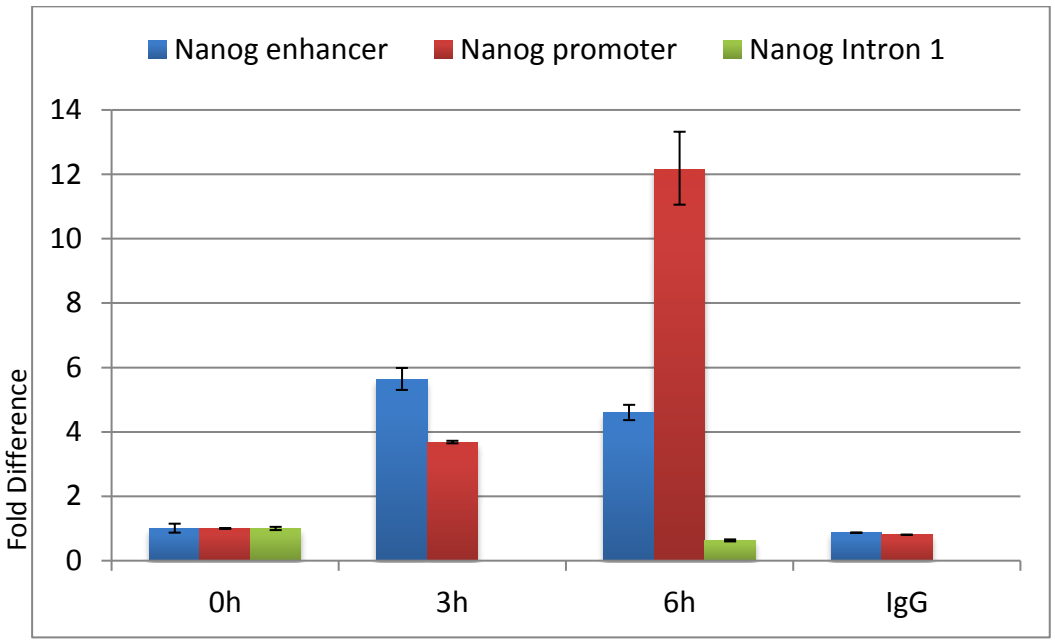

B.

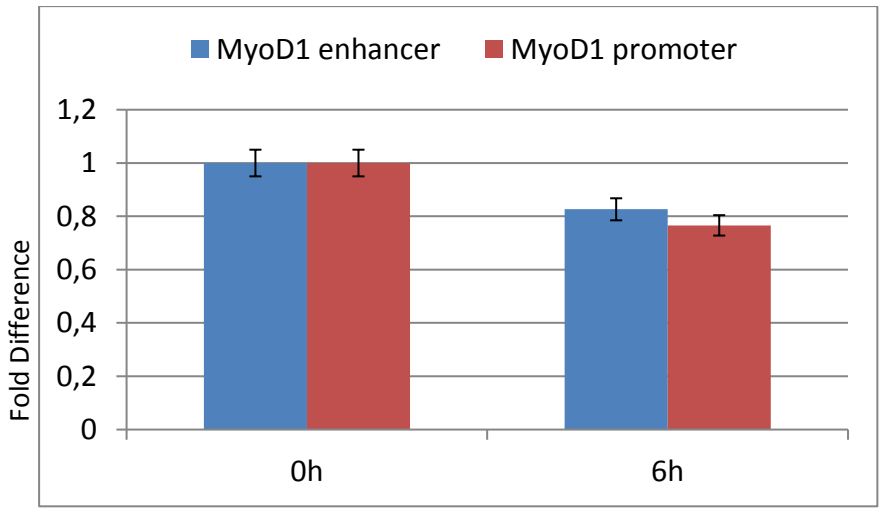

Figure 3.2 Level of 5hmC on the regulatory regions of Nanog gene in NIH3T3 cells after AOE treatment

Sheared chromatin from 2 x 10^6 cells was immunoprecipitated with 4 µg of 5hmC antibody and the levels of specific DNA sequences (as indicated) were quantified by qPCR. A. The graph shows the changes in fold differences of 5hmC levels on the Nanog enhancer (blue), promoter (red) and the Nanog intron 1 (green) in NIH3T3 cells treated with AOE. Immunoprecipitation with IgG is a negative control. B. The graph shows the changes in fold differences of 5hmC levels on the MyoD1 enhancer (blue) and promoter (red) in control cells (0h) and after 6 hours of AOE treatment. Biological repeat number= 5 and error bars indicate standard deviations in technical replicates.

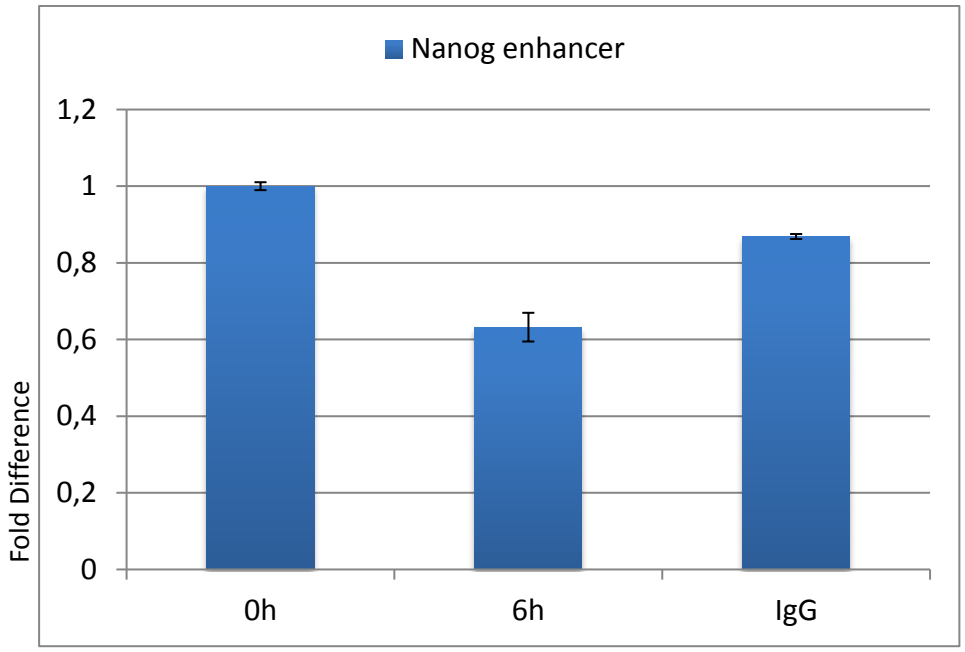

Figure 3.3 Level of 5hmC enrichment on the Nanog enhancer after XOE treatment

Sheared chromatin from 2 x 10^6 cells was immunoprecipitated with 4 µg of 5hmC antibody and the levels of specific DNA sequences (as indicated) were quantified by qPCR. The graph shows the changes in fold differences of the 5hmC level on the Nanog enhancer in control cells (0h) and cells 6 hours of XOE treatment. Immunoprecipitation with IgG is a negative control. Biological repeat number= 3 and error bars indicate standard deviations in technical replicates.

3.2.3 Conclusions

Using ChIP as an assay, this study demonstrated that the level of 5hmC was increased on the mouse Nanog enhancer and promoter after treatment with AOE.

Hydroxymethylation of the promoter sequence increased between 3 and 6 hours of incubation with AOE and reached to 12-fold over the control. This experiment was consistent with previous results, which showed the demethylation of the mouse Nanog promoter in AOE and suggests that 5hmC is induced as an intermediate step in the demethylation pathway.

The level of 5hmC on the mouse Nanog enhancer increased significantly in 3 hours of treatment with AOE compared to that of promoter, showing that hydroxymethylation began on the enhancer prior to the promoter. Between the 3 and 6 hour, the 5hmC level did not increase and remained almost at the similar level, indicating the enhancer is remodelled prior to the promoter by hydroxymethylation. This result highlights the fact that the epigenetic modifications on promoter regions are generally more stable and enhancer regions are more plastic to undertake these modifications (Visel et al., 2009, Chen et al., 2012, Peters et al., 2015). Furthermore, the promoter region may be less accessible to the demethylation machinery and subsequent hydroxymethylation of the promoter might be triggered by hydroxymethylation of the enhancer.

While 5hmC was enriched on cis-regulatory regions of the pluripotency gene Nanog, it was not induced on the enhancer of the MyoD1 gene, which is involved exclusively in development of muscle cells, and is not included in reprogramming

process. These results confirm the specificity of the remodelling activities by AOE, suggesting they are limited to genes involved in the regulation of pluripotency.

Intriguingly, recent work suggests that when somatic cells are exposed to oocyte factors they attain the epigenetic features of oocytes (Jullien et al., 2014). Analysis of the axolotl oocyte transcriptome indicates that in this species pluripotency is maternally programmed, suggesting that oocyte factors can reconfigure somatic chromatin to a state that is compatible with the activation and maintenance of pluripotency factors.

There was no enrichment of 5hmC on Nanog enhancer in somatic cells treated in XOE. Although this result seems contradictory to the previous results showing XOE can reduce the methylation level on pluripotent gene promoters, indeed, it might answer why XOE is less efficient than AOE in the demethylation of these regions. For example, AOE has greater ability to demethylate the promoters of the pluripotency genes, Nanog and Oct4 (Bian et al., 2009) than XOE.

3.3 Histone modifications on the mouse Nanog gene regulatory regions induced by amphibian oocyte extract

3.3.1 Background

Nucleosomes can contain numerous post-translational modifications on their amino-termini of tails, which alter the interactions between histones, DNA and transcription factors, thereby, providing chromatin with a dynamic structure (Wolffe and Hayes, 1999). Taken together, these alterations have an important role in the control of transcription and so are involved in regulation of development, cell division, and reprogramming.

The acetylation and/or methylation of lysine residues within histone H3 are widely studied modifications which have important roles in the condensation and stabilization of chromatin (Grunstein, 1997). Acetylation of histone lysine tails are related to transcriptionally active regions, which act in part by changing biochemical features of the histone residues (Struhl and Adachi, 1998). This induces an uncondensed chromatin structure which increases the likelihood of transcription factors binding to DNA. Overall, acetylated lysine residues mostly contribute to positive regulation of transcriptional activity (Struhl and Adachi, 1998).

Methylation of histones occurs on lysine residues as mono-, di-, or tri-methylation motifs. Arginine residues can be mono- or di-methylated (Strahl et al., 1999). The specific function of histone methylation depends on which lysine residue is specifically modified: While tri-methylation of lysine 9 or 27 of histone H3 has a

repressive role on transcriptional activity, mono- or tri-methylation of lysine 4 regulates gene expression in positive manner (Strahl and Allis, 2000, Kimura, 2013). And, extension of methyl groups is another factor designating the activity of histone methylation: While tri-methylation of lysine 4 residue of histone H3 is located on active promoters, mono-methylation of the same residue exists on active enhancers (Barski et al., 2007).

However, there are still unknown mechanisms for newly discovered modifications which affect development and reprogramming. In the ENCODE project, histone modifications, H3K27ac, H3K4me1, H3K4me2, H3K4me3 and H3K79me2, were found within the cis-regulatory regions of genes, such as promoters and enhancers, however, only active enhancers are enriched in H3K4me1 and H3K27ac (Creyghton et al., 2010, Zentner et al., 2011, Bogdanovic et al., 2012) (Figure 3.4). Later studies showed that these activating histone marks on enhancers have a significant role in determining the temporal and tissue-specific regulation of gene expression (Bogdanovic et al., 2012, Capra, 2015). Active enhancers require both H3K27ac and H3K4me1 marks (Creyghton et al., 2010, Hawkins et al., 2011, Rada-Iglesias and Wysocka, 2011, Bonn et al., 2012). Also, H3K4me3 and H3K36me3 marks are found as defining active enhancers (Pekowska et al., 2011, Zentner et al., 2011).

It was previously demonstrated that putative distal regulatory elements (PDREs) function in zebrafish embryogenesis by examining three histone modifications on active enhancers, H3K4me3, H3K4me1 and H3K27ac, by ChIP-seq analysis. The enhancers enriched by these modifications, especially H3K4me1, encourage

binding of transcription factors, like p300 and CBP coactivators (Heintzman et al., 2007, Kim et al., 2010b). While H3K4me1 is constitutively enriched at poised enhancers, H3K27ac is enriched at only tissue-specific active enhancers (Bonn et al., 2012), therefore, enrichment of H3K27ac allows binding of pluripotency factors, as well as tissue-specific transcriptional factors. Also, defining 'differentially acetylated regions' (DARs) in the zebrafish genome indicated that these regions are characteristically varied for acetylation of H3K27 status in different stages (Bogdanovic et al., 2012), showing the level of H3K27ac changes during development, depending on transcriptional activity of the gene. For instance, in early embryogenesis, binding of Nanog was detected on these distal regulatory regions which are enriched with the H3K27ac mark and any decrease in H3K27ac level on enhancers is associated with gene expression specific for differentiation (Bogdanovic et al., 2012).

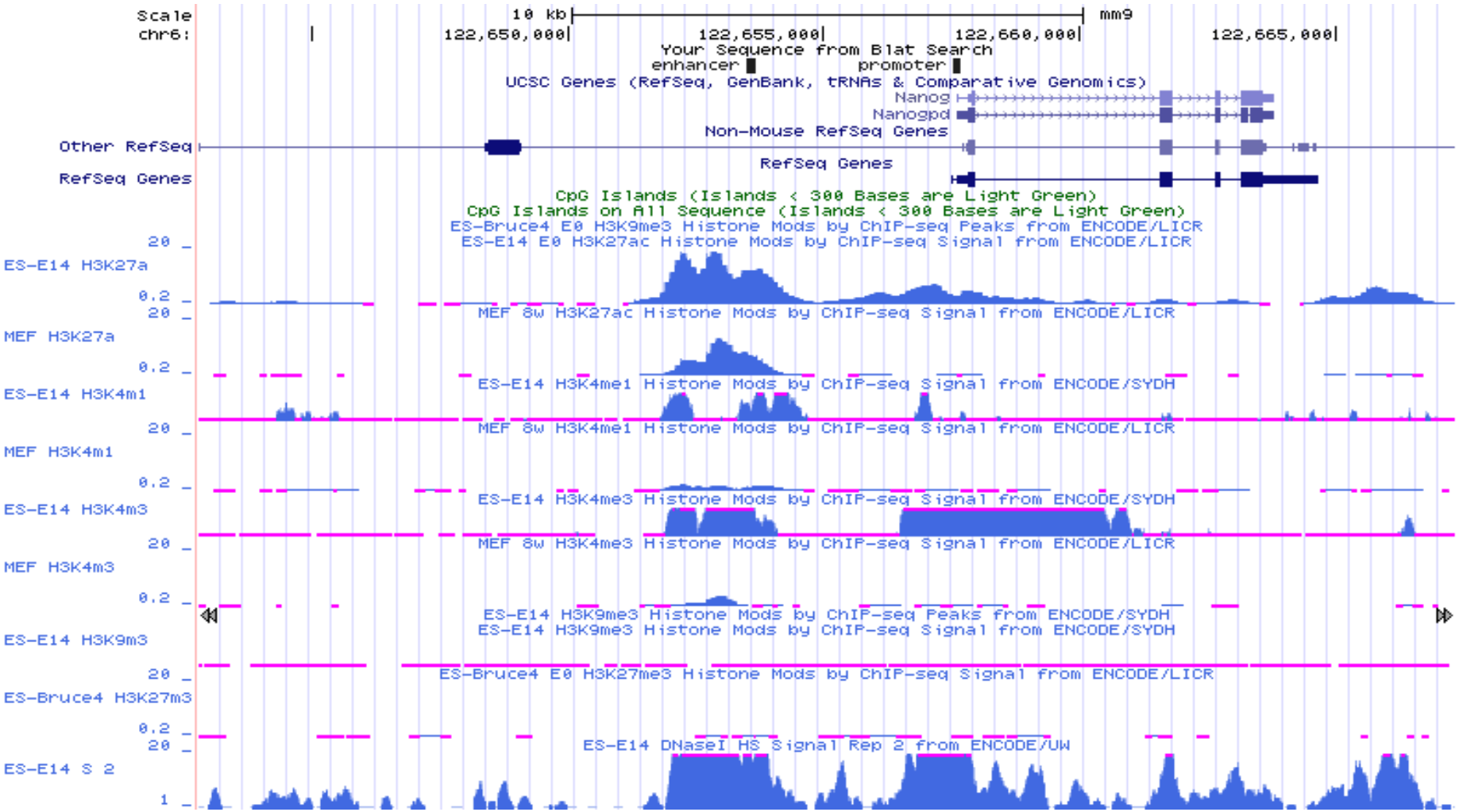
Scale
chr6:
10 kb
mm9
122,650,000
122,655,000
122,660,000
122,665,000
Your Sequence from Blat Search
enhancer
promoter
UCSC Genes (RefSeq, GenBank, tRNAs & Comparative Genomics)
Nanog
Nanogpd
Non-Mouse RefSeq Genes
Other RefSeq
RefSeq Genes
RefSeq Genes
CpG Islands (Islands < 300 Bases are Light Green)
CpG Islands on All Sequence (Islands < 300 Bases are Light Green)
ES-Bruce4 E0 H3K9me3 Histone Mods by ChIP-seq Peaks from ENCODE/LICR
ES-E14 E0 H3K27ac Histone Mods by ChIP-seq Signal from ENCODE/LICR
20
ES-E14 H3K27a
0.2
20
MEF 8w H3K27ac Histone Mods by ChIP-seq Signal from ENCODE/LICR
MEF H3K27a
0.2
ES-E14 H3K4me1 Histone Mods by ChIP-seq Signal from ENCODE/SYDH
ES-E14 H3K4m1
20
MEF 8w H3K4me1 Histone Mods by ChIP-seq Signal from ENCODE/LICR
MEF H3K4m1
0.2
ES-E14 H3K4me3 Histone Mods by ChIP-seq Signal from ENCODE/SYDH
ES-E14 H3K4m3
20
MEF 8w H3K4me3 Histone Mods by ChIP-seq Signal from ENCODE/LICR
MEF H3K4m3
0.2
ES-E14 H3K9me3 Histone Mods by ChIP-seq Peaks from ENCODE/SYDH
ES-E14 H3K9me3 Histone Mods by ChIP-seq Signal from ENCODE/SYDH
ES-E14 H3K9m3
20
ES-Bruce4 E0 H3K27me3 Histone Mods by ChIP-seq Signal from ENCODE/LICR
ES-Bruce4 H3K27m3
0.2
20
ES-E14 DNaseI HS Signal Rep 2 from ENCODE/UW
ES-E14 S 2
1

Figure 3.4: Epigenetic modifications on the mouse Nanog locus in differentiated and undifferentiated cells. The mouse Nanog locus is located on chromosome 6 as indicated in the figure. The enhancer and promoter sequences which were used in this project are indicated by two black squares. The distance between the Nanog enhancer and promoter is approximately 4 kb. Various histone modifications on the mouse Nanog locus are shown in the mouse ES cells and MEFs (UCSC Genome Browser).

Taken together, there are defined enhancers which are active and poised (refers to inactive) during development and reprogramming. Acetylation of the H3K27 residue can distinctively mark active enhancers, but not poised enhancers, while the monomethylated H3K4 residue occurs on both active and poised enhancers. In other words, while H3K27ac is a stage-specific histone mark on active enhancers, H3K4me1 permanently marks enhancers of genes which will become activated (Bonn et al., 2012); therefore H3K27ac has a more dynamic deposition than H3K4me1.

In this study, I focused on the induction of acetylation of H3K27 and mono-methylation of H3K4 on the Nanog regulatory regions (Figure 3.4) in somatic chromatin remodelled by treatment with AOE.

3.3.2 Results

3.3.2.1 H3K27ac enrichment on the Nanog enhancer after AOE treatment

To measure the H3K27 acetylation level before or after extract treatment, ChIP was performed using a commercial H3K27ac antibody (Active Motif, catalog no. 39133) with IgG immunoprecipitation as negative control. qPCR for Nanog enhancer and promoter regions was accompanied with the MyoD1 enhancer and promoter, and Nanog intron 1 regions as negative controls.

As Figure 3.5 shows, acetylated H3K27 was enriched on the mouse Nanog enhancer sequences in NIH3T3 cells after axolotl oocyte extract treatment. The levels were increased by 2.5 fold within 3 hours and stayed fairly constant through 6 hours of further incubation, relative to signal from untreated cells or IgG controls. Nanog promoter amplification from immunoprecipitated DNA was similar to that obtained from untreated cells or from IgG controls. This result indicates that H3K27ac showed no increase in signal corresponding to Nanog promoter sequences after 3 or 6 hours of extract treatment. There was no detected signal for increase on the MyoD1 regulatory regions or intron 1 of Nanog genomic region, indicating the specificity of the remodelling activity.

I also tested for the addition of H3K27ac on the Nanog regulatory regions after AOE treatment of mouse embryo fibroblasts (MEFs). Results showed a similar trend (even more efficient); H3K27ac increased by almost 9 and 12 fold between 3

and 6 hours of treatment, while there was no increase on Nanog promoter. Also, no increase was detected on MyoD1 regulatory regions (Figure 3.6).

These data suggest that axolotl oocyte extract promotes addition of H3K27ac specifically on the Nanog enhancer, a well-characterized regulatory region (Kidder et al., 2009). In contrast, this mark is not added to the Nanog promoter. H3K27ac is a mark exclusively found on transcriptionally active enhancers in other cell types (Capra, 2015), indicating the specificity of the enzymatic activities in AOE, and suggesting that AOE configures the chromatin around the Nanog gene in a transcriptionally active state.

Measurement of the level of H3K27ac after XOE treatment

I then tested if Xenopus oocyte extract had similar activity with the same experimental approach. As shown in the graph, the level of H3K27ac on the mouse Nanog enhancer showed no increase after XOE treatment of 3T3 cells (Figure 3.7). This experiment shows that Xenopus oocyte extract is not capable of adding the H3K27ac mark to the regulatory Nanog enhancer in differentiated mouse cells.

A.

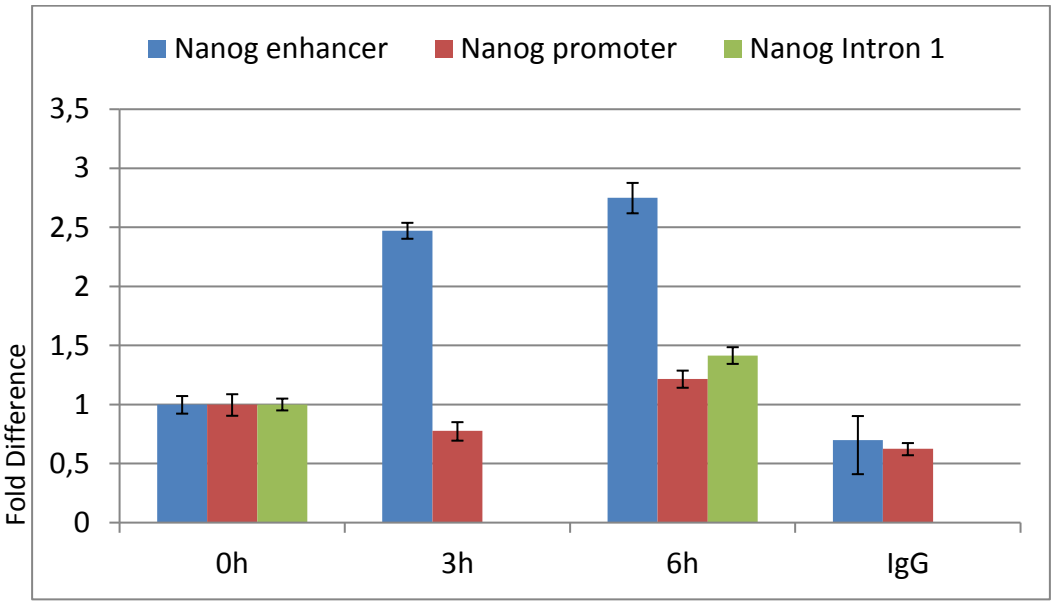

B.

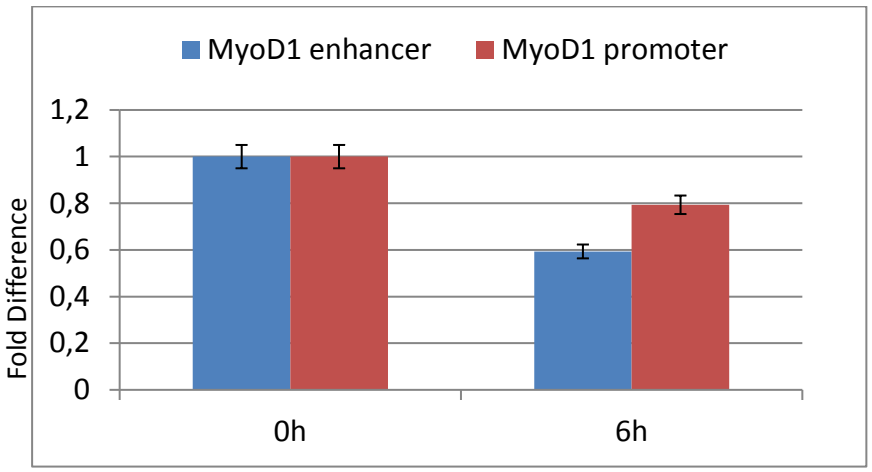

Figure 3.5 Level of H3K27ac on the regulatory regions of the Nanog gene in NIH3T3 cells after AOE treatment

Sheared chromatin from 2 x 10^6 cells was immunoprecipitated with 5 µg of H3K27ac antibody and the levels of specific DNA sequences (as indicated) were quantified by qPCR. A. The graph shows the changes in fold differences of H3K27ac levels on the Nanog enhancer (blue), promoter (red) and the Nanog intron 1 sequence (green) in NIH3T3 cells treated with AOE. Immunoprecipitation with IgG is negative control. B. The graph shows the changes in fold differences of H3K27ac levels on the MyoD1 enhancer (blue) and promoter (red) in control (0h) and 6 hours of AOE treatment. Biological repeat number= 6 and error bars indicate standard deviations in technical replicates.

A.

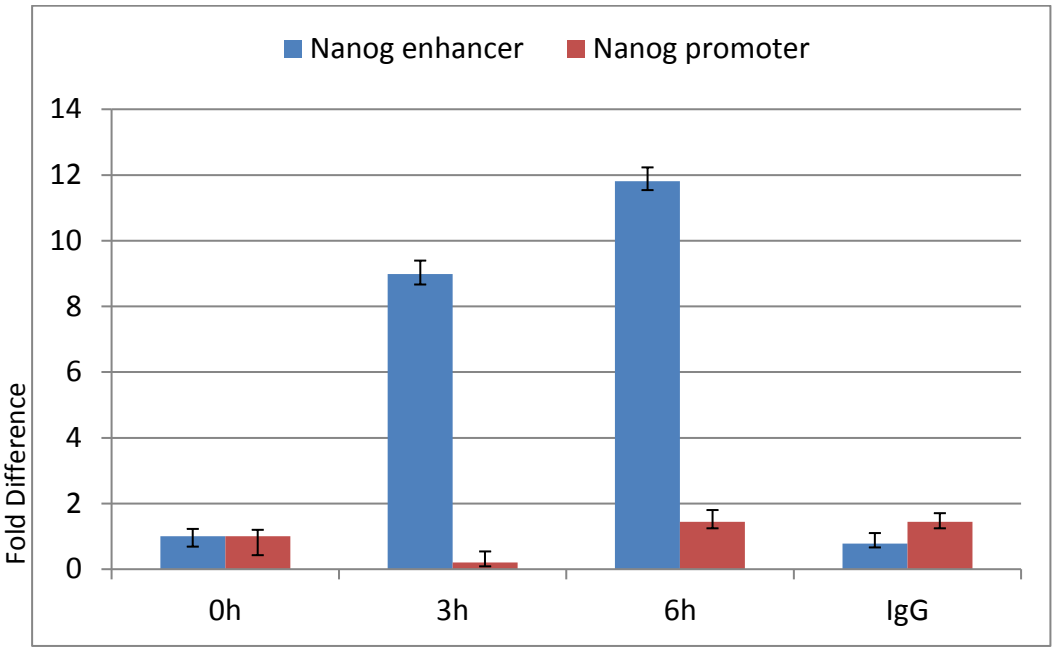

B.

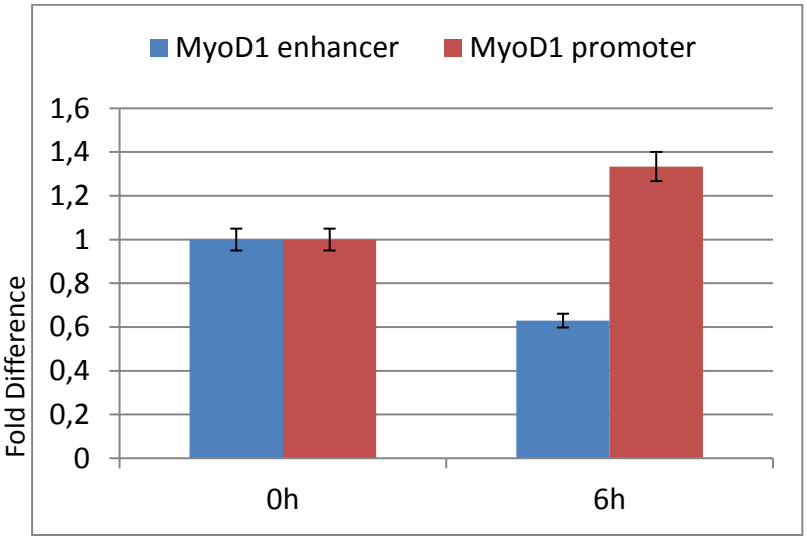

Figure 3.6 Level of H3K27ac on the regulatory regions of the Nanog gene in MEFs cells after AOE treatment

Sheared chromatin from 2 x 10^6 cells was immunoprecipitated with 5 µg of H3K27ac antibody and the levels of specific DNA sequences (as indicated) were quantified by qPCR. A. The graph shows the changes in fold differences of H3K27ac levels on the Nanog enhancer (blue) and promoter (red) in MEFs treated with AOE. Immunoprecipitation of IgG is negative control. B. The graph shows the changes in fold differences of H3K27ac levels on the MyoD1 enhancer (blue) and promoter (red) sequences in control (0h) and 6 hours of AOE treatment. Biological repeat number= 3 and error bars indicate standard deviations in technical replicates.

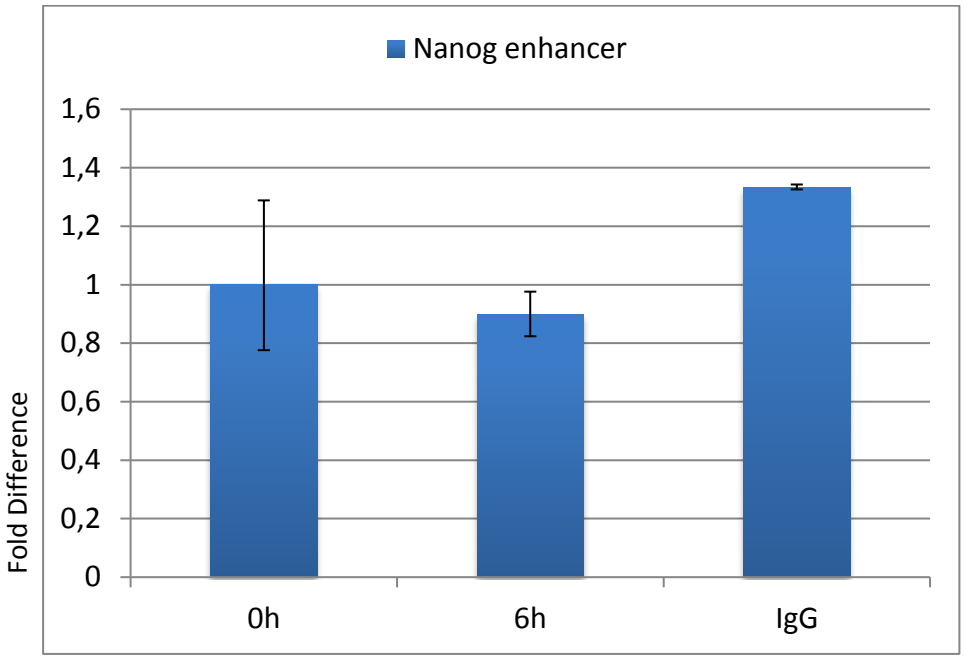

Figure 3.7 Level of H3K27ac on the Nanog enhancer after XOE treatment

Sheared chromatin from 2 x 10^6 cells was immunoprecipitated with 5 µg of H3K27ac antibody and the levels of specific DNA sequences (as indicated) were quantified by qPCR. The graph shows the changes in fold differences of histone H3K27ac level on the Nanog enhancer in control and 6 hours of XOE treatment. Immunoprecipitation of IgG is negative control. Biological repeat number= 3 and error bars indicate standard deviations in technical replicates.

3.3.2.2 H3K4me1 enrichment on the Nanog enhancer and promoter after AOE treatment

The mono-methylated form of H3K4 is enriched on poised and active enhancers. I therefore asked if this histone modification is also induced on Nanog regulatory sequences by AOE. After permeabilization and incubation over several time points in extract from the oocytes of axolotl or Xenopus, as indicated in the Figure 3.8 and 3.9, chromatin was subjected to ChIP in the absence (IgG) or presence of an antibody specific to H3K4me1 (Active Motif, catalog no. 39297). Immunoprecipitation of IgG was used as a negative control. Nanog enhancer and promoter sequences were amplified by qPCR as before, accompanied by negative control regions, the MyoD1 enhancer and promoter, and intron 1 of genomic Nanog region.

As Figure 3.8 shows, the results of qPCR suggest that the level H3K4me1 increased 6 fold on the Nanog enhancer in NIH3T3 cells over the first 3 hours of incubation in AOE, compared to untreated cells, and IgG pull-down, shows antibody specificity. Little change was observed over a further 3 hours of incubation. Interestingly, only low levels of H3K4me1 were observed on the promoter sequences of Nanog, about 2 fold. There was no increase detected for the mark on the negative control regions, MyoD1 enhancer or promoter again demonstrating the specificity of the chromatin remodelling activities within AOE.

The level of H3K4me1 enrichment on Nanog enhancer and promoter after XOE treatment

Using the same approach as above, the capacity of XOE was tested for adding this activating histone mark. As shown in Figure 3.9, the fold difference calculation using the mean Ct values showed that there was no increase in the level of H3K4me1 on the Nanog enhancer after treatment with Xenopus oocyte extract for 6 hours, compared to the untreated cells. This experiment indicates that Xenopus oocyte extract cannot add the H3K4me1 mark to Nanog enhancer sequences.

A.

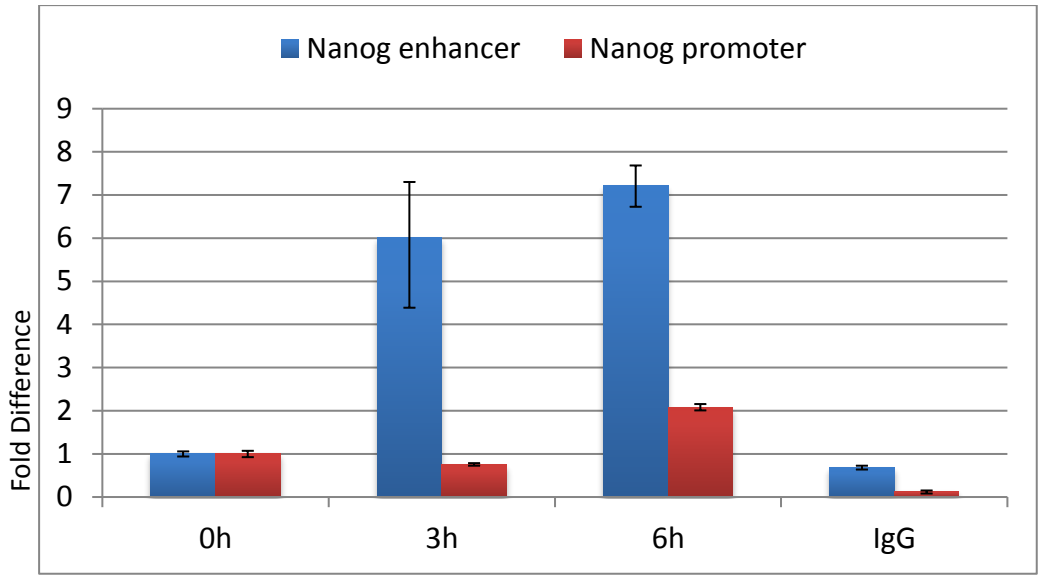

B.

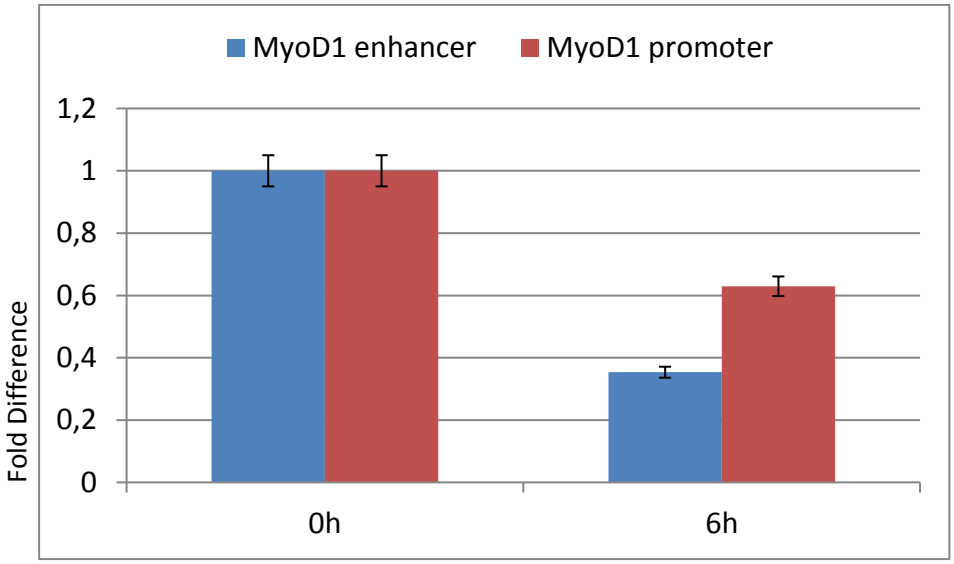

Figure 3.8 Level of H3K4me1 on the regulatory regions of the Nanog gene in NIH3T3 cells after AOE treatment

Sheared chromatin from 2 x 10^6 cells was immunoprecipitated with 5 µg of H3K4me1 antibody and the levels of specific DNA sequences (as indicated) were quantified by qPCR. A. The graph shows the changes in fold differences of H3K4me1 levels on the Nanog enhancer (blue) and promoter (red) in NIH3T3 cells treated with AOE. Immunoprecipitation of IgG is negative control. B. The graph shows the changes in fold differences of H3K4me1 levels on the MyoD1 enhancer (blue) and the MyoD1 promoter (red) in control (0h) and 6 hours of AOE treatment. Biological repeat number= 3 and error bars indicate standard deviations in technical replicates.

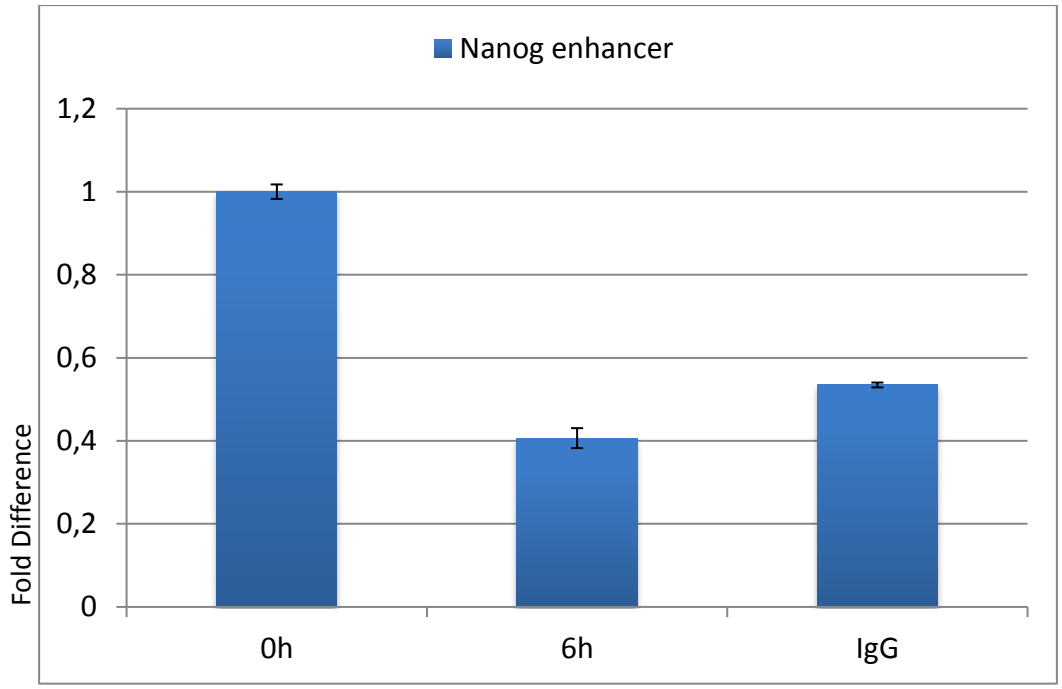

Figure 3.9 Level of H3K4me1 on the Nanog enhancer after XOE treatment

Sheared chromatin from 2 x 10^6 cells was immunoprecipitated with 5 µg of H3K4me1 antibody and the levels of specific DNA sequences (as indicated) were quantified by qPCR. The graph shows the changes in fold differences of H3K4me1 level on the Nanog enhancer in control (0h) and 6 hours of XOE treatment. Immunoprecipitation IgG is negative control. Biological repeat number= 3 and error bars indicate standard deviations in technical replicates.

3.3.3 Conclusions

Using ChIP, I demonstrated that the enhancer-specific markers H3K4me1 and H3K27ac are enriched on the Nanog enhancer, but not on the Nanog promoter, upon axolotl oocyte extract treatment. Creyghton et al. demonstrated that active enhancers are distinguishable from inactive or poised enhancers by the presence of H3K27ac on enhancers which already contain H3K4me1; and during reprogramming enhancers are remodelled by these activating histone marks (Creyghton et al., 2010). The results that I obtained provide evidence that axolotl oocyte has the capacity for remodelling the mouse Nanog enhancer by adding the activating histone marks, H3K27ac and H3K4me1 to the enhancer. This validates previous results which show its ability to change histone modification profiles of Nanog, a pluripotency gene, while it does not have an effect on regulatory regions of differentiation marker gene such as MyoD1. This suggests that the remodelling is specific to pluripotency genes.

Xenopus oocyte extract treatment does not have the ability to add either H3K27ac or H3K4me1 to the Nanog enhancer. Previously our lab showed that while axolotl oocyte extract was able to add activating marks, H3K4me3 and H3K9ac, to the Nanog and Oct4 promoters of somatic cells, Xenopus oocyte extract cannot. The reprogramming mechanism of axolotl is obviously different than that of the Xenopus. The ability to add activating histone modifications to the regulatory regions of pluripotency genes enhances the reprogramming capacity of these cells by preparing the somatic chromatin environment to reactivate pluripotency genes.

3.4 General Conclusions

In this chapter, I demonstrated that axolotl oocytes contain activities that rapidly remodel mouse somatic chromatin. To investigate remodelling activity, I focused on 5hmC and histone modifications H3K27ac and H3K4me1, on regulatory regions of the mouse Nanog gene. Previous studies from our lab showing AOE can demethylate the mouse Nanog promoter more efficiently than XOE, and can add activating histone marks, while XOE cannot; I used XOE as a negative control in my experiments. These results revealed that AOE employs a different reprogramming mechanism than XOE. For instance, the factors remodelling chromatin in AOE such as DNA hydroxylases, i.e. the Tet family, catalyse hydroxymethylation of the mouse Nanog enhancer and promoter. It was shown previously that Tet1 and Tet2 interact with Nanog protein to be recruited on target sites (Costa et al., 2013). AOE contains a Nanog ortholog, suggesting that the same demethylation mechanism is used in axolotl and mouse. After demonstrating that AOE can remodel the mouse Nanog gene, in the next chapter, I focused on the factors axNanog and H2A.Z their participation in the remodelling of the chromatin associated with the Nanog gene.

CHAPTER 4

REGULATION OF THE MOUSE NANOG GENE BY FACTORS INCLUDED IN AXOLOTL OOCYTE EXTRACTS

4.1 INTRODUCTION

Factors present in AOE can direct the sequence-specific remodelling of chromatin and the reactivation of mouse Nanog expression in mammalian somatic nuclei. In this chapter, I focus on the regulation of the mouse Nanog enhancer by the pluripotency factor axNanog, and H2A.Z, a histone variant.

4.1.1 Regulation of the mouse Nanog gene by axolotl ortholog of Nanog, axNanog

Nanog gene expression is necessary for the acquisition of pluripotency during the reprogramming of differentiated cells (Chambers et al., 2003, Mitsui et al., 2003). Providing the homeodomain protein Nanog to somatic chromatin with other pluripotency factors increases the reprogramming efficiency, since the transcription factor Nanog targets the regulatory regions of Nanog gene and activates endogenous expression (Silva et al., 2009, Theunissen et al., 2011b).

Incubating differentiated cells in factors from amphibian oocytes is an effective reprogramming method, as demonstrated with oocytes from Xenopus (Gurdon,

1986, Gurdon and Wilmut, 2011) and axolotl (Alberio et al., 2005, Bian et al., 2009). It was previously shown in our lab that mouse fibroblasts incubated in Xenopus and axolotl oocytes are able to re-express the endogenous Oct4 gene (Bian et al., 2009). However, only the axolotl oocyte was capable of initiating endogenous Nanog expression (Bian et al., 2009).

Axolotl oocytes contain pluripotency factors that are conserved in mammals, such as axNanog and axOct4 (Bachvarova et al., 2004, Dixon et al., 2010). Nanog, however, is not conserved in frogs. Thus, isolation of a Nanog ortholog from axolotl demonstrated a major difference in the early regulation of development between these two amphibians. AxNanog and its mouse ortholog have similar capacities to activate pluripotency in differentiated cells. Although axNanog does not contain a tryptophan repeat (WR) domain, and thus cannot form homodimers, it inhibits differentiation in mouse embryonic stem cells (Dixon et al., 2010).

The homeodomain of Nanog targets binding sites on pluripotency genes in the mammalian genome, such as Nanog and Oct4 (Chen et al., 2008). AxNanog, in monomer form, recognises the same targets. By performing ChIP assays in mouse ES cells, it was shown that mouse Nanog homodimers, axNanog monomers and WR domain-deleted Nanog (also a monomer) can recognise Nanog and Oct4 promoters (Dixon et al., 2010).

AxNanog binds directly to the mouse Nanog promoter as demonstrated by both luciferase and ChIP assays (Dixon et al., 2010). Therefore, axNanog protein in AOE might participate in the initiation of the Nanog gene. To test this, I investigated

whether axNanog present in AOE could bind Nanog targets in mouse differentiated cells.

Enhancers located in distant non-coding regions of a locus can regulate gene activity (Chen et al., 2012). With the help of tissue-specific epigenetic alterations, enhancer activity varies from one cell type to another during development. Promoters mostly carry more uniform epigenetic modifications in different cell types (Chen et al., 2012, Heintzman et al., 2009, Visel et al., 2009). The mechanisms that initiate the epigenetic modifications on regulatory regions of pluripotent genes are not fully understood. However, 5-hydroxymethylation of promoter and enhancer DNA, and histone modifications H3K27ac and H3K4me1 on the enhancer of the mouse Nanog gene have very important roles in Nanog gene regulation and these modifications might be targeted to the Nanog locus by transcription factors in the axolotl oocyte extract.

Chen et al (2008) demonstrated that there are putative binding sites for Nanog identified by ChIP coupled with massively parallel short-tag-based sequencing (ChIP-seq). This was based on alignment of ChIP-seq reads after Nanog immunoprecipitation (Chen et al., 2008). The binding motif of Nanog protein, which was indicated in this study (Figure 4.1), is indicated below. I pointed to its putative binding sites on the Nanog enhancer and promoter regions (blue), which were amplified by the primers that I used here (Kidder et al., 2009).

A.

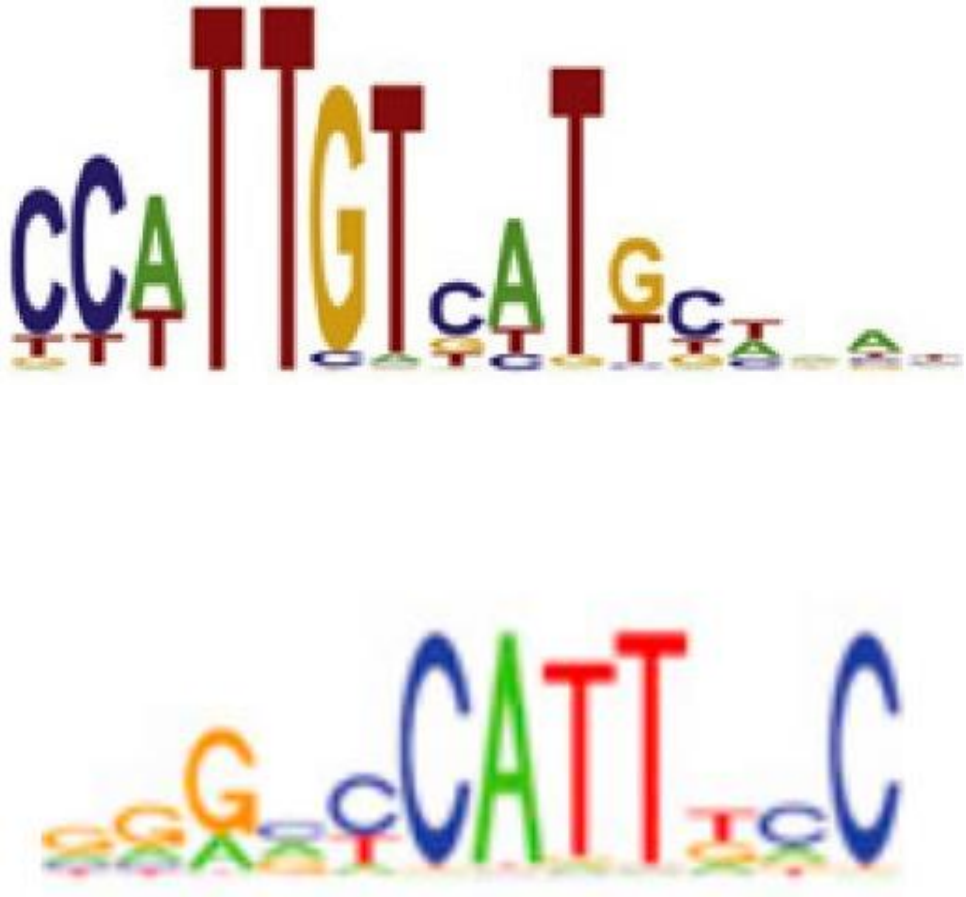

B.

Nanog promoter

GGAGAATAGGGGGTGGGTAGGGTAGGAGGCTTGAGGGGGGAGGAGCA
GGACCTACCCTTTAAATCTATCGCCTTGAGCCGTTGGCCTTCAGATAGG
CTGATTTGGTTGGTGTCTTGCTCTTTCTGTGGGAAGGCTG

Nanog enhancer

CTCGAATGTTGGGCTTAGGAATGGGGAGACAAGAGCCATCACAGAATG
CCTATTGTCCTTCAATATGTTAGCGATGGGCCCCGTGCTTTAGATTTTAG
GCTTGTATTTTCTTTGTGTGTGTGTGTGTTTGTTTTGTTTCTGTTTCTTTA
GGCAGTCTGGAGATCAGGCTGGCTTTCAACTCCCTGTGATGCCCCTACC
TCTC

Figure 4.1 Nanog binding sites A. Nanog binding sites were detected using ChIP-seq data (first panel, Chen et al., 2008; second panel, Whyte et al., 2013). B. Putative binding regions are marked in the Nanog enhancer and promoter. Chen et al., 2008 binding sites are marked by blue; Whyte et al., 2013 binding sites are marked by underline.

4.1.2 Enrichment of histone variant H2A.Z deposition on the mouse Nanog gene

Nucleosomes including histone H2A are essentially similar to those including its variant H2A.Z (Suto et al., 2000); furthermore, H2A.Z has around 60% sequence similarity to H2A (Zlatanova and Thakar, 2008). However, their effect on chromatin structure is different. Nucleosomes enriched with H2A are more stable on chromatin, favouring a heterochromatin state. Nucleosomes enriched with H2A.Z result in chromatin being more relaxed, favouring euchromatin (open chromatin form). Residues on the surface of H2A.Z generate an extended acidic patch on nucleosomes. This feature of H2A.Z promotes chromatin remodelling. Replacement of histone H2A with the H2A.Z variant is a result of an ATP-dependent reaction performed by chromatin remodelling enzymes in a replication-independent manner (Hardy et al., 2009). H2A.Z deposition is mostly a genome-wide alteration for transcriptional activity. Therefore, it is thought to be required for normal gene expression in ESCs.

The H2A.Z amino acid sequence provides it with unique properties compared to H2A. There are three residues (Gln substitution with Gly92, Asp97 and Ser98) located in the C-terminus of H2A.Z that result in a unique external surface of the nucleosome; the area generated by H2A.Z deposition is highly acidic. This acidic patch results in loosening of chromatin allowing specific transcription factors to bind (Subramanian et al., 2013). Thereby, enrichment of H2A.Z exchange accelerates the access of transcription factors to chromatin (Hu et al., 2013).

Even though H2A.Z is deposited in nucleosomes throughout the genome (Sarcinella et al., 2007), H2A.Z nucleosomes are mostly located around active genes and their upstream regulatory regions (Ranjan et al., 2013). It was also shown that H2A.Z is deposited more broadly at the active or poised promoters, which suggests its deposition is related to transcription factor binding (Gevry et al., 2007, Gallant-Behm et al., 2012). It is enriched at the regions related to transcriptional activity which carry activating epigenetic marks. These epigenetic events around H2A.Z-enriched areas show that H2A.Z is coupled to up-regulated transcriptional activity (Ranjan et al., 2013). For instance, methylation of DNA and deposition of H2A.Z are antagonist factors in plant and animal genomes (Conerly et al., 2010, Zemach et al., 2010). Zemach et al. (2010) showed that during lymphomagenesis, H2A.Z was depleted around transcription start sites, in which DNA methylation was enriched. Linking these two alterations, it is clear that H2A.Z deposition might have an indirect role in facilitating DNA demethylation by loosening the chromatin and generating a more suitable environment for enzymes

to bind. Therefore, H2A.Z can fulfil the role of a pioneer factor (Soufi et al., 2012) that facilitates axNanog activity during reprogramming with oocyte molecules.

On the other hand, it has been reported that H2A.Z can incorporate into chromatin not only in active loci but also at loci where transcription is repressed. It was shown that in ESCs deposition of H2A.Z is also associated with Polycomb-repressive complex 2 (PRC2) at the promoters of transcriptionally repressed gene (Creyghton et al., 2008), and at the repressed gene enhancers enriched with repressive histone marks, such as H3K27me3 (Hu et al., 2013). The disparity seen here is likely a result of specific H2A.Z modifications that have yet to be elucidated. Obviously, the function of H2A.Z in chromatin remodelling may vary according to which type of histone modifications (on H2A.Z and other histones) are enriched at the region. For instance, methylation of lysine residues on H2A.Z lead to transcription silencing (Binda et al., 2013), while acetylation-enriched H2A.Z ($H2AZ^{ac}$) is located at transcriptionally active promoters (Valdes-Mora et al., 2012, Dalvai et al., 2013). Additionally, H2A.Z function also changes according to its association with other modified histones. For example, H2A.Z deposition accompanied to the modifications on histone H3 Lysine 4 monomethylation (H3K4me1) and Lysine 27 trimethylation (H3K27me3) were used to identify active or inactive enhancer regions, respectively, in hematopoietic stem cells and somatic cells. These enhancers are functionally active and/or poised in hematopoietic stem cells when H3K4me1 is enriched, while they are functionally inactive in differentiated cells when H3K27me3 is enriched (Binda, 2013). That is,

modifications on H2A.Z, other histones, or DNA itself change the profile of H2A.Z function to inform the transcriptional activity of specific loci.

It has recently been shown that H2A.Z has a physical interaction with Nanog in ES cells by ChIP assay and overexpressed H2A.Z is characteristic of the pluripotent state of ES cells; on the other hand, knock down of H2A.Z expression in mouse ES cells promotes differentiation (Wang et al., 2015). Also, it was reported that during OSKM reprogramming of somatic cells, expression of H2A.Z was increased (Wang et al., 2015). Taken together, H2A.Z plays an appreciable role in the reprogramming of eukaryotic chromatin and the maintenance of pluripotency.

Histone variant H2A.Z is expressed in axolotl oocyte (as well as in mouse embryonic stem cells), but it is not expressed in Xenopus oocyte (Matt Loose, unpublished data, personal communication). Given that H2A.Z has dual roles in gene regulation depending on activating and repressing epigenetic modifications, we wanted to interrogate the incorporation of this histone variant during chromatin remodelling at the Nanog locus in response to treatment with AOE. To address this question, I tested the enrichment of H2A.Z on mouse Nanog regulatory regions using ChIP.

4.2 Results

4.2.1 AxNanog binds on the mouse Nanog enhancer and promoter in NIH3T3 and MEF cells.

To test if axNanog binds to the enhancer of the Nanog gene, NIH3T3 cells were permeabilized with digitonin and then incubated in the extract for 3 or 6 hours. After cell lysis and shearing chromatin, axNanog-bound DNA was immunoprecipitated using an antibody raised against the axolotl ortholog of Nanog protein (For Nanog antibody specificity, see Appendix, Figure S2). qPCR was used for the enhancer and promoter regions of Nanog gene. Sequences encoding the enhancer and promoter of MyoD1, as well as the first Nanog intron, were included as negative controls.

Amplification of the Nanog enhancer linearly increased about 3 fold in 3 hours and about 4.5 fold in 6 hours of incubation in oocyte extract. Nanog promoter amplification also showed an increase; about 2 fold and 4 fold in 3 and 6 hours of extract incubation, respectively. These results indicated that axNanog binds to regulatory regions of the mouse Nanog gene and implied that binding to the enhancer was more efficient than that to the promoter in NIH3T3 cells (Figure 4.2). The same DNA isolated by ChIP assay using axNanog antibody was used in qPCR with MyoD1 enhancer and promoter regions. The mean C_t values for MyoD1 for both 0 and 6 hours were lower than that of Nanog regulatory regions, and there is no significant change in time, indicating that neither the MyoD1 enhancer

nor promoter is a target for axNanog. The Nanog intron 1 was also used as a negative control.

I repeated these experiments using MEFs, which also showed a response to treatment with AOE. The increase of axNanog binding to the Nanog promoter in 6 hours, in this case, was about 12 fold. In both cell types, the IgG pull down negative control was lower than axNanog pull-down in untreated cells (Figure 4.3).

It was previously shown that Xenopus genome does not encode an ortholog for Nanog (Hellsten et al., 2010). Consistent with this, binding of the axNanog antibody to mouse chromatin was not observed after treatment with the oocyte extract from Xenopus (Figure 4.4).

A.

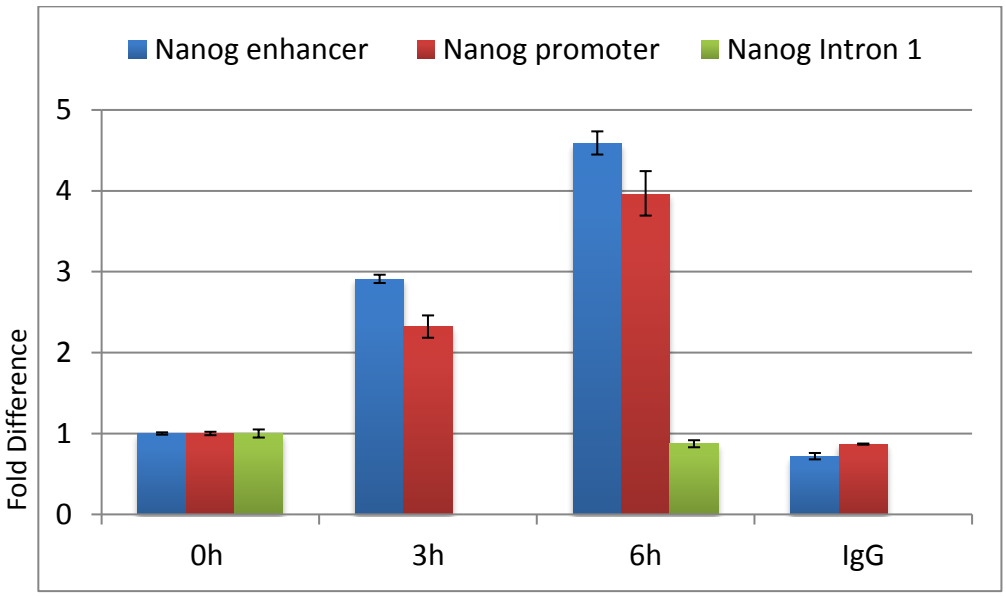

B.

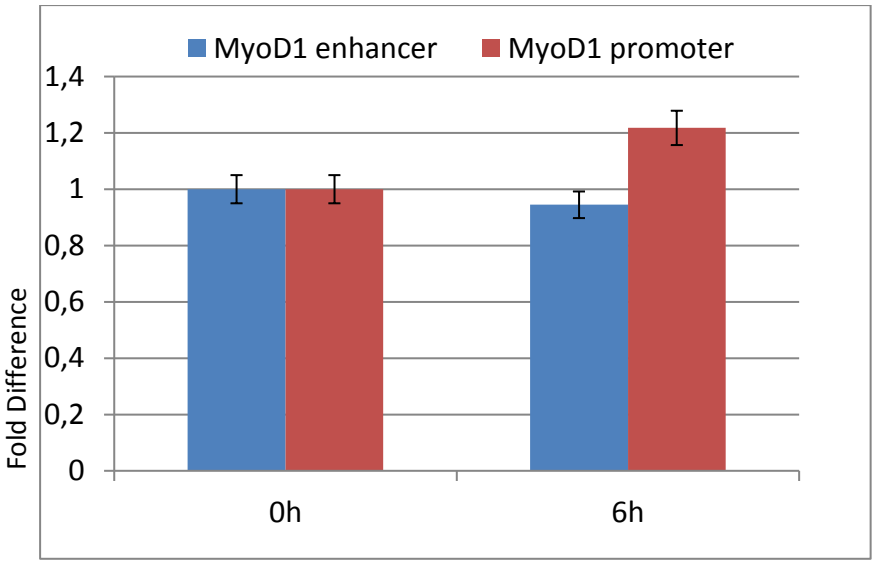

Figure 4.2 AxNanog binding on the regulatory regions of the Nanog gene in NIH3T3 cells after AOE treatment

Sheared chromatin from 2 x 10^6 cells was immunoprecipitated with 5 µg AxNanog antibody and the levels of specific DNA sequences (as indicated) were quantified by qPCR. A. The graph shows the changes in fold differences of AxNanog binding levels on the Nanog enhancer (blue), the Nanog promoter (red) and Nanog intron 1 (green) in 0, 3, and 6 hours of AOE treatment. Immunoprecipitation with IgG is negative control. B. The graph shows the changes in fold differences of AxNanog binding levels on the MyoD1 enhancer (blue), promoter (red) and in control (0h) and 6 hours of AOE treatment. Biological repeat number= 9 and error bars indicate standard deviations in technical replicates.

A.

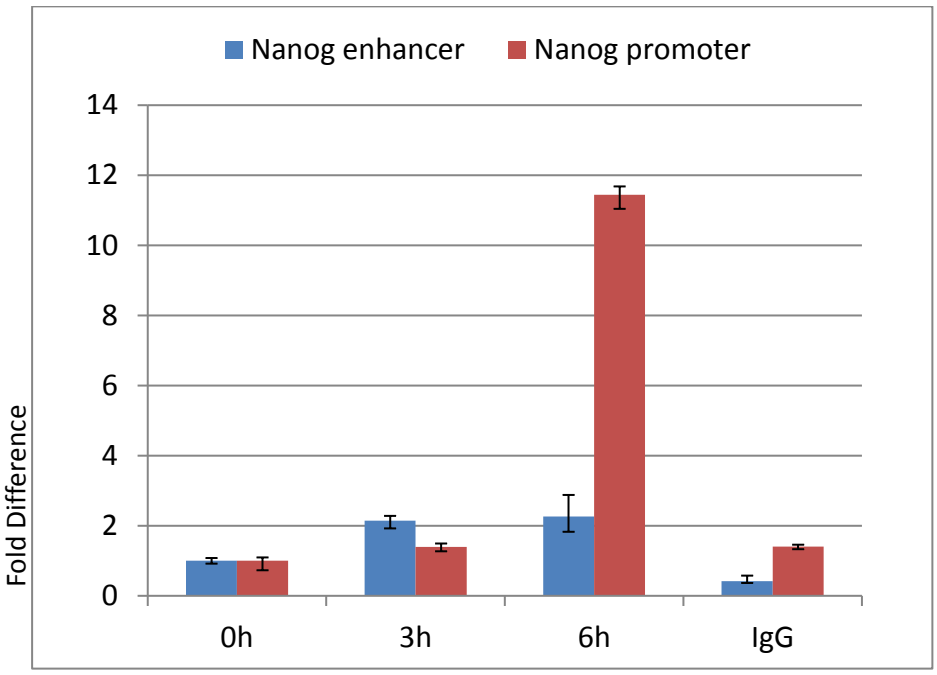

B.

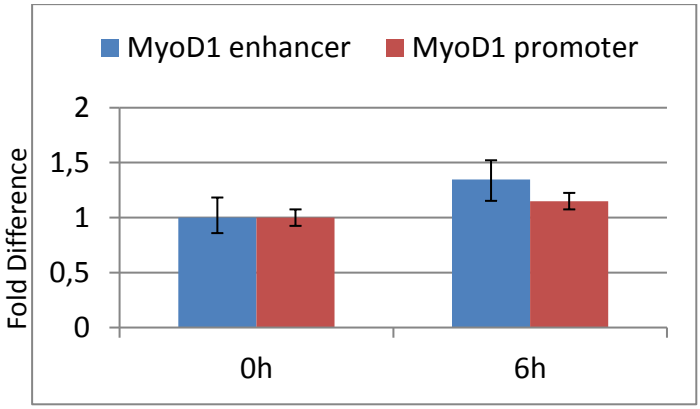

Figure 4.3 AxNanog binding on the regulatory regions of the Nanog gene in MEFs after AOE treatment

Sheared chromatin from 2 x 10^6 cells was immunoprecipitated with 5µg AxNanog antibody and the levels of specific DNA sequences (as indicated) were quantified by qPCR. A. The graph shows the changes in fold differences of AxNanog binding levels on the Nanog enhancer (blue) and promoter (red) in control (0h), 3 and 6 hours of AOE treatment. Immunoprecipitation with IgG is a negative control. B. The graph shows the changes in fold differences of AxNanog binding levels on the MyoD1 enhancer (blue) in control (0h) and 6 hours of AOE treatment. Biological repeat number= 3 and error bars indicate standard deviations in technical replicates.

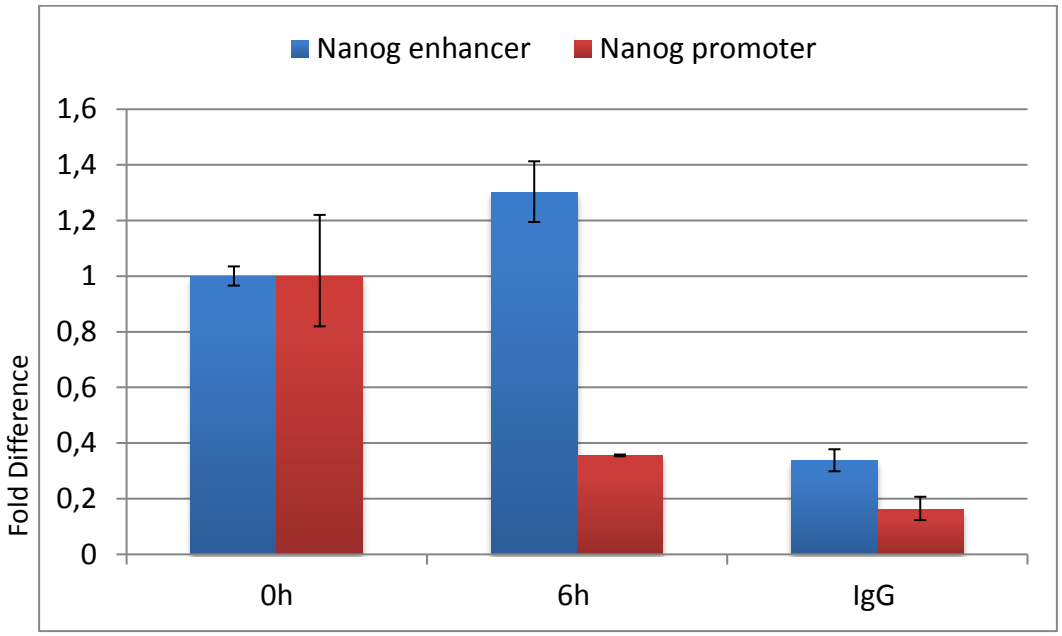

Figure 4.4 AxNanog binding on the regulatory regions of the Nanog gene after XOE treatment

Sheared chromatin from 2 x 10^6 cells was immunoprecipitated with 5 µg AxNanog antibody and the levels of specific DNA sequences (as indicated) were quantified by qPCR. A. The graph shows the changes in fold differences of AxNanog binding levels on the Nanog enhancer (blue) and promoter (red) in control and 6 hours of AOE treatment. Immunoprecipitation with IgG is negative control. Biological repeat number= 3 and error bars indicate standard deviations in technical replicates.

4.2.2 The level of axNanog binding on the Nanog enhancer of reprogrammed NIH3T3 cells is comparable to that seen in ES cells.

I then compared the Nanog levels in extract treated NIH3T3 cells with those of ES cells, which naturally express Nanog (Navarro et al., 2012). In this particular experiment, the percentage of input method was used to calculate the increase of Nanog binding levels and was compared with each other, since the level of binding is important in the control groups (untreated cells). The analysis resulted in qPCR with similar low Ct values, ranging from Ct 21 to 23, for untreated and treated cells, indicating a high level of Nanog-bound Nanog enhancer region in mouse ES cells. In untreated NIH3T3 cells, the Ct values were significantly higher (ranging from 27 to 28.5) than those of AOE-treated NIH3T3 cells (ranging from 23 to 24). Therefore, as indicated in the graph, the level of Nanog-bound Nanog enhancer in the differentiated mouse cells after AOE treatment reached a level similar to that of ES cells (Figure 4.5). However, it should be noted that this experiment could be validated with extra experiments showing whether the antibody can distinguish mouse and axolotl Nanog. For instance, a western blotting can be carried out to test if the antibody can detect the endogenous Nanog in mouse ES cells. Nanog depleted ES cells could also be included in this experiment.

When NIH3T3 cells were treated with Xenopus oocyte extract for 6 hours, on the other hand, Nanog enhancer amplification was similar to that of untreated cells. Together, these results suggest that the chromatin of somatic cells can be remodelled to a pluripotent configuration by AOE.

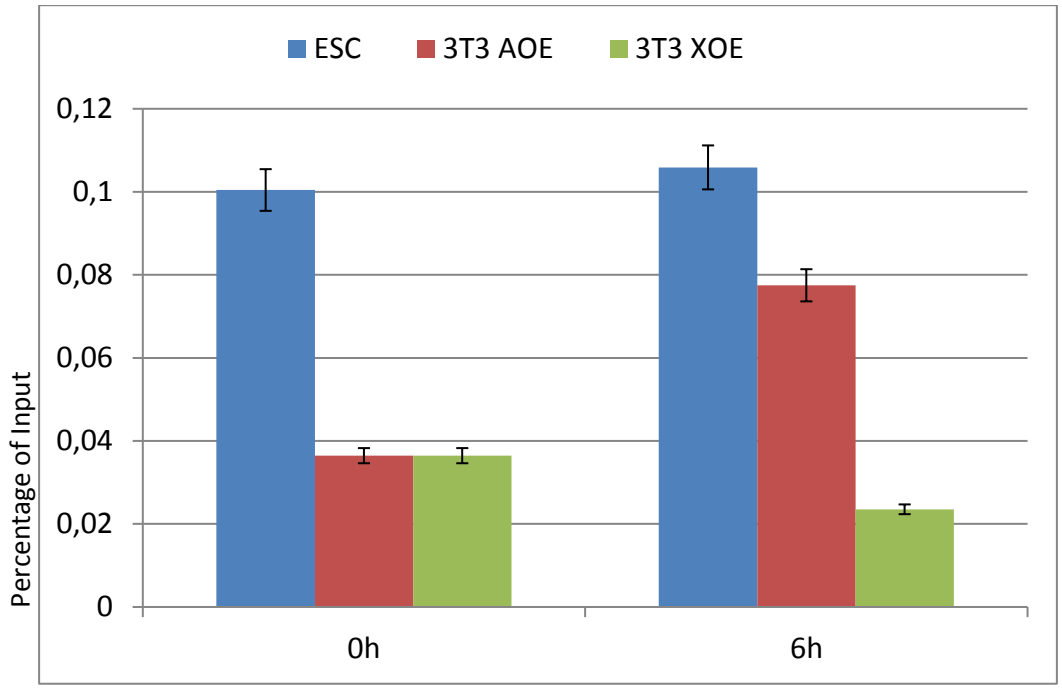

Figure 4.5 AxNanog binding on the Nanog enhancer in mouse ES and NIH3T3 cells after AOE and XOE treatment

Sheared chromatin from 2 x 10^6 cells was immunoprecipitated with 5 µg AxNanog antibody and quantified by qPCR. The graph shows the changes on percentage of inputs of Nanog binding levels on the Nanog enhancers in mouse ES cells (blue), NIH3T3 cells treated with AOE (red) and NIH3T3 cells treated with XOE (green). Biological repeat number= 3 and error bars indicate standard deviations in technical replicates.

4.2.3 Statistical analyses of axNanog binding on the Nanog enhancer and promoter after axolotl oocyte extract treatment

Changes in axNanog binding to the Nanog enhancer: For the first part of the statistical analyses, we checked whether there are statistically significant differences in axNanog binding to the Nanog enhancer region between 0, 3 and 6 hour time points of axolotl oocyte extract treatment. Measurements were made at the α=0.05 level of significance. I decided to use the difference values of DNA measurements before and after treatment for each time point. Since we are comparing three related samples and these samples include only 31 observations in total, we used the Friedman Test (Friedman, 1939, Friedman, 1937) which is the nonparametric alternative of parametric repeated measures ANOVA. The hypothesis, related SPSS output and boxplots are below.

Hypothesis:

$$H_0: M_1 = M_2 = M_3\ (The\ median\ test\ scores\ are\ equal)$$

$$H_a: Not\ all\ of\ the\ medians\ are\ equal$$

Test Statistics:

Ranks

	Mean Rank
AOENeNanog0Hour	2.33
AOENeNanog3Hour	2.44
AOENeNanog6Hour	1.22

Test Statistics

N	9
Chi-Square	8.222
Df	2
Asymp. Sig.	.016

a Friedman Test

Since p-value = 0.016 < 0.05 = α , we reject the null hypothesis. We have concluded that there are statistically significant differences among three time points (0, 3 and 6 hours) for amplification of the Nanog enhancer in the cells treated in AOE. The boxplot below (Figure 4.6) shows the distribution of these time points; it was obvious to see the decrease at 6 hours.

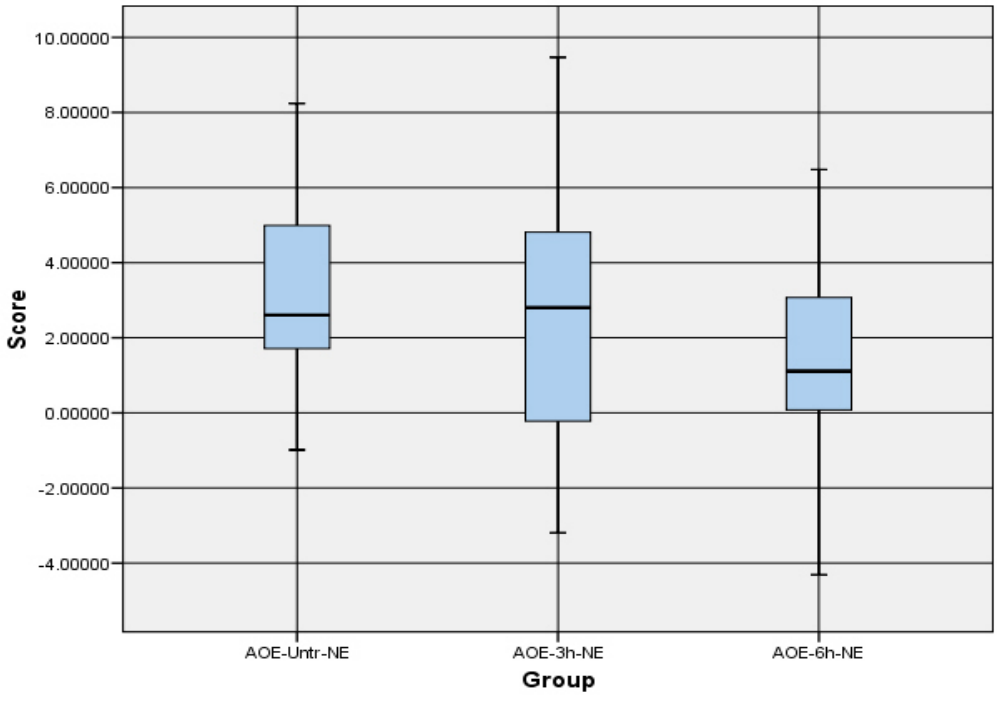

Figure 4.6 Box Plot for the Nanog enhancer

Changes in axNanog binding to the Nanog promoter: For the second part of the test I checked whether there are statistically significant differences between Nanog promoter amplification measurements after 0, 3 and 6 hours of AOE treatment at the α=0.05 level of significance. I used difference values of DNA measurements before and after treatment for each time points. Since we have 3 related samples and these include only 15 observations in total, I again preferred to use the Friedman Test (Friedman, 1939, Friedman, 1937). The hypothesis, related SPSS output and boxplots are below.

Hypothesis:

$$H_0: M_1 = M_2 = M_3 \ (The\ median\ test\ scores\ are\ equal)$$

$$H_a: Not\ all\ of\ the\ medians\ are\ equal$$

Test Statistics:

Ranks

	Mean Rank
AOENpNanog0Hour	3.00
AOENpNanog3Hour	1.33
AOENpNanog6Hour	1.67

Test Statistics

N	3
Chi-Square	4.667
Df	2
Asymp. Sig.	.097

a Friedman Test

Since p-value = 0.097 > 0.05 = α_2 , we cannot reject the null hypothesis at $\alpha_2 = 0.05$ level of significances. There is not enough evidence to conclude that there is a statistically significant difference among three time points for Nanog promoter binding in AOE. We can associate this with the various results and limited numbers of measurements. The boxplot below (Figure 4.7) shows the distribution of three time points; the decrease at 3 and 6 hours is obvious. It is important to note that we have just 3 measurements for 3 hour that is why the median value is at the very low part of the graph.

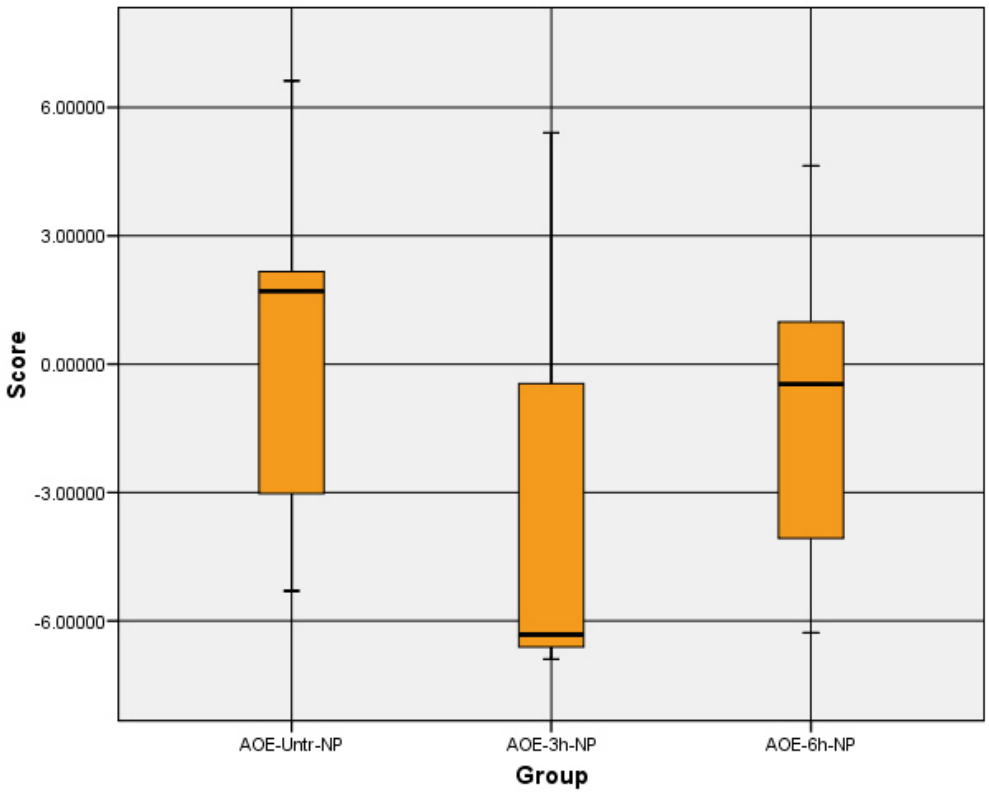

Figure 4.7 Box Plot for the Nanog promoter

4.2.4 Deposition of histone variant H2A.Z on the Nanog enhancer and promoter after axolotl oocyte extract treatment

H2A.Z deposition is an important step in facilitating transcription initiation (Bargaje et al., 2012). To test if H2A.Z exchange accompanies somatic chromatin remodelling by AOE, ChIP was used as described above using 4 µg of a commercial H2A.Z antibody (Active motif, 39113). IgG antibody was used as a negative control. Following ChIP, amplification of the Nanog enhancer and promoter sequences were measured by qPCR.

As Figure 4.8 shows, H2A.Z binding increased 7-fold on both the Nanog enhancer and promoter regions, compared to untreated cells, after 3 hours of incubation. After 6 hours, it remained at a similar level (6.5-fold) on the enhancer and decreased slightly on the promoter region. This result suggests that H2A.Z binds to these regions rapidly and it might be among the first factors to bind on chromatin during the oocyte reprogramming process. The mean Ct value for IgG immunoprecipitation was similar to that of immunoprecipitation of H2A.Z in untreated cells, showing that the pull down was specific for the H2A.Z antibody. The enhancer and promoter sequences of the MyoD1 gene were also analysed by qPCR and showed a slight increase, between 1.5 and 2 fold, in binding by H2A.Z. This slight increase is not surprising because H2A.Z binds uniformly throughout the genome, even on cell-type specific differentiation genes. However, the difference between the levels of its binding on Nanog and MyoD1 shows that its activity might be promoted by pluripotency factors in the oocyte. When binding to Nanog intron 1 was analysed as a negative control, it showed no change in H2A.Z

binding after AOE treatment (Figure 4.8). It should be noted that this antibody can detect the mouse H2A.Z which already exists at low level in the mouse fibroblasts. Thus, the increase of H2A.Z binding could be the result of the reallocation of endogenous (mouse derived) or axolotl H2A.Z onto the nucleosomes around Nanog regulatory regions. To test whether it is the murine or axolotl H2A.Z that is incorporated in the chromatin, H2A.Z depleted NIH3T3 cells could be treated with AOE and immunoprecipitated with the H2A.Z antibody. Another solution could be to block the H2A.Z function in the AOE and use this extract to treat differentiated cells.

Figure 4.9 shows that there was no change in the level of H2A.Z deposition on the Nanog enhancer after XOE treatment as expected, since H2A.Z was not detected in XOE by transcriptome analysis (unpublished data).

Comparison of axNanog and H2A.Z binding levels on the Nanog enhancer after AOE treatment

Since both axNanog and H2A.Z showed efficient binding to the Nanog enhancer after 3 hours of axolotl oocyte extract treatment, a 1 hour time-point was added to the experiment. This 1 hour time-point would be useful to determine which factor binds first to the Nanog enhancer in the chromatin microenvironment.

As the graph in Figure 4.10 shows, axNanog binding was not detected on the Nanog enhancer of NIH3T3 cells exposed to AOE for only 1 hour. However, after 3 and 6 hours of treatment, axNanog binding was at around 2.75 fold increase

compared to untreated cells, similar to previous results. In contrast, even after 1 hour of AOE treatment, the histone variant H2A.Z was bound to the Nanog enhancer 2 fold more than in untreated cells. This level increased very little by 6 hours, suggesting that exchange of the H2A.Z variant was complete within an hour of exposure to extract.

A.

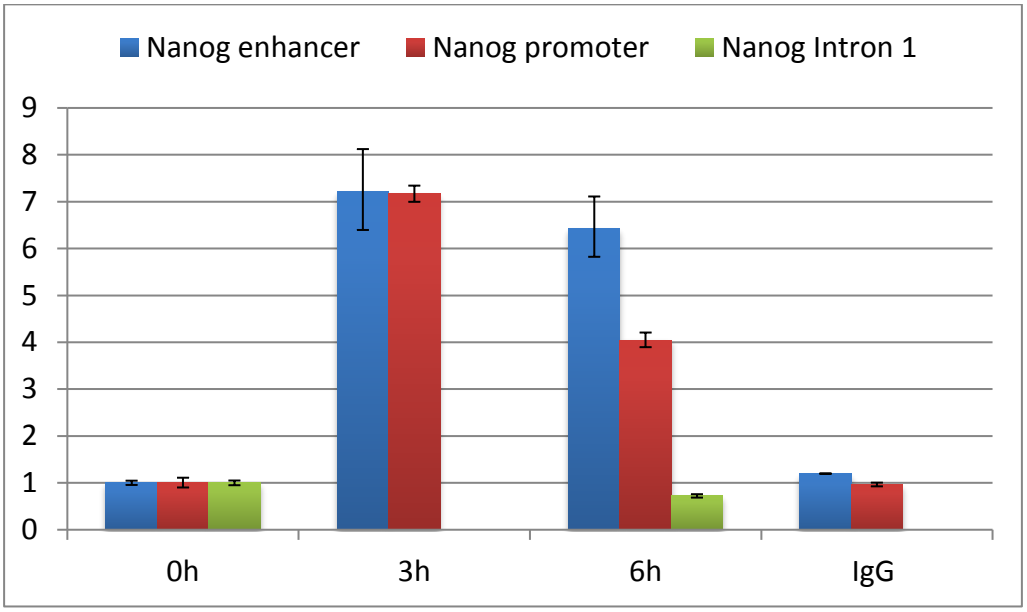

B.

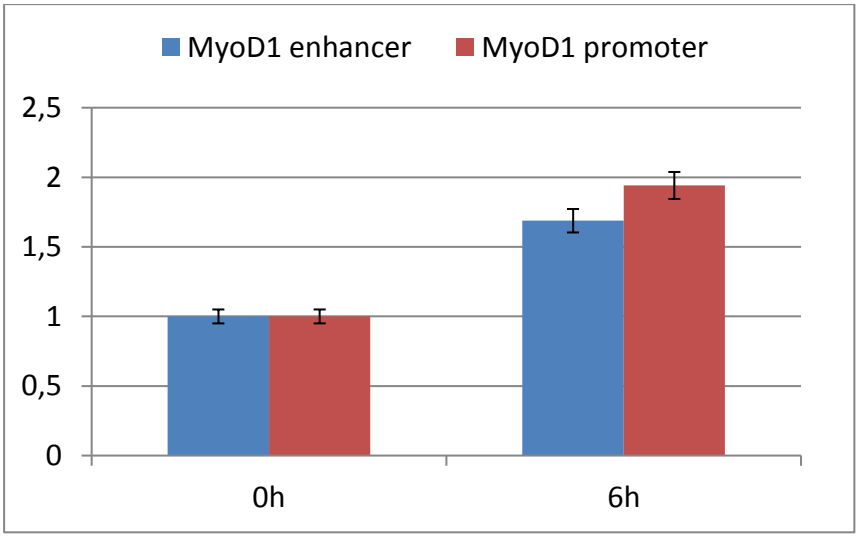

Figure 4.8 H2A.Z binding on the regulatory regions of the Nanog gene in NIH3T3 cells after AOE treatment

Sheared chromatin from 2 x 10^6 cells was immunoprecipitated with 5 µg AxNanog antibody and the levels of specific DNA sequences (as indicated) were quantified by qPCR. A. The graph shows the changes in fold differences of histone variant H2A.Z binding levels on the Nanog enhancer (blue), promoter (red) and the Nanog intron 1 (green) in NIH3T3 cells treated with AOE. Immunoprecipitation with IgG is negative control. B. The graph shows the changes in fold differences of H2A.Z binding levels on the MyoD1 enhancer (blue) and promoter (red) in control (0h) and 6 hours of AOE treatment. Biological repeat number= 5 and error bars indicate standard deviations in technical replicates.

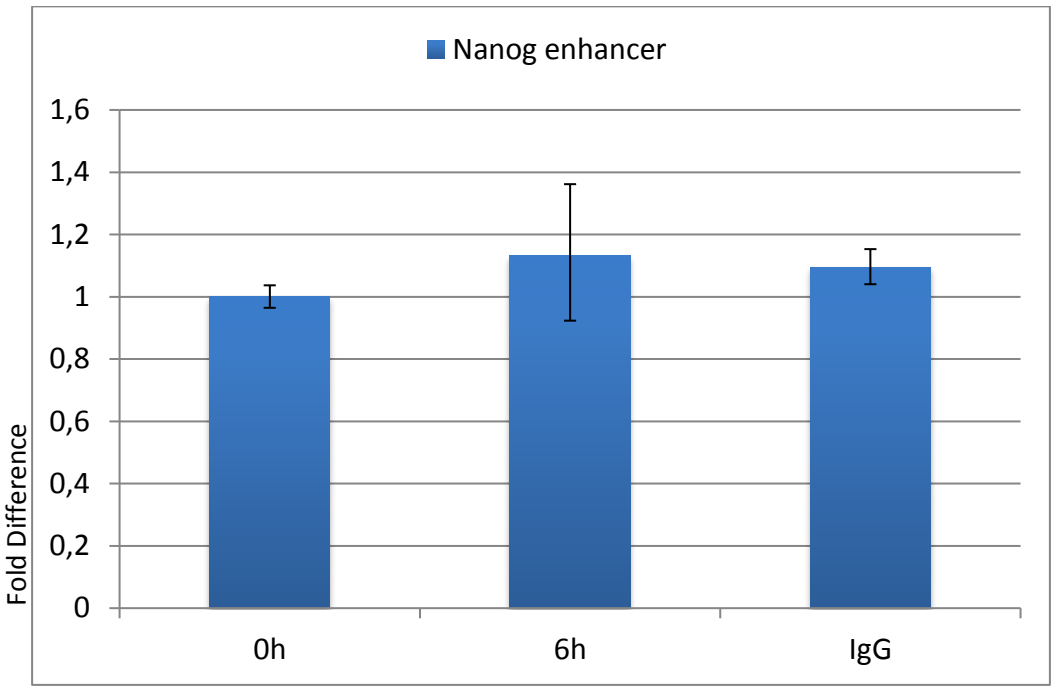

Figure 4.9 Level of H2A.Z on the Nanog enhancer after XOE treatment

Sheared chromatin from 2 x 10^6 cells was immunoprecipitated with 4 µg of H2A.Z antibody and the levels of specific DNA sequences (as indicated) were quantified by qPCR. The graph shows the changes in fold differences of H2A.Z binding levels on the Nanog enhancer (blue) in control (0h) and 6 hours of XOE treatment. Immunoprecipitation with IgG is negative control. Biological repeat number= 3 and error bars indicate standard deviations in technical replicates.

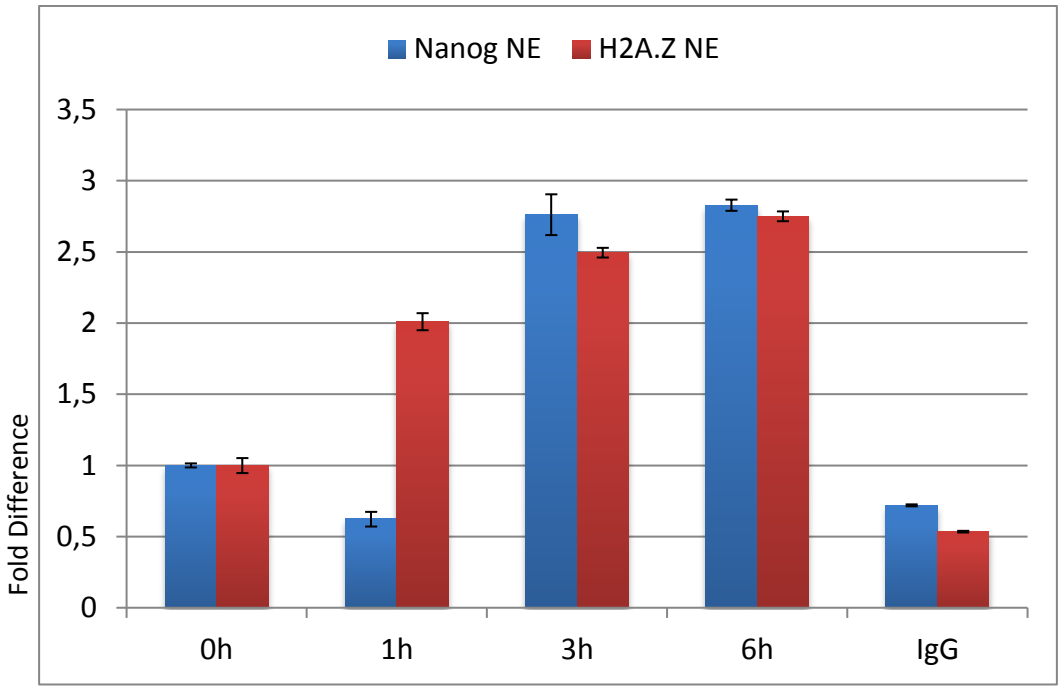

Figure 4.10 Comparison between Nanog and H2A.Z binding on the Nanog enhancer region in NIH3T3 cells after AOE treatment

Sheared chromatin from 2 x 10^6 cells was immunoprecipitated with 5 µg for each AxNanog and H2A.Z antibody and the levels of specific DNA sequences (as indicated) were quantified by qPCR. The graph shows the changes in fold differences of the Nanog (blue) and histone variant H2A.Z (red) binding levels on the Nanog enhancer in NIH3T3 cells treated with AOE. Immunoprecipitation IgG is negative control. Biological repeat number= 3 and error bars indicate standard deviations in technical replicates.

Western blotting for H2A.Z deposition on chromatin after AOE treatment

To ensure that H2A.Z from the axolotl oocytes was deposited on somatic chromatin, I performed Western blotting on cells before and after incubation in the extract. Embryonic stem cells were used as a positive control since it is known that H2A.Z is enriched in nucleosome depleted regions of pluripotent chromatin, especially near active regulatory elements (Ku et al., 2012). Untreated and AOE-treated NIH3T3 cells were compared for H2A.Z deposition on chromatin. To perform western blotting, histones were extracted from 2 x 10^5 cells before or after treatment with AOE for 6 hours. Detection of Histone H3 was used as loading control.

Figure 4.11 shows a Western blot probed with H2A.Z antibody showing high levels of H2A.Z on the chromatin derived from embryonic stem cells. The signal obtained in the AOE-treated NIH3T3 cells showed a robust H2A.Z accumulation on chromatin, while signal from untreated cells was undetectable or very low. As indicated previously, to understand if this accumulation is actually the H2A.Z from AOE or the endogenous mouse H2A.Z, the result could be further tested by using H2A.Z-depleted fibroblasts or H2A.Z-blocked AOE. However, this assay indicated that 6 hours of AOE treatment was sufficient for accumulation of the variant H2A.Z on somatic chromatin (Figure 4.11).

The data above shows that H2A.Z is incorporated into chromatin rapidly and before axNanog in somatic cells upon the treatment with axolotl oocyte extract. ChIP was then performed with Xenopus oocyte extract with the same approach and showed that H2A.Z immunoprecipitation from untreated (0 hour) cells and

cells incubated in Xenopus oocyte extract were similar to the levels of immunoprecipitation in IgG controls (Figure 4.8 and 4.9) . These data were supported by Western blotting that there was no increase in the deposition of histone H2A.Z on the Nanog enhancer (Figure 4.11), even after 6 hours of treatment with Xenopus oocyte extract, confirming the specificity of results with AOE.

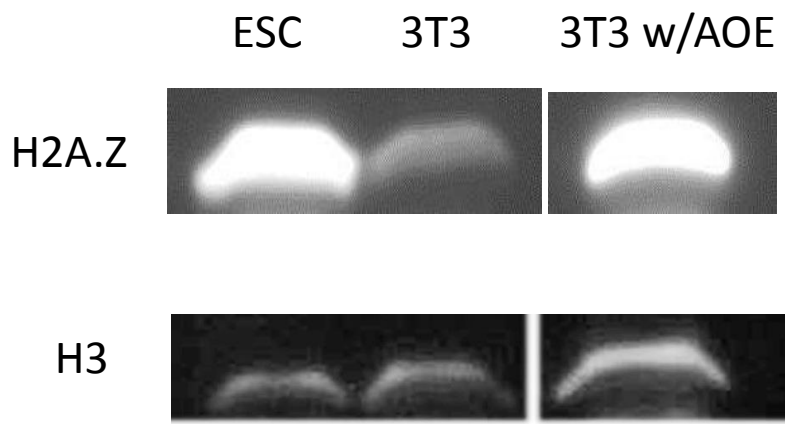

Figure 4.11 Western blotting shows H2A.Z is enriched on the NIH3T3 chromatin after AOE treatment.

Histones were extracted from 2 x 10^5 of mouse ES cells (positive control) or NIH3T3 cells before (negative control) and after AOE treatment and analysed by Western blotting using 1:2000 diluted antibodies specific for H2A.Z and H3 (loading control). Signals was visualized in the Bio-ChemiDoc System after 20 minutes exposure.

4.2.5 Blocking Nanog function in axolotl oocyte extract

I next investigated the sequence of events leading to chromatin remodelling. To address this question, Nanog function was blocked or reduced by pre-incubating axolotl oocyte extract with 20 µg of axNanog antibody for 45 minutes in +4 °C. Control extracts were pre-incubated with IgG. Permeabilized NIH3T3 cells were split to three groups; untreated cells, treated cells in axolotl oocyte extract and treated cells in Nanog-depleted axolotl oocyte extract. Chromatin from each group of cells was immunoprecipitated with previously optimised antibodies for H3K27ac, 5hmC and H2A.Z, and axNanog (as control for antibody specificity).

The graph in Figure 4.12 shows that axNanog binding increased about 4-fold in IgG antibody-treated AOE, while it was only 1.75 fold in axNanog-depleted AOE, indicating the antibody specificity. Acetylation of H3K27 increased 3.5 fold in 6 hours in IgG treated extracts, similar to previous results. However, H3K27 acetylation increased only about 2.2 fold, on the Nanog enhancer of cells treated with the depleted oocyte extract.

5-hydroxymethylation of cytosine increased in NIH3T3 chromatin by about 4.5-fold after 6 hours in axolotl oocyte extract; this increase was only about 2-fold when cells were treated with the axNanog depleted oocyte extract.

Histone variant H2A.Z binding was tested under the same conditions. In this case, the inhibition of Nanog activity did not affect the binding of H2A.Z, which showed an increase of around 2.5-3 fold on the Nanog enhancer in cells treated with extract containing either the function blocking axNanog antibody or IgG,

suggesting that Nanog activity is not required for the deposition of H2A.Z on Nanog regulatory regions (Figure 4.12).

This experiment confirmed that H2A.Z provided by the AOE is enriched on nucleosomes near the Nanog enhancer before axNanog binds. Moreover, it suggested that enrichment of both 5hmC and H3K27ac on the Nanog enhancer is dependent on axNanog activity. In light of these data I propose the following sequence of events leading to remodelling of the Nanog gene: (1) H2A.Z binds to the Nanog enhancer and loosens the chromatin within this region to allow axNanog binding; (2) then, binding of axNanog promotes enrichment of 5hmC and H3K27ac.

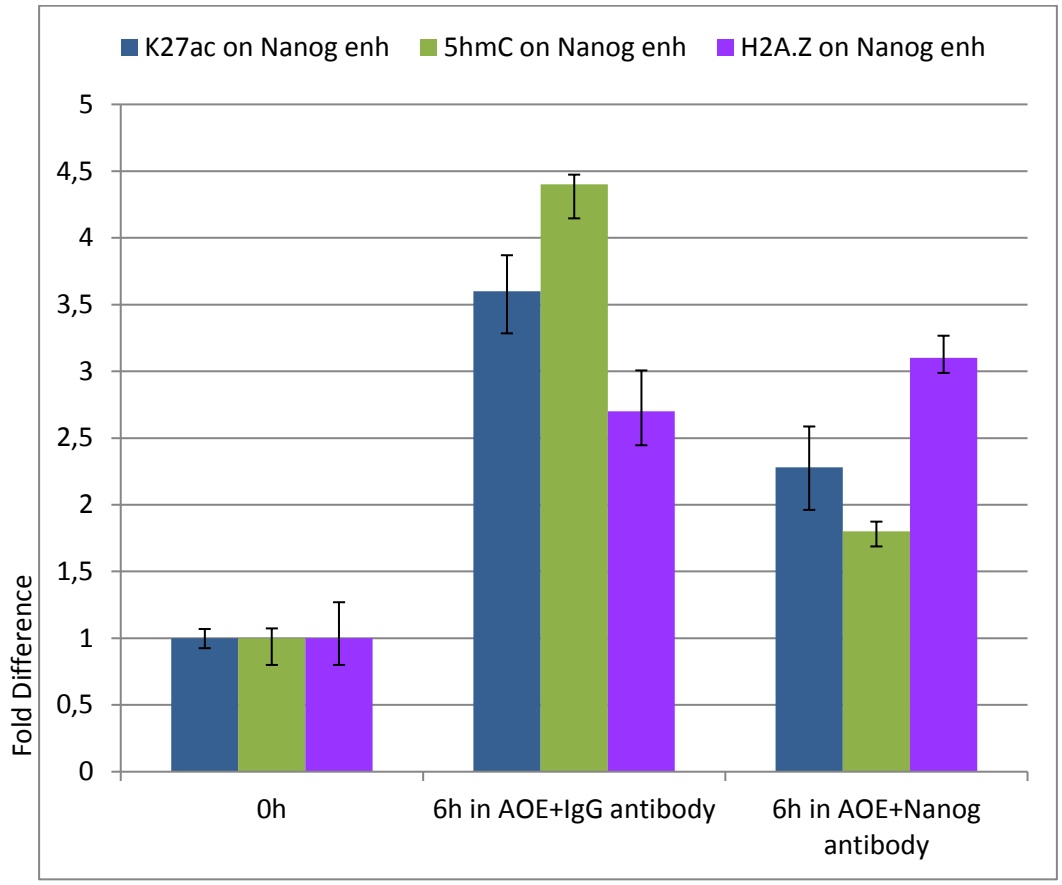

Figure 4.12 Nanog function-blocking in AOE

Sheared chromatin from 2 x 10^6 cells was immunoprecipitated with 5µg H3K27ac, 5hmC and H2A.Z antibodies to test Nanog function on these alterations. 3T3 cells were incubated for 6 hours with 200 µl AOE which was incubated with IgG or Nanog antibodies. Nanog was blocked in AOE by incubating AOE with 20 µg of Nanog antibody for 1 hour in +4 °C. The levels of immunoprecipitated DNA were tested on the Nanog enhancer sequence by qPCR. Biological repeat number= 3 and error bars indicate standard deviations in technical replicates.

4.3 Conclusions

Reprogramming of the Nanog gene in mammalian somatic cells

In this chapter, I have shown that the axolotl ortholog of the Nanog transcription factor binds to the enhancer region of the Nanog gene in mammalian somatic chromatin after 3 hours of axolotl oocyte extract treatment. ChIP assays in NIH3T3 cells and MEFs above showed that after 3 hours of AOE incubation binding of axNanog to the enhancer was slightly more efficient than its binding on the promoter (Figure 4.2 and 4.3). However, in MEFs, binding to the promoter occurred efficiently within a further 3 hours (6 hours in total). This result is consistent with the finding that re-activation of the Nanog enhancer might prompt its promoter activation (Kim et al., 2011). These experiments suggest that axolotl oocytes can provide factors to re-activate the mouse Nanog enhancer. Moreover, axNanog specifically binds to the Nanog regulatory regions, but does not bind to the MyoD1 regulatory sequences, showing the specificity of Nanog binding. My results also showed that there was no change in the level of Nanog binding after Xenopus oocyte treatment, which was used as negative control (Figure 4.4) consistent with the absence of a Nanog orthologs in Xenopus.

I demonstrated that Nanog pull-down levels were almost identical to mouse ES cells in the AOE-treated fibroblasts. This experiment shows that the extract of axolotl oocyte can elevate the level of Nanog protein-bound Nanog enhancer, to that of mouse ES cells. This result is consistent with results from our lab showing endogenous Nanog gene re-expression in mouse fibroblasts which were incubated in axolotl oocyte nuclei.

AOE adds pioneering factors to reprogramming system

I also showed that axolotl oocyte extract stimulates histone variant H2A.Z exchange in the nucleosomes on and near both the enhancer and promoter of the Nanog gene within an hour of treatment. The level of H2A.Z enrichment increased between 1 and 3 hours of treatment, it remained at similar levels thereafter (Figure 4.8). This suggests that H2A.Z deposition is completed within 1-3 hours.

Confirming the fact that deposition of H2A.Z is a genome-wide event, there was about a 2-fold increase in signal on and near MyoD1 enhancer and promoter regions after 6 hours of treatment with axolotl oocyte extract. Bi-functional H2A.Z exchange occurs on differentiation marker genes (Creyghton et al., 2008, Hu et al., 2013) and pluripotency genes (Wang et al., 2015) in ES cells. However, different levels of deposition (2-fold on MyoD1 and 7-fold on Nanog enhancer) suggested that H2A.Z evicts H2A more efficiently on pluripotency genes with the incorporation of other pluripotent regulators during reprogramming. Also, at the Nanog locus, H2A.Z deposition was strongly associated with the transcription activating histone marks H3K27ac, H3K4me1, and 5-hmC, suggesting a role in facilitating transcriptional activation (Ranjan et al., 2013; Conerly et al., 2010).

Transcriptome comparisons of histone variant H2A.Z between mouse embryonic stem cells and oocytes from Xenopus and axolotl showed that H2A.Z gene expression levels are remarkably high in mouse embryonic stem cells and axolotl oocytes, while there is very low signal for H2A.Z expression in Xenopus oocytes (M. Loose, unpublished). Consistent with this, I showed that H2A.Z was not

deposited in the Nanog enhancer region of somatic cells after treatment with Xenopus oocyte extract.

H2A.Z participates in destabilizing chromatin and activating gene expression (Subramanian et al., 2015). One of the most important findings in this thesis project involves the comparison between the dynamics of H2A.Z and axNanog binding to enhancer sequences. H2A.Z binding commences earlier than axNanog binding on the Nanog enhancer and promoter (Figure 4.10). This result was supported by axNanog function-blocking experiment, which shows that Nanog is not required for H2A.Z deposition (Figure 4.12). These two experiments clearly demonstrate that the deposition of histone variant H2A.Z on the Nanog enhancer occurs in a Nanog-independent manner, suggesting that H2A.Z acts as a pioneer factor.

CHAPTER 5

EFFECT OF AMPHIBIAN OOCYTE EXTRACT TREATMENT ON BINDING OF OCT4 TO THE MOUSE PLURIPOTENCY GENES

5.1 INTRODUCTION

In the Chapters 3 and 4, I have shown that axolotl oocyte extract has a capacity to add the epigenetic marks, 5hmC, H3K27ac, and H3K4me1, to the somatic chromatin and for providing transcription and pioneering factors, axNanog and H2A.Z, to initiate chromatin remodelling in mouse fibroblasts. In this chapter, I show the capability of AOE to prepare the chromatin on the pluripotency gene Nanog for binding by Oct4.

Epigenetic memory

Cell identity is established by the stable transcriptional profile. Stable cell-type specific gene expression is regulated by epigenetic modifications such as posttranslational histone modifications, exchange of histone variants and DNA methylation (Goldberg et al., 2007, Xie et al., 2013). Mis-regulated gene expression, such as inappropriate expression of c-myc, can lead to cancer formation (Kim et al., 2010a). Epigenetic memory is a mechanism that provides

stability of cell identity during differentiation. The former profile of epigenetic marks, thus of gene expression, are inherited by cells throughout development by a mechanism which can be described as 'memory' (Shipony et al., 2014).

Stable gene expression in adult cells can be changed to resemble embryonic gene expression by pluripotency-inducing experimental approaches which alter the epigenetic profile. However, the retention of a previous epigenetic profile during reprogramming causes persistence of the original gene transcription profile which is specific for the cell type (Blelloch et al., 2006, Pasque et al., 2012, Nashun et al., 2015). An example of epigenetic memory is the silencing of pluripotency genes and continued transcription of cell lineage-specific genes after reprogramming is induced. When the expression of pluripotency genes is incomplete, it points to the maintenance of epigenetic memory (Halley-Stott and Gurdon, 2013). In other words, the forced expression of pluripotency genes is capable of switching the differentiated cells to undifferentiated state once the epigenetic memory is abolished. Persistence of silenced and/or active genes will create a resistance to establishing pluripotency and eventually incomplete or unsuccessful reactivation of pluripotency genes to direct the reprogramming process (Halley-Stott and Gurdon, 2013; Shipony et al., 2014).

It was previously reported that iPS cells contain residual hypermethylation (Doi et al., 2009; Ball et al., 2009). However, a comparison between reprogramming by Yamanaka factors and SCNT shows important differences in resetting epigenetic marks on somatic chromatin, especially methylation of DNA. For instance, DNA demethylation begins immediately in transferred donor nuclei (Santos et al.,

2002); on the contrary it takes a much longer time in iPS cells (Mikkelsen et al., 2008). In a later study, the DNA methylation patterns of iPS and nuclear-transferred cells were compared by CHARM and pyrosequencing analysis: there were only 229 differentially methylated regions (DMRs) between SCNT-derived pluripotent cells and ES cells, while this number of DMRs reached to 5,304 between iPS and ES cells, and most were hypermethylated on these sites, demonstrating that the methylation pattern of ES and SCNT-derived cells is more similar than that of iPS cells (Kim et al., 2010). These results suggest that epigenetic memory might result in inefficient and slow DNA demethylation during transcription factor-induced reprogramming.

Similarly, the retention of histone modifications, and also histone variants, reduces the chance of completing the reprogramming process, as it is known that differentiation-associated genes are silenced in pluripotent cells by the repressive histone marks. For instance, SCNT experiments with Xenopus showed that genes which mark individual somatic lineages in donor nuclei were still expressed (Ng and Gurdon, 2005). Indeed, the high level of the histone H3 variant H3.3 in Xenopus eggs might be a reason for the continued lineage marker gene expression after SCNT, illustrating for epigenetic memory (Ng and Gurdon, 2008b). Moreover, the histone H2 variant macroH2A, which has a role in reducing the transcriptional activity, also contributes to the limitations of Xenopus oocyte nuclear reprogramming (Pasque et al., 2011a, Pasque et al., 2011b).

Residual methylation and histone marks detected in iPS cells are a limitation for reprogramming efficiency as well as re-differentiation of these cells into a new

somatic cell lineage. Comparisons between producing differentiated tissues from SCNT-derived cells and iPS cells with ES cells from a blastocyst indicated that regardless of the original tissue, nuclear-transferred cells have a capacity equivalent to ES cells, while iPS cells were more restricted (Kim et al., 2010a). One reason for this might be the number of hypermethylated DMRs on ES cell-specific genes, which is higher in iPS cells than in SCNT-derived cells. Moreover, it was shown that the level of the repressive histone mark H3K27me3 was higher in ES cells from blastocysts of naturally fertilized embryos than that of SCNT derived embryos. This is also indicative of the resilient epigenetic profile of differentiated nuclei in the reprogrammed cells (Zhang et al., 2009). H3K27me3 plays a significant role in the suppression of differentiation genes in ES cells; therefore, differentiation-related genes might be activated in the ES cells from SCNT embryos (Zhang et al., 2009).

It was also discussed in a recent paper that reprogramming by SCNT, and oocyte extracts, is more effective in overcoming epigenetic barriers when compared to iPS cells induced by transcription factors (Firas et al., 2014). Apparently, oocytes possess efficient enzymatic activities for remodelling/relaxing the differentiated chromatin (Perry and Wakayama, 2002, Simonsson and Gurdon, 2004, Bian et al., 2009, Murata et al., 2010, Pfeiffer et al., 2011). Indeed, eight 'candidate oocyte reprogramming factors (CORFs) were identified by cross-species transcriptional analysis: ARID2, ASF1A, ASF1B, DPPA3, ING3, MSL3, H1FOO and KDM6B (Awe and Byrne, 2013). Recent studies have demonstrated a synergy between oocyte reprogramming and Yamanaka factors, indicating that oocyte factors can enhance

the reprogramming activity of Yamanaka factors: Ganier et al. showed that incubation of MEFs, which express OSKM factors, in the Xenopus egg extract accelerates the reprogramming efficiency of the factors (Ganier et al., 2011). Cibelli's group also showed that the OSKM-induced reprogramming was very inefficient in inducing pluripotency in human adult dermal fibroblasts, but introducing ASF1A, a histone-remodelling chaperone which is included in human oocyte, was sufficient to trigger reprogramming (Gonzalez-Munoz et al., 2014).

It was also shown that the Nanog interactome is reconfigured during reprogramming and the loci which are in contact with the Nanog locus are mostly upregulated in early reprogramming (pre-iPSCs). These findings are consistent with the acquisition of transcriptionally activating epigenetic modifications. For instance these sites are enriched with H3K4me3, have reduced levels of H3K27me3, and are bound by Klf4 (Sridharan et al., 2009, Apostolou et al., 2013). All of these factors establish a bridge providing a stable interaction between the Nanog promoter and enhancer, as well as other pluripotency gene regulators, to maintain pluripotency in the reprogrammed cells. I demonstrated in the previous chapters that AOE is effective in adding activating epigenetic marks to the enhancer and promoter of the mouse Nanog gene, therefore, it might be facilitating reconstruction of the Nanog interactome and promote Oct4 binding.

I therefore tested whether AOE can improve the binding of Oct4 to the mouse Nanog gene regulatory regions and compared these results with the effect of XOE using the same approach.

5.2 RESULTS

5.2.1 Effect of AOE treatment on the binding of Oct-4 as a Yamanaka factor

Expression of the Nanog homeodomain protein is crucial to the transition to ground state pluripotency, in other words, Nanog is “the gateway to the pluripotent ground state” (Silva, et al. 2009). In this experiment, we focused on whether factors in axolotl oocytes could accelerate the effect of Yamanaka factors and create a synergy in reprogramming. To address this question, an NIH3T3 cell line was generated with Tet-inducible Oct4 and Sox2 expression. Oct4 and Sox2 are two of the main pluripotency inducers belonging to the Yamanaka factor tetrad; they form a heterodimer and function as pioneering factors in re-activation of Nanog gene expression during reprogramming (Kuroda et al., 2005; Silva et al., 2009). In this strategy, using the doxycycline-induced Oct4/Sox2 NIH3T3 cell line, it is possible to observe if AOE can increase endogenous Oct4 binding efficiency.

The approach in more detail: First, the inducible Oct4/Sox2 NIH3T3 cell line was generated by lentivirus produced in HEK293T cells that were transfected with Oct-4 (Addgene, Plasmid 20323, TetO-FUW-oct4) and Sox2 (Addgene, Plasmid 20326, TetO-FUW-sox2) plasmids. Selection of the cells including Oct4/Sox2 plasmids was carried out by 500 µg/ml of zeocin antibiotic (Life Technologies, R25005) treatment for 1 week. In selected cells, expression of Oct4 and Sox2 factors was initiated by doxycycline treatment for 24 hours. To ensure expression of

endogenous Oct4 in the cell line, immunostaining assay was carried out with an Oct4 antibody (Santa Cruz, catalog no. 5279).

5.2.1.1 Detecting Oct4 expression:

In this experiment, mouse ES cells were used as a positive control since the Oct4 gene is constitutively active in these cells. The inducible Oct4/Sox2 NIH3T3 cell line was tested for Oct4 expression before and after doxycycline treatment, indicated as - dox and + dox, respectively. In Figure 5.1, each panel includes three images showing bright field, DAPI staining (showing stained nucleus in blue) and Oct4-immunostaining (showing Oct4 expression in green). Endogenous expression of Oct4 was detected in mouse ES cells as a positive control, while there was no signal detected in cells before doxycycline treatment in the cell line, as negative control. The last panel shows that there is a robust immunostain resulting from Oct4 expression after 24 hours of doxycycline treatment, indicating that induction of Oct4 expression in the cell line (Figure 5.1).

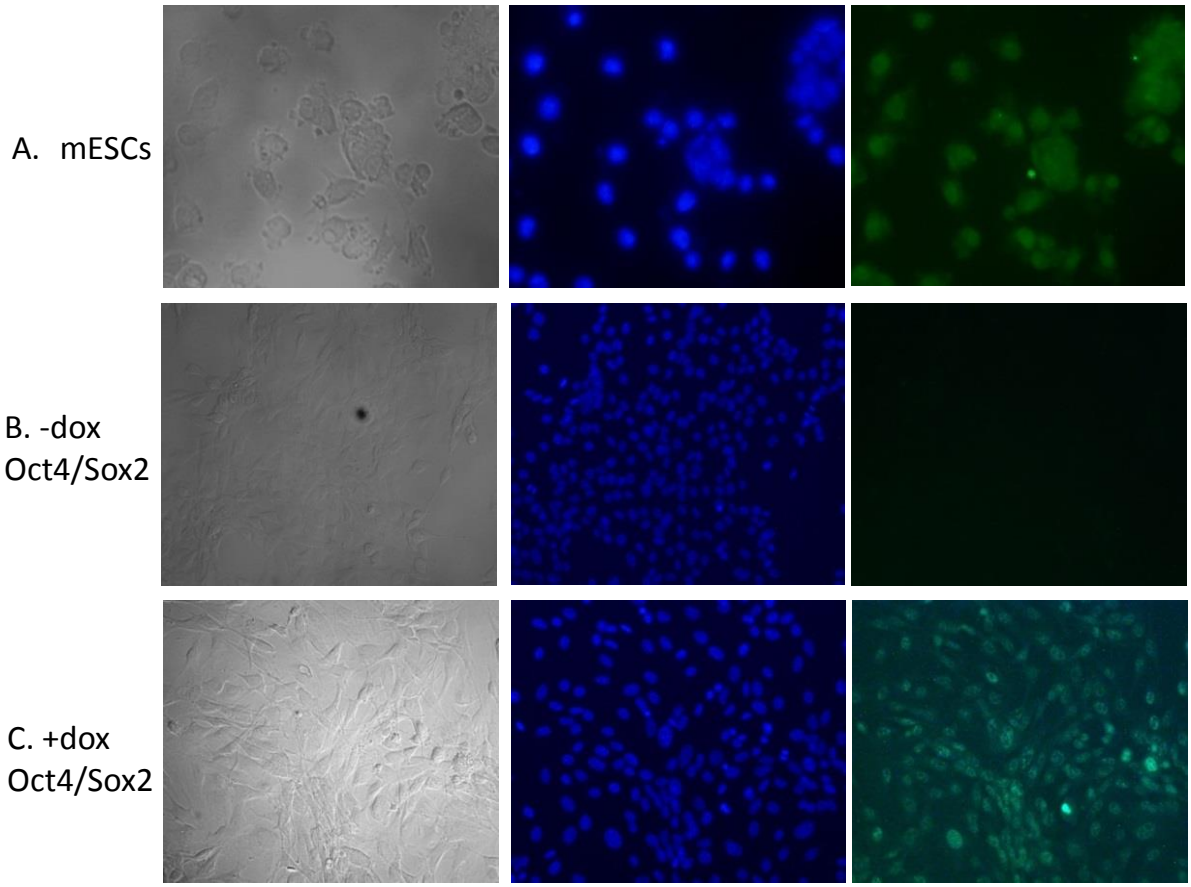

Figure 5.1 Immunostaining of Oct4 antibody.

Bright field, DAPI staining and immunostaining of Oct4 in A. mouse ES cells, B. -dox Oct4/Sox2 inducible NIH3T3 cells, and C) +dox Oct4/Sox2 inducible NIH3T3 cells.

5.2.1.2 Immunoprecipitation of Oct4 after AOE treatment:

To test if AOE treatment can enhance the effect of Yamanaka factors, Oct4 binding to the regulatory regions of the Nanog gene was tested in the Oct4/Sox2 cell line before (-dox) and after (+dox) doxycycline treatment. In order to induce the expression of Oct4 and Sox2, the cell line was treated with 2 µg/ml of doxycycline for 24 hours. This brief time of treatment would avoid the induction of pre-iPS cells which would have obscured the interpretation of the data. Following permeabilization with digitonin, AOE incubation was applied for 6 hours to 2 x 10^6 of dox- or dox+ cells. Untreated and AOE-treated dox- and dox+ cells were lysed and were subjected to ChIP assay using a specific Oct4 antibody (Santa Cruz, catalog no. 5279). IgG was used as a negative control. Regions of the Nanog enhancer and promoter, and also negative control sequences, including the MyoD1 promoter and Nanog intron 1, were assessed by qPCR. In this experiment, the percentage of input values was used to compare the amplification in each time point.

The difference between untreated (0h) groups of -dox and +dox Oct4/Sox2 cells indicates the effect of endogenous Oct4 expression on Oct4 immunoprecipitation, which is 1.97 (on the enhancer) and 2.5 fold (on the promoter) increased in +dox cells compared to -dox cells. It means that induction of endogenous Oct4 expression by 24 hours of doxycycline treatment increased the Oct4 binding on the Nanog enhancer only 1.97-fold and 2.5-fold on the Nanog promoter. However, a 13.7-fold increase was observed for the binding of Oct4 to the Nanog enhancer upon 6 hours AOE treatment in +dox Oct4/Sox2 cells; an increase of 3.7-fold was

observed for the Nanog promoter (Figure 5.2). This means that AOE enhances (13.7 fold) the binding of Oct4 to the enhancer region of Nanog gene in mouse differentiated cells expressing Oct4. This suggests that AOE contains factors making the specific DNA regulatory regions accessible to Oct4; therefore enhances the activity of Yamanaka factors on pluripotency rate-limiting gene, Nanog. AOE apparently generates a chromosomal environment which is suitable for transcriptional activation of pluripotency genes by exogenous pluripotency factors.

A.

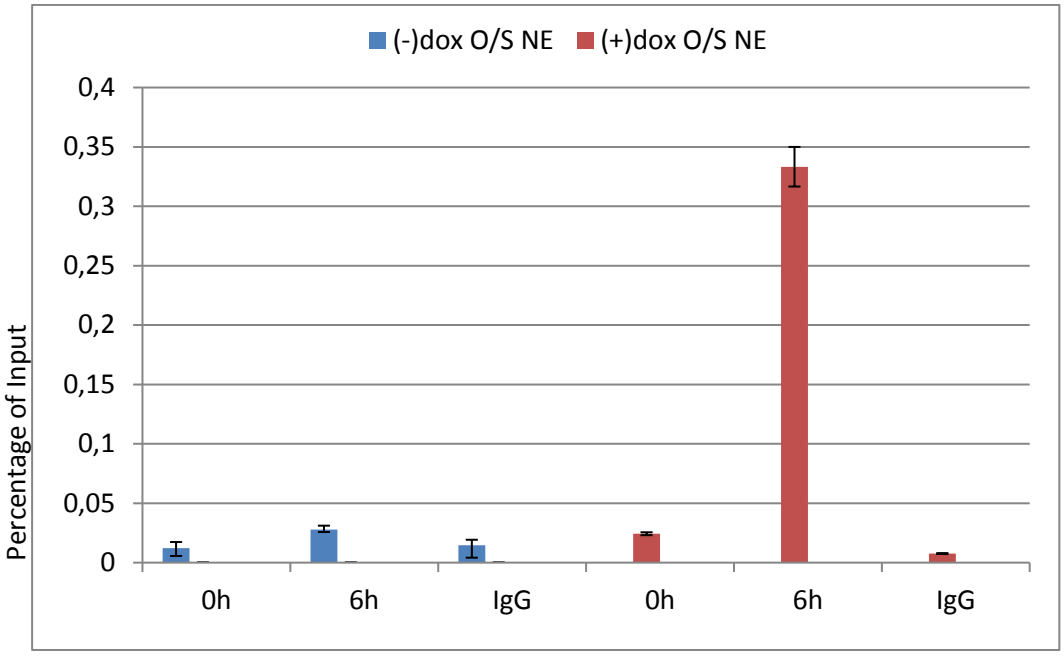
(-)dox O/S NE
(+)dox O/S NE
Percentage of Input
0,4
0,35
0,3
0,25
0,2
0,15
0,1
0,05
0
0h
6h
IgG
0h
6h
IgG

B.

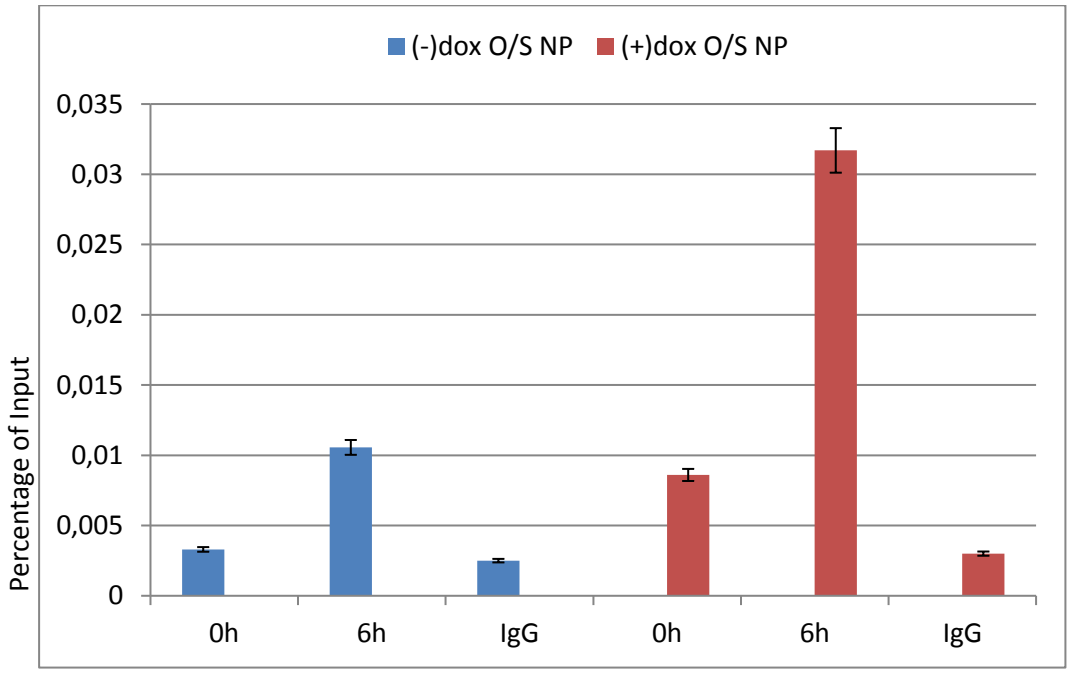
(-)dox O/S NP
(+)dox O/S NP
Percentage of Input
0,035
0,03
0,025
0,02
0,015
0,01
0,005
0
0h
6h
IgG
0h
6h
IgG

C.

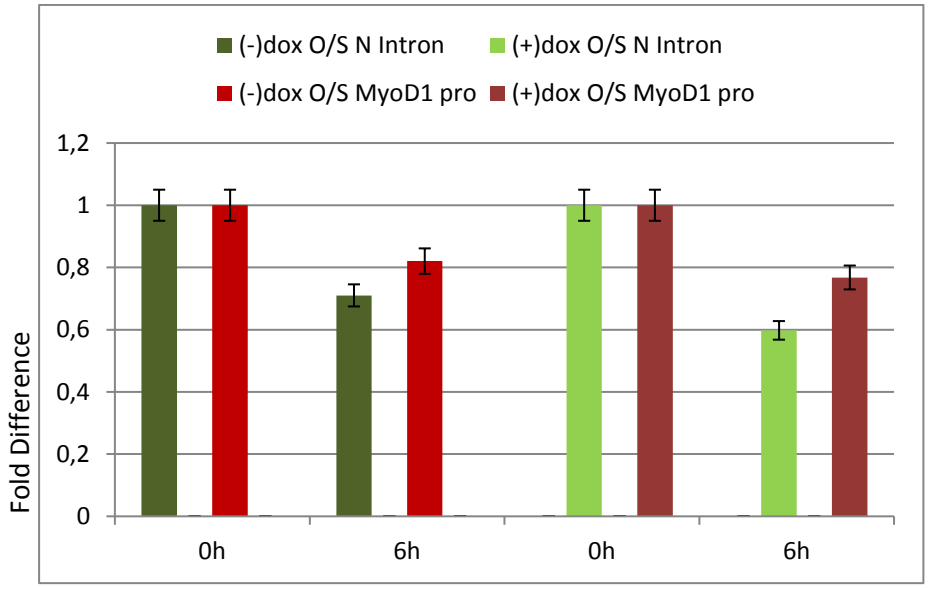

Figure 5.2 Oct4 binding on the regulatory regions of the Nanog gene in the inducible Oct4/Sox2 NIH3T3 cells after AOE treatment

Sheared chromatin from 2 x 10^6 cells was immunoprecipitated with 5 µg Oct4 antibody and the levels of specific DNA sequences (as indicated) were quantified by qPCR. The graphs show the percentage of input values of Oct4 binding on the Nanog enhancer (A), promoter (B), and the fold difference values of Oct4 binding on the Nanog intron 1 and MyoD1 promoter (C) in the -dox and +dox cells treated with AOE. Immunoprecipitation with IgG is negative control. Biological repeat number= 3 and error bars indicate standard deviations in technical replicates.

Immunoprecipitation of Oct4 after XOE treatment:

I next tested if XOE can enhance Oct4 binding on the mouse Nanog enhancer: the NIH3T3 Oct4/Sox2 cell line was treated for 24 hours with doxycycline (+dox). The cells were permeabilized and incubated with XOE for 6 hours. Control cells were not induced with doxycycline (-dox). Oct4-bound regions were immunoprecipitated with Oct4 antibody and the Nanog enhancer was amplified by qPCR. IgG immunoprecipitation was used as negative control for antibody specificity. The graph in Figure 5.3 shows that there is not a significant change in the levels of Oct4 binding on the mouse Nanog enhancer region, suggesting that XOE does not have an impact on the binding of Yamanaka Factors.

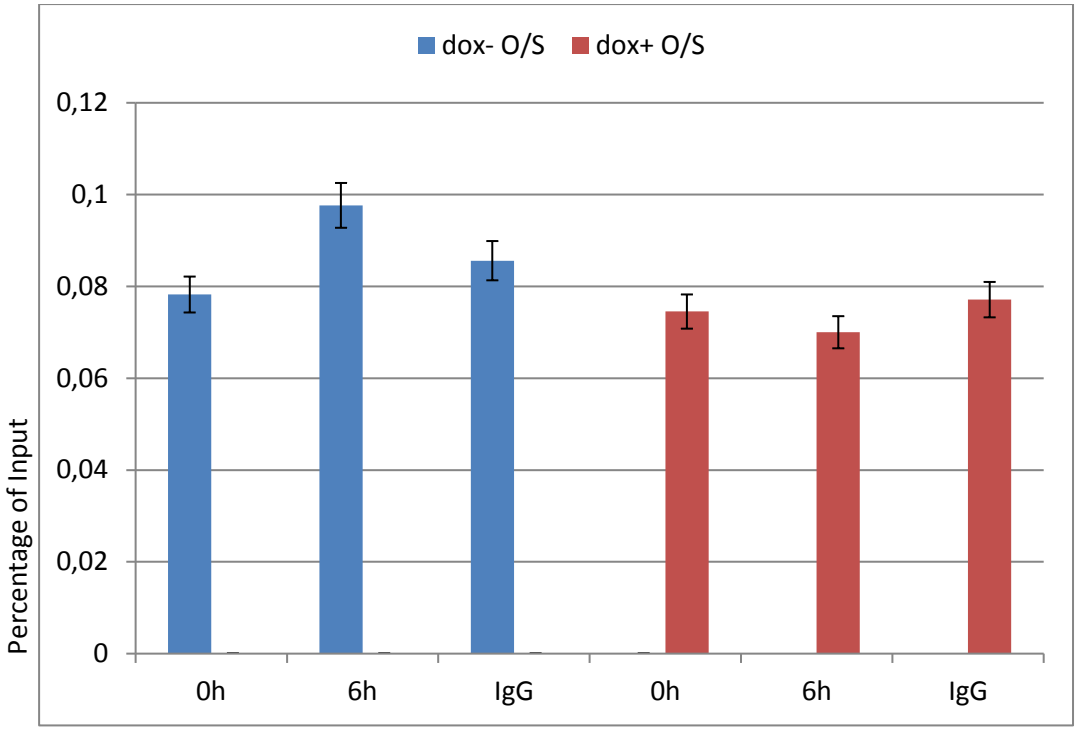

Figure 5.3 Oct4 binding on the Nanog enhancer in the inducible Oct4/Sox2 NIH3T3 cells after XOE treatment

Sheared chromatin from 2 x 10^6 cells was immunoprecipitated with 5 µg Oct4 antibody and the levels of specific DNA sequences (as indicated) were quantified by qPCR. The graph shows the percentage of input values of Oct4 binding levels on the Nanog enhancer (A), promoter (B), and the Nanog intron 1 and MyoD1 promoter (C) in dox- and dox+ cells treated with AOE. Immunoprecipitation with IgG is negative control. Biological repeat number= 3 and error bars indicate standard deviations in technical replicates.

5.3 CONCLUSIONS

In this chapter, I have tested if the extracts from Amphibian oocytes can enable binding of Yamanaka factors' to the regulatory regions of the mouse Nanog gene. I demonstrated that AOE can enhance Oct4 binding in a fibroblast cell line carrying doxycycline inducible Oct4 and Sox2 genes, showing an increase in Oct4 binding efficiency. In the Oct4-expressing fibroblasts (+dox) after 6 hours of AOE treatment, the Oct4 binding on the mouse Nanog enhancer and promoter increased about 14- and 4-fold, respectively; on a non-coding region of Nanog gene, Nanog intron 1 and a promoter of a differentiation gene, MyoD1, there was no change in this cell line after 6 hours of AOE treatment, showing that AOE can specifically enhance Oct4 binding to Nanog regulatory regions. There was no effect detected after 6 hours of XOE treatment. In previous studies it was shown that Yamanaka factors are sufficient to induce pluripotency in differentiated cells and fulfil the stringent reprogramming criteria, however, efficiency of reversing the epigenetic modifications, thereby reprogramming efficiency, is very low (Kim et al., 2010; Firas et al., 2014).

CHAPTER 6

DISCUSSION

6.1 AOE ALTERS THE EPIGENETIC PROFILE ON THE MOUSE NANOG GENE

In this project I showed that AOE can catalyse the oxidation of methylated cytosines to hydroxymethylated cytosines on the regulatory regions of Nanog in mouse somatic chromatin. It has been shown that the oxidation of 5mC is an intermediate step in DNA demethylation, which is catalysed by Tet family enzymes which are overexpressed in ES cells (Ito et al., 2010; Wu and Zhang, 2011). It is well established that DNA methylation makes chromatin more compact and less accessible to transcription factors (Bird, 2002, Schaefer and Lyko, 2007). In contrast, 5hmC is mostly enriched in euchromatin in mouse ES cells, facilitating transcription factor binding cells (Ficz et al., 2011), implying 5hmC itself has roles in gene regulation for maintaining pluripotency in ES cells. Therefore, it was important to show the increasing levels of 5hmC, as an intermediate in demethylation process, on regulatory regions of the mouse Nanog gene, suggesting AOE can promote DNA demethylation to create a profile resembling to ES cells in mouse somatic cells.

Also, I demonstrated that the level of 5hmC selectively increased on the promoter and enhancer regions of the Nanog gene but not on the promoter or enhancer of

MyoD1 a marker for differentiation. This indicated that AOE can initiate hydroxymethylation specifically on pluripotency genes during reprogramming in differentiated cells. Transcriptomic analysis indicated that Tet1 and Tet2 are expressed at low level in the oocytes of both Xenopus and axolotl (unpublished data). It was shown that Nanog directly associates with Tet1 and Tet2 and co-occupy on the pluripotency related genes in mouse ES cells, this interaction enhances the reprogramming activity (Costa et al., 2013). I propose that axNanog might have a similar ability on Tet1 and Tet2 in AOE, axNanog might be interacting with Tets and co-occupy the pluripotency genes and this might be initiating the hydroxymethylation of the regulatory regions of the mouse Nanog gene. The negative control of the above experiment with XOE which does not have Nanog did not show any increase of 5hmC. As expected, there was no increase in 5hmC on the first intron region of Nanog gene which was used as a negative control, as introns remain methylated in transcriptionally active genes in mammalian genome (Laurent et al., 2010). While regulatory regions of genes are demethylated, gene bodies are mostly methylated during transcription (Jones, 1999, Hellman and Chess, 2007, Laurent et al., 2010). However, 5-hydroxymethylation was detected at the gene bodies in human ES cells (Stroud et al., 2011), thereby, it should be noted that very early time points were studied and that the intronic/exonic sequences might later be hydroxymethylated/demethylated. The results I obtained indicate that the gene regulatory regions of the mouse Nanog gene were primarily hydroxymethylated, presumably catalysed by the Tet enzymes expressed in oocytes (unpublished) and present in AOE.

There was no increase in the level of 5hmC on enhancer or promoter regions of the Nanog gene after 6 hours of XOE treatment. However, previous studies showed that XOE has the capacity to remove methyl groups on cytosines in the Nanog and Oct4 promoters (Simonsson and Gurdon, 2004). While it might seem contradictory that two amphibian species' oocytes generate different results in the reprogramming of 5mC to 5hmC, AOE and XOE differ greatly in their reprogramming capacities and mechanisms. My results suggest that AOE and XOE might be involved in distinct demethylation processes when applied on differentiated cells. Although, the expression of Tet genes were detected at low levels (much lower than that of ES cells) in both Xenopus and axolotl oocytes, AOE can induce hydroxymethylation by catalysing the oxidation of 5mC, while it is not catalysed by XOE. This suggests that hydroxymethylation is not involved in the mechanism for demethylation by XOE. XOE can remove the methyl groups on cytosine, but cannot produce the hydroxyl group to convert 5hmC from 5mC. It was previously shown that BER is involved in the chromatin remodelling in mouse PGCs as a DNA repair mechanism acting in active DNA demethylation (Hajkova et al., 2010). These results suggest that DNA repair pathways might be involved in the demethylation of XOE-treated somatic chromatin, while in AOE this is carried out primarily by the Tet family enzymes; again, should be noted that DNA repair mechanisms might also be in charge in AOE-demethylation.

I further demonstrated that AOE can add the transcription activating histone modifications H3K27ac and H3K4me1 specifically to the enhancer of the Nanog in differentiated mouse cells, but not on the enhancer of the MyoD1 gene. There

was also no increase in the level of H3K27ac and H3K4me1 on the first intron of the Nanog gene. Previous results from our lab demonstrated that AOE can add activating histone marks, such as H3K9ac, to the promoters of Nanog and Oct4. Therefore AOE is capable of not only altering the epigenetic marks on DNA but it can also actively remodel the histone code of differentiated cells during reprogramming within a short time frame.

H3K27ac and H3K4me1 are enriched on the mouse Nanog enhancer even after 3 hours of AOE treatment. As described above, H3K4me1 is specific for poised enhancers, while H3K27ac is enriched on active enhancers (Creyghton et al., 2010, Bogdanovic et al., 2012). Using ChIP, I showed that 3-6 hours of AOE treatment is sufficient to initiate epigenetic reprogramming of the Nanog gene in somatic chromatin of murine cells (Table 6.1). My results show that AOE can add transcriptional activating marks to pluripotency genes in the differentiated chromatin of mouse cells. In contrast, XOE cannot add H3K27ac or H3K4me1 to the Nanog enhancer even after 6 hours of treatment. These results support previous studies showing that the level of H3K9ac, an activating mark on promoters, did not show any increase in differentiated chromatin upon XOE treatment (Bian et al., 2009).

	AOE		XOE	
	Nanog enhancer	**Nanog promoter**	**Nanog enhancer**	**Nanog promoter**
5hmC	↗	↗	**O**	**X**
5mC	↘	⇢	**X**	⇢
H3K27ac	↗	**O**	**O**	**X**
H3K4me1	↗	**O**	**O**	**X**

Table 6.1 Summary of epigenetic alterations that occur on regulatory regions of the mouse Nanog gene.

↗ :Indicates increasing, ↘ : Indicates decreasing, **O** : indicates no change,

X :indicates not available data, ⇢ : Indicates decreasing shown in previous studies

6.2 AOE PROVIDES FACTORS TO INITIATE RAPID CHROMATIN REMODELLING

Using ChIP with an antibody to axolotl Nanog, I demonstrated that axolotl Nanog binds to the enhancer and promoter of the mouse Nanog efficiently. Moreover, the binding occurs rapidly, within 3 hours. The specificity of this interaction is demonstrated by the inability of AOE to precipitate regulatory sequences of the MyoD1 gene. I also showed that after incubating NIH3T3 and mouse ES cells for 6 hours in AOE treatment, equivalent levels of axNanog was bound to the mouse Nanog enhancer locus in both cell types. Endogenous Nanog expression is crucial to reaching the pluripotent ground state during the final phases of reprogramming (Silva et al., 2009), suggesting that the ability of AOE to target the enhancer and promoter regions of pluripotency genes in murine cell lines makes it a useful tool for elucidating reprogramming mechanisms involved in the acquisition of ground state pluripotency.

I showed that AOE promoted the deposition of the histone variant H2A.Z on regulatory regions of the mouse Nanog gene as rapidly as within 1 hour of exposure to the extract. Enrichment of H2A.Z in the nucleosomes is mostly associated with transcriptionally active sites enriched with activating epigenetic marks (Gallant-Behm et al., 2012; Hu et al., 2013; Dalvai et al., 2013). H2A.Z exchange provides more flexible chromatin allowing interactions between histones and transcription factors (Subramanian et al., 2013; Hu et al., 2013). Therefore, the increased levels of H2A.Z on the Nanog enhancer and promoter of the mouse somatic cells indicate that AOE can change chromatin configuration to

facilitate reprogramming of the Nanog gene. Moreover, a recent study by Wang et al. (2014) revealed the importance of H2A.Z in pluripotency and reprogramming by showing that the level of H2A.Z expression is much lower in differentiated cells than in ES cells and H2A.Z knock-down in mouse ES cells causes a striking decrease in Nanog protein level. Furthermore, H2A.Z expression was elevated during the reprogramming of differentiated cells, while formation of iPS colonies was abolished by knocking-down H2A.Z in cells reprogrammed by introduction of Yamanaka factors (Wang et al., 2015). It was also shown that Nanog overexpression can rescue reprogramming after H2A.Z knock-down in differentiated cells and, moreover, H2A.Z has a role in modulating Nanog protein levels, indicating a strong interaction between H2A.Z and Nanog during reprogramming to pluripotency (Wang et al., 2015). These findings support a role for of H2A.Z and Nanog during reprogramming by AOE.

I also demonstrated that AOE induced an increase of H2A.Z on the MyoD1 enhancer, showing that genes involved in differentiation can also be enriched by H2A.Z (Taberlay et al., 2011). As indicated above, enrichment of H2A.Z is not sufficient to define active genes in the absence of activating histone marks; the role of H2A.Z can only be determined by the chromatin environment as well as by its level of enrichment. It is possible that activating histone marks on nucleosomes flanking the transcriptionally active regulatory regions cause an increase in H2A.Z deposition (Hu et al., 2013).

6.3 REPROGRAMMING OF THE MOUSE NANOG GENE BEGINS ON THE ENHANCER

Hydroxymethylation of CpGs and axNanog binding was initiated on the Nanog enhancer before either activity was detectable on the promoter. Experiments testing the level of axNanog binding showed an increase over 6 hours, while the level of 5hmC on the enhancer did not show an additional increase (remained at a similar level) between 3 and 6 hours of extract treatment, suggesting that re-activation of the mouse Nanog gene by oocyte factors begins with remodelling of the enhancer prior to modification of the promoter. This suggests that the Nanog enhancer is more amenable to chromatin remodelling and indicates that the epigenetic status of the promoter is somewhat more stable. This result is in agreement with other studies showing that enhancers accumulate methylation more gradually than promoters; enhancers boost transcriptional activity from promoters in a gradient, depending on the tissue and the stage of the cell (Aran et al., 2013). Also, enhancers undertake less uniform histone modifications than promoters, suggesting they can tissue-specifically regulate promoter activity by being less stable with more bivalent marks (Chen et al., 2012). My results, therefore, address questions about the initiation of reprogramming and re-expression of mouse Nanog gene.

6.4 AXNANOG AND H2A.Z START THE DYNAMICS OF REPROGRAMMING OF THE NANOG GENE

Analysis of the timing of H2A.Z and axNanog binding showed that after AOE treatment H2A.Z is deposited more rapidly on the Nanog enhancer than axNanog. This result suggests that H2A.Z deposition is among the early events in Nanog reprogramming by AOE, preceding the binding of axNanog. This finding was supported by axNanog function-blocking experiments in which increased H2A.Z deposition was unaffected by inhibition of axNanog binding, suggesting that remodelling of the Nanog enhancer by H2A.Z occurs independent of axNanog binding (Figure 6.1). Furthermore, H2A.Z might be increasing axNanog activity during initiation stages, as mentioned previously, H2A.Z has roles in promoting the activity of the mouse Nanog protein, thus, enhancing the efficiency of reprogramming (Wang et al., 2015). Importantly, the inhibition of axNanog binding resulted in lower levels of H3K27ac and 5hmC enrichment on the enhancer. These results suggest that axNanog initiates the epigenetic alterations that result in transcriptional activation of pluripotency genes.

6.5 ACTIVITY OF PLURIPOTENT FACTORS ACCELERATED BY AOE

I demonstrated that a 6 hour treatment with AOE enhanced binding of the transcription factor Oct4 to the mouse Nanog enhancer. ChIP data showed that in mouse fibroblasts expressing Oct4/Sox2, Oct4 binding on the enhancer of Nanog gene, was enhanced around 14 fold. This result is important from the perspective

of reprogramming. In the course of the present ChIP experiment, only Oct4 binding was analysed. However, considering that Oct4 and Sox2 form heterodimers and bind on target genes, such as Nanog, Oct4, Sox2, Fbx15 (Chambers et al., 2003; Okumura et al., 2005, Nishimoto et al., 1999) this result suggests that AOE increases the Oct4/Sox2 heterodimer binding on the Nanog enhancer. These molecules are two of the original Yamanaka factors required to induce reprogramming in differentiated cells. Previous studies showed that transcription factor-induced reprogramming is effective and sufficient to establish pluripotency in differentiated cells; however, it has a low efficiency. One of the reasons might be that oocytes provide chromatin remodellers that can overcome the persistent somatic epigenetic profile (Firas et al., 2014; Halley-Stott and Gurdon, 2013). Moreover, there are studies showing that combination of these two reprogramming methods can reverse stable epigenetic modifications more efficiently (Ganier et al., 2011; Gonzalez-Munoz et al., 2014).

Note to the requirement for cell divisions to reactivate the pluripotency genes with transcription factors, oocyte reprogramming provides a combination of factors to the somatic cells with no need for cell division. This includes pluripotency factors, epigenome modifiers and also chromatin remodellers that change the chromatin environment. According to the literature, chromatin looping factors, Mediator and cohesin, play an important role for establishing Nanog gene activation in ES cells (Kagey et al., 2010). These interactions are regained during reprogramming and play important roles in rearranging the pluripotency-specific Nanog interactome which is established prior to the

reactivation of the Nanog locus (Apostolou et al., 2013). It would be interesting to test the binding of these factors on the murine Nanog regulatory regions following AOE incubation of mouse fibroblasts with chromosome confirmation capture (3C) assay to understand if AOE can induce the pluripotency state-specific Nanog-interactome. Existence of these factors can be also tested by ChIP assay, since Mediator and cohesin components and Nipbl (cohesin loading factor) occupy the enhancer and promoter regions of core pluripotency factors in ES cells (Okumura-Nakanishi et al., 2005; Kagey et al., 2010). These experiments could be important for understanding higher-order organisation of the chromatin before and after it is exposed to AOE. Moreover, these experiments might provide a clue to the function of super-enhancers which affect broad regions to activate genes, and possibly Mediator and cohesin have a role in this formation.

Interference of epigenetic memory was found as an efficiency reducing in oocyte reprogramming using Xenopus oocytes (Ng and Gurdon, 2007). This problem can be partially overcome with inhibitors for specific modifications that change the gene expression profile, such as Trichostatin A which is an inhibitor for histone deacetylase (Bui et al., 2010). To better understand the efficiency of reprogramming with Yamanaka factors and oocyte reprogramming, it would be interesting to test the effect of inhibitors for DNMTs to ease the DNA demethylation on regulatory regions of pluripotency genes. If positive results are obtained, that would mean that transcription-factor based reprogramming could be improved by the presence of such inhibitors.

Overall, AOE does not only provide the factors to initiate re-expression of the mouse Nanog gene by epigenetic alterations, but may also improve the effect of Yamanaka factors, thereby, increasing reprogramming efficiency. It appears that AOE can improve the efficiency of Yamanaka factors by remodelling chromatin structure.

Figure 6.1 Model of the sequence of events which occur upon AOE treatment

The figure shows the sequence of putative events which occur in the mouse somatic chromatin following incubation with AOE. Chromatin structure dominantly exists as closed chromatin in a differentiated cell and when pluripotency was induced by AOE incubation. As a pioneering factor H2A.Z deposes on the nucleosomes flanking the regulatory regions of Nanog gene, and loosens the chromatin and this makes the chromatin more accessible for the transcription factor axNanog included in AOE. AxNanog and Tet proteins co-occupy these regions and histone modifications follow these events as indicated in the figure in 6 hours of AOE treatment. To establish pluripotency the enhancer and the promoter of Nanog gene interact by the help of Mediator and Cohesin.

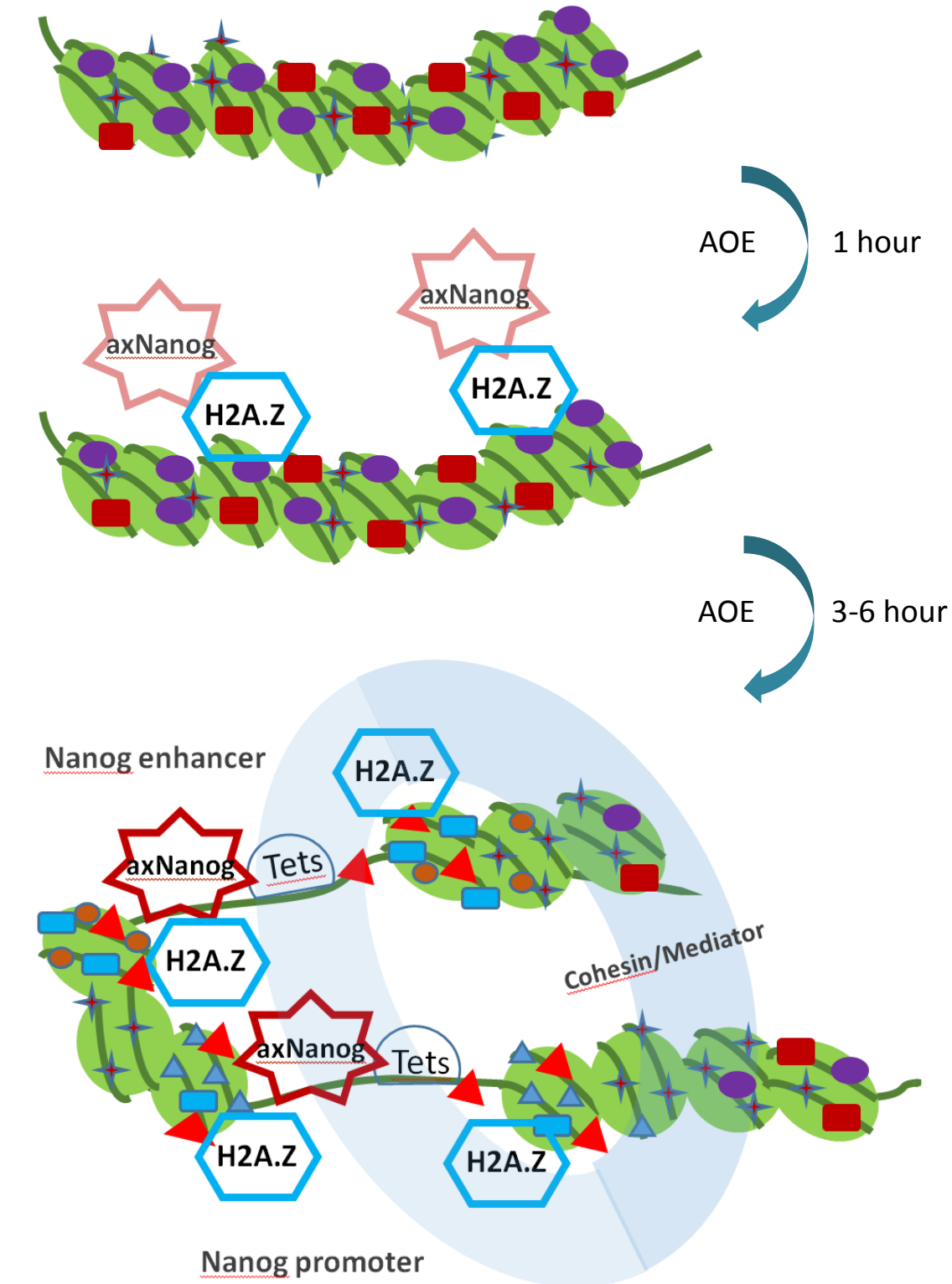
AOE
1 hour
axNanog
axNanog
H2A.Z
H2A.Z
AOE
3-6 hour
Nanog enhancer
H2A.Z
axNanog
Tets
H2A.Z
Cohesin/Mediator
axNanog
Tets
H2A.Z
H2A.Z
Nanog promoter
Repressive marks
Activating marks
H3K9me3
H3K27ac
H3K27me3
H3K4me1
5hmC
DNA Methylation
H3K4me3

In summary, I showed that the axolotl oocyte extract is capable of changing the epigenetic profile of mouse somatic cells to pluripotent and this reversal of epigenome is initiated rapidly and possibly in a deterministic manner. AOE can fulfil a rapid reprogramming activity by the pluripotency factors which are also included in the mouse ES cells that are not included in Xenopus oocytes (Johnson, A.D.; unpublished data). Indeed, my experiments showed that XOE does not have the same capability to reverse the epigenetic status of differentiated chromatin. For instance, XOE cannot add the activating histone marks on the pluripotency genes, while AOE can. My results support the theory that the mechanisms responsible for the establishment of pluripotency are conserved from urodeles to mammals.

Recalling the cell fusion experiments in which ES cells can reprogram the differentiated cell nuclei, the pluripotency is a dominant feature in ES cells (Foshay et al., 2012). It is important to note that the similarity of gene expression profile between the axolotl oocytes and the mouse ES cells suggests dominant pluripotency features to the axolotl oocytes, which might even help to solve the problems for reprogramming efficiency caused by epigenetic memory. This makes the axolotl oocytes are useful tool for the oocyte reprogramming assays.

REFERENCE LIST

AKKERS, R. C., VAN HEERINGEN, S. J., JACOBI, U. G., JANSSEN-MEGENS, E. M., FRANCOIJS, K. J., STUNNENBERG, H. G. & VEENSTRA, G. J. 2009. A hierarchy of H3K4me3 and H3K27me3 acquisition in spatial gene regulation in Xenopus embryos. *Dev Cell,* 17**,** 425-34.

ALBERIO, R., JOHNSON, A. D., STICK, R. & CAMPBELL, K. H. 2005. Differential nuclear remodeling of mammalian somatic cells by Xenopus laevis oocyte and egg cytoplasm. *Exp Cell Res,* 307**,** 131-41.

ALLEGRUCCI, C., RUSHTON, M. D., DIXON, J. E., SOTTILE, V., SHAH, M., KUMARI, R., WATSON, S., ALBERIO, R. & JOHNSON, A. D. 2011. Epigenetic reprogramming of breast cancer cells with oocyte extracts. *Mol Cancer,* 10**,** 7.

ANGELOV, D., MOLLA, A., PERCHE, P. Y., HANS, F., COTE, J., KHOCHBIN, S., BOUVET, P. & DIMITROV, S. 2003. The histone variant macroH2A interferes with transcription factor binding and SWI/SNF nucleosome remodeling. *Mol Cell,* 11**,** 1033-41.

APOSTOLOU, E., FERRARI, F., WALSH, R. M., BAR-NUR, O., STADTFELD, M., CHELOUFI, S., STUART, H. T., POLO, J. M., OHSUMI, T. K., BOROWSKY, M. L., KHARCHENKO, P. V., PARK, P. J. & HOCHEDLINGER, K. 2013. Genome-wide Chromatin Interactions of the Nanog Locus in Pluripotency, Differentiation, and Reprogramming. *Cell Stem Cell,* 12**,** 699-712.

ARAN, D., SABATO, S. & HELLMAN, A. 2013. DNA methylation of distal regulatory sites characterizes dysregulation of cancer genes. *Genome Biol,* 14**,** R21.

AVILION, A. A., NICOLIS, S. K., PEVNY, L. H., PEREZ, L., VIVIAN, N. & LOVELL-BADGE, R. 2003. Multipotent cell lineages in early mouse development depend on SOX2 function. *Genes Dev,* 17**,** 126-40.

AWE, J. P. & BYRNE, J. A. 2013. Identifying candidate oocyte reprogramming factors using cross-species global transcriptional analysis. *Cell Reprogram,* 15**,** 126-33.

BACHVAROVA, R. F., MASI, T., DRUM, M., PARKER, N., MASON, K., PATIENT, R. & JOHNSON, A. D. 2004. Gene expression in the axolotl germ line: Axdazl, Axvh, Axoct-4, and Axkit. *Dev Dyn,* 231**,** 871-80.

BANNISTER, A. J. & KOUZARIDES, T. 2011. Regulation of chromatin by histone modifications. *Cell Res,* 21**,** 381-95.

BAR-NUR, O., RUSS, H. A., EFRAT, S. & BENVENISTY, N. 2011. Epigenetic memory and preferential lineage-specific differentiation in induced pluripotent stem cells derived from human pancreatic islet beta cells. *Cell Stem Cell,* 9**,** 17-23.

BARGAJE, R., ALAM, M. P., PATOWARY, A., SARKAR, M., ALI, T., GUPTA, S., GARG, M., SINGH, M., PURKANTI, R., SCARIA, V., SIVASUBBU, S., BRAHMACHARI, V. & PILLAI, B. 2012. Proximity of H2A.Z containing nucleosome to the transcription start site influences gene expression levels in the mammalian liver and brain. *Nucleic Acids Res,* 40**,** 8965-78.

BARRES, R., YAN, J., EGAN, B., TREEBAK, J. T., RASMUSSEN, M., FRITZ, T., CAIDAHL, K., KROOK, A., O'GORMAN, D. J. & ZIERATH, J. R. 2012. Acute Exercise Remodels Promoter Methylation in Human Skeletal Muscle. *Cell Metabolism,* 15**,** 405-411.

BARRETO, G., SCHAFER, A., MARHOLD, J., STACH, D., SWAMINATHAN, S. K., HANDA, V., DODERLEIN, G., MALTRY, N., WU, W., LYKO, F. & NIEHRS, C. 2007. Gadd45a promotes epigenetic gene activation by repair-mediated DNA demethylation. *Nature,* 445**,** 671-5.

BARSKI, A., CUDDAPAH, S., CUI, K., ROH, T. Y., SCHONES, D. E., WANG, Z., WEI, G., CHEPELEV, I. & ZHAO, K. 2007. High-resolution profiling of histone methylations in the human genome. *Cell,* 129**,** 823-37.

BATLLE-MORERA, L., SMITH, A. & NICHOLS, J. 2008. Parameters influencing derivation of embryonic stem cells from murine embryos. *Genesis,* 46**,** 758-67.

BHATTACHARYA, D., TALWAR, S., MAZUMDER, A. & SHIVASHANKAR, G. V. 2009. Spatio-temporal plasticity in chromatin organization in mouse cell differentiation and during Drosophila embryogenesis. *Biophys J,* 96**,** 3832-9.

BIAN, Y., ALBERIO, R., ALLEGRUCCI, C., CAMPBELL, K. H. & JOHNSON, A. D. 2009. Epigenetic marks in somatic chromatin are remodelled to resemble pluripotent nuclei by amphibian oocyte extracts. *Epigenetics,* 4**,** 194-202.

BIDDLE, A., SIMEONI, I. & GURDON, J. B. 2009. Xenopus oocytes reactivate muscle gene transcription in transplanted somatic nuclei independently of myogenic factors. *Development,* 136**,** 2695-703.

BINDA, O. 2013. On your histone mark, SET, methylate! *Epigenetics,* 8**,** 457-63.

BINDA, O., SEVILLA, A., LEROY, G., LEMISCHKA, I. R., GARCIA, B. A. & RICHARD, S. 2013. SETD6 monomethylates H2AZ on lysine 7 and is required for the maintenance of embryonic stem cell self-renewal. *Epigenetics,* 8**,** 177-83.

BIRD, A. 2002. DNA methylation patterns and epigenetic memory. *Genes Dev,* 16**,** 6-21.

BLELLOCH, R., WANG, Z. D., MEISSNER, A., POLLARD, S., SMITH, A. & JAENISCH, R. 2006. Reprogramming efficiency following somatic cell nuclear transfer is influenced by the differentiation and methylation state of the donor nucleus. *Stem Cells,* 24**,** 2007-2013.

BOGDANOVIC, O., FERNANDEZ-MINAN, A., TENA, J. J., DE LA CALLE-MUSTIENES, E., HIDALGO, C., VAN KRUYSBERGEN, I., VAN HEERINGEN, S. J., VEENSTRA, G. J. & GOMEZ-SKARMETA, J. L. 2012. Dynamics of enhancer chromatin signatures mark the transition from pluripotency to cell specification during embryogenesis. *Genome Res,* 22**,** 2043-53.

BONISCH, C. & HAKE, S. B. 2012. Histone H2A variants in nucleosomes and chromatin: more or less stable? *Nucleic Acids Res,* 40**,** 10719-41.

BONN, S., ZINZEN, R. P., GIRARDOT, C., GUSTAFSON, E. H., PEREZ-GONZALEZ, A., DELHOMME, N., GHAVI-HELM, Y., WILCZYNSKI, B., RIDDELL, A. & FURLONG, E. E. 2012. Tissue-specific analysis of chromatin state identifies temporal signatures of enhancer activity during embryonic development. *Nat Genet,* 44**,** 148-56.

BOOTH, M. J., BRANCO, M. R., FICZ, G., OXLEY, D., KRUEGER, F., REIK, W. & BALASUBRAMANIAN, S. 2012. Quantitative sequencing of 5-methylcytosine and 5-hydroxymethylcytosine at single-base resolution. *Science,* 336**,** 934-7.

BOOTH, M. J., OST, T. W., BERALDI, D., BELL, N. M., BRANCO, M. R., REIK, W. & BALASUBRAMANIAN, S. 2013. Oxidative bisulfite sequencing of 5-methylcytosine and 5-hydroxymethylcytosine. *Nat Protoc,* 8**,** 1841-51.

BORA-SINGHAL, N., NGUYEN, J., SCHAAL, C., PERUMAL, D., SINGH, S., COPPOLA, D. & CHELLAPPAN, S. 2015. YAP1 Regulates OCT4 Activity and SOX2 Expression to Facilitate Self-Renewal and Vascular Mimicry of Stem-Like Cells. *Stem Cells,* 33**,** 1705-18.

BORGEL, J., GUIBERT, S., LI, Y., CHIBA, H., SCHUBELER, D., SASAKI, H., FORNE, T. & WEBER, M. 2010. Targets and dynamics of promoter DNA methylation during early mouse development. *Nat Genet,* 42**,** 1093-100.

BOSTICK, M., KIM, J. K., ESTEVE, P. O., CLARK, A., PRADHAN, S. & JACOBSEN, S. E. 2007. UHRF1 plays a role in maintaining DNA methylation in mammalian cells. *Science,* 317**,** 1760-1764.

BRIGGS, R. & KING, T. J. 1952. Transplantation of Living Nuclei From Blastula Cells into Enucleated Frogs' Eggs. *Proc Natl Acad Sci U S A,* 38**,** 455-63.

BUGANIM, Y., FADDAH, D. A., CHENG, A. W., ITSKOVICH, E., MARKOULAKI, S., GANZ, K., KLEMM, S. L., VAN OUDENAARDEN, A. & JAENISCH, R. 2012. Single-cell expression analyses during cellular reprogramming reveal an early stochastic and a late hierarchic phase. *Cell,* 150**,** 1209-22.

BURGESS, R. J. & ZHANG, Z. 2013. Histone chaperones in nucleosome assembly and human disease. *Nat Struct Mol Biol,* 20**,** 14-22.

BYRNE, J. A., SIMONSSON, S., WESTERN, P. S. & GURDON, J. B. 2003. Nuclei of Adult Mammalian Somatic Cells Are Directly Reprogrammed to oct-4 Stem Cell Gene Expression by Amphibian Oocytes. *Current Biology,* 13**,** 1206-1213.

CAMP, E., SANCHEZ-SANCHEZ, A. V., GARCIA-ESPANA, A., DESALLE, R., ODQVIST, L., ENRIQUE O'CONNOR, J. & MULLOR, J. L. 2009. Nanog regulates proliferation during early fish development. *Stem Cells,* 27**,** 2081-91.

CAPRA, J. A. 2015. Extrapolating histone marks across developmental stages, tissues, and species: an enhancer prediction case study. *BMC Genomics,* 16**,** 104.

CAREY, B. W., MARKOULAKI, S., HANNA, J. H., FADDAH, D. A., BUGANIM, Y., KIM, J., GANZ, K., STEINE, E. J., CASSADY, J. P., CREYGHTON, M. P., WELSTEAD, G. G., GAO, Q. & JAENISCH, R. 2011. Reprogramming factor stoichiometry influences the epigenetic state and biological properties of induced pluripotent stem cells. *Cell Stem Cell,* 9**,** 588-98.

CATENA, R., TIVERON, C., RONCHI, A., PORTA, S., FERRI, A., TATANGELO, L., CAVALLARO, M., FAVARO, R., OTTOLENGHI, S., REINBOLD, R., SCHOLER, H. & NICOLIS, S. K. 2004. Conserved POU binding DNA sites in the Sox2 upstream enhancer regulate gene expression in embryonic and neural stem cells. *J Biol Chem,* 279**,** 41846-57.

CHAKRAVARTHY, S., GUNDIMELLA, S. K., CARON, C., PERCHE, P. Y., PEHRSON, J. R., KHOCHBIN, S. & LUGER, K. 2005. Structural characterization of the histone variant macroH2A. *Mol Cell Biol,* 25**,** 7616-24.

CHALLEN, G. A., SUN, D., JEONG, M., LUO, M., JELINEK, J., VASANTHAKUMAR, A., MEISSNER, A., ISSA, J. P., GODLEY, L., LI, W. & GOODELL, M. A. 2011. Dnmt3a Is Essential for Hematopoietic Stem Cell Differentiation. *Blood,* 118**,** 178-178.

CHAMBERS, I., COLBY, D., ROBERTSON, M., NICHOLS, J., LEE, S., TWEEDIE, S. & SMITH, A. 2003. Functional expression cloning of Nanog, a pluripotency sustaining factor in embryonic stem cells. *Cell,* 113**,** 643-55.

CHANG, E. Y., FERREIRA, H., SOMERS, J., NUSINOW, D. A., OWEN-HUGHES, T. & NARLIKAR, G. J. 2008. MacroH2A allows ATP-dependent chromatin remodeling by SWI/SNF and ACF complexes but specifically reduces recruitment of SWI/SNF. *Biochemistry,* 47**,** 13726-32.

CHATFIELD, J., O'REILLY, M. A., BACHVAROVA, R. F., FERJENTSIK, Z., REDWOOD, C., WALMSLEY, M., PATIENT, R., LOOSE, M. & JOHNSON, A. D. 2014. Stochastic specification of primordial germ cells from mesoderm precursors in axolotl embryos. *Development,* 141**,** 2429-40.

CHEN, C. Y., MORRIS, Q. & MITCHELL, J. A. 2012. Enhancer identification in mouse embryonic stem cells using integrative modeling of chromatin and genomic features. *BMC Genomics,* 13**,** 152.

CHEN, R. Z., PETTERSSON, U., BEARD, C., JACKSON-GRUSBY, L. & JAENISCH, R. 1998. DNA hypomethylation leads to elevated mutation rates. *Nature,* 395**,** 89-93.

CHEN, T. P., UEDA, Y., DODGE, J. E., WANG, Z. J. & LI, E. 2003. Establishment and maintenance of genomic methylation patterns in mouse embryonic stem cells by Dnmt3a and Dnmt3b. *Molecular and Cellular Biology,* 23**,** 5594-5605.

CHEN, X., XU, H., YUAN, P., FANG, F., HUSS, M., VEGA, V. B., WONG, E., ORLOV, Y. L., ZHANG, W., JIANG, J., LOH, Y. H., YEO, H. C., YEO, Z. X., NARANG, V., GOVINDARAJAN, K. R., LEONG, B., SHAHAB, A., RUAN, Y., BOURQUE, G., SUNG, W. K., CLARKE, N. D., WEI, C. L. & NG, H. H. 2008. Integration of external signaling pathways with the core transcriptional network in embryonic stem cells. *Cell,* 133**,** 1106-17.

CHEN, Y., CHEN, Q., MCEACHIN, R. C., CAVALCOLI, J. D. & YU, X. 2014. H2A.B facilitates transcription elongation at methylated CpG loci. *Genome Res,* 24**,** 570-9.

CHEN, Y., KUNDAKOVIC, M., AGIS-BALBOA, R. C., PINNA, G. & GRAYSON, D. R. 2007. Induction of the reelin promoter by retinoic acid is mediated by Sp1. *Journal of Neurochemistry,* 103**,** 650-665.

CHEW, J. L., LOH, Y. H., ZHANG, W., CHEN, X., TAM, W. L., YEAP, L. S., LI, P., ANG, Y. S., LIM, B., ROBSON, P. & NG, H. H. 2005. Reciprocal transcriptional regulation of Pou5f1 and Sox2 via the Oct4/Sox2 complex in embryonic stem cells. *Mol Cell Biol,* 25**,** 6031-46.

CHIEN, C. S., WANG, M. L., CHU, P. Y., CHANG, Y. L., LIU, W. H., YU, C. C., LAN, Y. T., HUANG, P. I., LEE, Y. Y., CHEN, Y. W., LO, W. L. & CHIOU, S. H. 2015. Lin28B/Let-7 Regulates Expression of Oct4 and Sox2 and Reprograms Oral Squamous Cell Carcinoma Cells to a Stem-like State. *Cancer Res,* 75**,** 2553-65.

CHOI, J., HEO, K. & AN, W. 2009. Cooperative action of TIP48 and TIP49 in H2A.Z exchange catalyzed by acetylation of nucleosomal H2A. *Nucleic Acids Res,* 37**,** 5993-6007.

CHOUDHARY, C., WEINERT, B. T., NISHIDA, Y., VERDIN, E. & MANN, M. 2014. The growing landscape of lysine acetylation links metabolism and cell signalling. *Nat Rev Mol Cell Biol,* 15**,** 536-50.

COKUS, S. J., FENG, S. H., ZHANG, X. Y., CHEN, Z. G., MERRIMAN, B., HAUDENSCHILD, C. D., PRADHAN, S., NELSON, S. F., PELLEGRINI, M. & JACOBSEN, S. E. 2008. Shotgun bisulphite sequencing of the Arabidopsis genome reveals DNA methylation patterning. *Nature,* 452**,** 215-219.

CONERLY, M. L., TEVES, S. S., DIOLAITI, D., ULRICH, M., EISENMAN, R. N. & HENIKOFF, S. 2010. Changes in H2A.Z occupancy and DNA methylation during B-cell lymphomagenesis. *Genome Res,* 20**,** 1383-90.

CORTAZAR, D., KUNZ, C., SELFRIDGE, J., LETTIERI, T., SAITO, Y., MACDOUGALL, E., WIRZ, A., SCHUERMANN, D., JACOBS, A. L., SIEGRIST, F., STEINACHER, R., JIRICNY, J., BIRD, A. & SCHAR, P. 2011. Embryonic lethal phenotype reveals a function of TDG in maintaining epigenetic stability. *Nature,* 470**,** 419-U210.

COSTA, Y., DING, J., THEUNISSEN, T. W., FAIOLA, F., HORE, T. A., SHLIAHA, P. V., FIDALGO, M., SAUNDERS, A., LAWRENCE, M., DIETMANN, S., DAS, S., LEVASSEUR, D. N., LI, Z., XU, M., REIK, W., SILVA, J. C. & WANG, J. 2013. NANOG-dependent function of TET1 and TET2 in establishment of pluripotency. *Nature,* 495**,** 370-4.

COSTANZI, C. & PEHRSON, J. R. 1998. Histone macroH2A1 is concentrated in the inactive X chromosome of female mammals. *Nature,* 393**,** 599-601.

COTTON, A. M., PRICE, E. M., JONES, M. J., BALATON, B. P., KOBOR, M. S. & BROWN, C. J. 2015. Landscape of DNA methylation on the X chromosome reflects CpG density, functional chromatin state and X-chromosome inactivation. *Hum Mol Genet,* 24**,** 1528-39.

CREYGHTON, M. P., CHENG, A. W., WELSTEAD, G. G., KOOISTRA, T., CAREY, B. W., STEINE, E. J., HANNA, J., LODATO, M. A., FRAMPTON, G. M., SHARP, P. A., BOYER, L. A., YOUNG, R. A. & JAENISCH, R. 2010. Histone H3K27ac separates active from poised enhancers and predicts developmental state. *Proc Natl Acad Sci U S A,* 107**,** 21931-6.

CREYGHTON, M. P., MARKOULAKI, S., LEVINE, S. S., HANNA, J., LODATO, M. A., SHA, K., YOUNG, R. A., JAENISCH, R. & BOYER, L. A. 2008. H2AZ is enriched at polycomb complex target genes in ES cells and is necessary for lineage commitment. *Cell,* 135**,** 649-61.

CUADRADO, A., CORRADO, N., PERDIGUERO, E., LAFARGA, V., MUNOZ-CANOVES, P. & NEBREDA, A. R. 2010. Essential role of p18Hamlet/SRCAP-mediated histone H2A.Z chromatin incorporation in muscle differentiation. *EMBO J,* 29**,** 2014-25.

DALVAI, M., FLEURY, L., BELLUCCI, L., KOCANOVA, S. & BYSTRICKY, K. 2013. TIP48/Reptin and H2A.Z requirement for initiating chromatin remodeling in estrogen-activated transcription. *PLoS Genet,* 9**,** e1003387.

DE GOBBI, M., GARRICK, D., LYNCH, M., VERNIMMEN, D., HUGHES, J. R., GOARDON, N., LUC, S., LOWER, K. M., SLOANE-STANLEY, J. A., PINA, C., SONEJI, S., RENELLA, R., ENVER, T., TAYLOR, S., JACOBSEN, S. E., VYAS, P., GIBBONS, R. J. & HIGGS, D. R. 2011. Generation of bivalent chromatin domains during cell fate decisions. *Epigenetics Chromatin,* 4**,** 9.

DIXON, J. E., ALLEGRUCCI, C., REDWOOD, C., KUMP, K., BIAN, Y., CHATFIELD, J., CHEN, Y. H., SOTTILE, V., VOSS, S. R., ALBERIO, R. & JOHNSON, A. D. 2010. Axolotl Nanog activity in mouse embryonic stem cells demonstrates that ground state pluripotency is conserved from urodele amphibians to mammals. *Development,* 137**,** 2973-80.

DONOHOE, M. E., SILVA, S. S., PINTER, S. F., XU, N. & LEE, J. T. 2009. The pluripotency factor Oct4 interacts with Ctcf and also controls X-chromosome pairing and counting. *Nature,* 460**,** 128-U147.

DREVENY, I., DEEVES, S. E., FULTON, J., YUE, B., MESSMER, M., BHATTACHARYA, A., COLLINS, H. M. & HEERY, D. M. 2014. The double PHD finger domain of MOZ/MYST3 induces alpha-helical structure of the histone H3 tail to facilitate acetylation and methylation sampling and modification. *Nucleic Acids Res,* 42**,** 822-35.

EDDY, E.M., CLARK, J., GONG, D. & FENDERSON, B.A. 1981. Origin and migration of primordial germ cells in mammals. *Gamete Res.*, 4:333-362.

ENCODE Project Consortium, 2011.

EVANS, M. J. & KAUFMAN, M. H. 1981. Establishment in culture of pluripotential cells from mouse embryos. *Nature,* 292**,** 154-6.

EVANS, T., WADE, C. M., CHAPMAN, F. A., JOHNSON, A. D. & LOOSE, M. 2014. Acquisition of Germ Plasm Accelerates Vertebrate Evolution. *Science,* 344**,** 200-203.

FICZ, G., BRANCO, M. R., SEISENBERGER, S., SANTOS, F., KRUEGER, F., HORE, T. A., MARQUES, C. J., ANDREWS, S. & REIK, W. 2011. Dynamic regulation of 5-hydroxymethylcytosine in mouse ES cells and during differentiation. *Nature,* 473**,** 398-402.

FILIPESCU, D., SZENKER, E. & ALMOUZNI, G. 2013. Developmental roles of histone H3 variants and their chaperones. *Trends Genet,* 29**,** 630-40.

FIRAS, J., LIU, X. & POLO, J. M. 2014. Epigenetic memory in somatic cell nuclear transfer and induced pluripotency: evidence and implications. *Differentiation,* 88**,** 29-32.

FRIEDMAN, M. 1937. The use of ranks to avoid the assumption of normality implicit in the analysis of variance. *Journal of the American Statistical Association,* 32**,** 675-701.

FRIEDMAN, M. 1939. The use of ranks to avoid the assumption of normality implicit in the analysis of variance, (vol 32, pg 675, 1937). *Journal of the American Statistical Association,* 34**,** 109-109.

GALLANT-BEHM, C. L., RAMSEY, M. R., BENSARD, C. L., NOJEK, I., TRAN, J., LIU, M., ELLISEN, L. W. & ESPINOSA, J. M. 2012. DeltaNp63alpha represses anti-proliferative genes via H2A.Z deposition. *Genes Dev,* 26**,** 2325-36.

GANIER, O., BOCQUET, S., PEIFFER, I., BROCHARD, V., ARNAUD, P., PUY, A., JOUNEAU, A., FEIL, R., RENARD, J. P. & MECHALI, M. 2011. Synergic reprogramming of mammalian cells by combined exposure to mitotic Xenopus egg extracts and transcription factors. *Proc Natl Acad Sci U S A,* 108**,** 17331-6.

GASPAR-MAIA, A., ALAJEM, A., MESHORER, E. & RAMALHO-SANTOS, M. 2011. Open chromatin in pluripotency and reprogramming. *Nat Rev Mol Cell Biol,* 12**,** 36-47.

GAUTIER, T., ABBOTT, D. W., MOLLA, A., VERDEL, A., AUSIO, J. & DIMITROV, S. 2004. Histone variant H2ABbd confers lower stability to the nucleosome. *EMBO Rep,* 5**,** 715-20.

GEVRY, N., CHAN, H. M., LAFLAMME, L., LIVINGSTON, D. M. & GAUDREAU, L. 2007. p21 transcription is regulated by differential localization of histone H2A.Z. *Genes Dev,* 21**,** 1869-81.

GLOBISCH, D., MUNZEL, M., MULLER, M., MICHALAKIS, S., WAGNER, M., KOCH, S., BRUCKL, T., BIEL, M. & CARELL, T. 2010. Tissue distribution of 5-hydroxymethylcytosine and search for active demethylation intermediates. *PLoS One,* 5**,** e15367.

GOLDBERG, A. D., ALLIS, C. D. & BERNSTEIN, E. 2007. Epigenetics: A landscape takes shape. *Cell,* 128**,** 635-638.

GOLDBERG, A. D., BANASZYNSKI, L. A., NOH, K. M., LEWIS, P. W., ELSAESSER, S. J., STADLER, S., DEWELL, S., LAW, M., GUO, X., LI, X., WEN, D., CHAPGIER, A., DEKELVER, R. C., MILLER, J. C., LEE, Y. L., BOYDSTON, E. A., HOLMES, M. C., GREGORY, P. D., GREALLY, J. M., RAFII, S., YANG, C., SCAMBLER, P. J., GARRICK, D., GIBBONS, R. J., HIGGS, D. R., CRISTEA, I. M., URNOV, F. D., ZHENG, D. & ALLIS, C. D. 2010. Distinct factors control histone variant H3.3 localization at specific genomic regions. *Cell,* 140**,** 678-91.

GOLDMAN, J. A., GARLICK, J. D. & KINGSTON, R. E. 2010. Chromatin remodeling by imitation switch (ISWI) class ATP-dependent remodelers is stimulated by histone variant H2A.Z. *J Biol Chem,* 285**,** 4645-51.

GOLIPOUR, A., DAVID, L., LIU, Y., JAYAKUMARAN, G., HIRSCH, C. L., TRCKA, D. & WRANA, J. L. 2012. A late transition in somatic cell reprogramming requires regulators distinct from the pluripotency network. *Cell Stem Cell,* 11**,** 769-82.

GONZALEZ-MUNOZ, E., ARBOLEDA-ESTUDILLO, Y., OTU, H. H. & CIBELLI, J. B. 2014. Cell reprogramming. Histone chaperone ASF1A is required for maintenance of pluripotency and cellular reprogramming. *Science,* 345**,** 822-5.

GREER, E. L. & SHI, Y. 2012. Histone methylation: a dynamic mark in health, disease and inheritance. *Nat Rev Genet,* 13**,** 343-57.

GRUNSTEIN, M. 1997. Histone acetylation in chromatin structure and transcription. *Nature,* 389**,** 349-52.

GUO, G., YANG, J., NICHOLS, J., HALL, J. S., EYRES, I., MANSFIELD, W. & SMITH, A. 2009. Klf4 reverts developmentally programmed restriction of ground state pluripotency. *Development,* 136**,** 1063-9.

GUO, W. L., CHUNG, W. Y., QIAN, M. P., PELLEGRINI, M. & ZHANG, M. Q. 2014. Characterizing the strand-specific distribution of non-CpG methylation in human pluripotent cells. *Nucleic Acids Research,* 42**,** 3009-3016.

GURDON, J. B. 1962. The developmental capacity of nuclei taken from intestinal epithelium cells of feeding tadpoles. *J Embryol Exp Morphol,* 10**,** 622-40.

GURDON, J. B. 1986. Nuclear transplantation in eggs and oocytes. *J Cell Sci Suppl,* 4**,** 287-318.

GURDON, J. B. & UEHLINGER, V. 1966. "Fertile" intestine nuclei. *Nature,* 210**,** 1240-1.

GURDON, J. B. & WILMUT, I. 2011. Nuclear transfer to eggs and oocytes. *Cold Spring Harb Perspect Biol,* 3.

HAJKOVA, P., JEFFRIES, S. J., LEE, C., MILLER, N., JACKSON, S. P. & SURANI, M. A. 2010. Genome-wide reprogramming in the mouse germ line entails the base excision repair pathway. *Science,* 329**,** 78-82.

HALLEY-STOTT, R. P. & GURDON, J. B. 2013. Epigenetic memory in the context of nuclear reprogramming and cancer. *Brief Funct Genomics,* 12**,** 164-73.

HANSIS, C., BARRETO, G., MALTRY, N. & NIEHRS, C. 2004. Nuclear reprogramming of human somatic cells by xenopus egg extract requires BRG1. *Curr Biol,* 14**,** 1475-80.

HANSSON, J., RAFIEE, M. R., REILAND, S., POLO, J. M., GEHRING, J., OKAWA, S., HUBER, W., HOCHEDLINGER, K. & KRIJGSVELD, J. 2012. Highly coordinated proteome dynamics during reprogramming of somatic cells to pluripotency. *Cell Rep,* 2**,** 1579-92.

HARDY, S., JACQUES, P. E., GEVRY, N., FOREST, A., FORTIN, M. E., LAFLAMME, L., GAUDREAU, L. & ROBERT, F. 2009. The euchromatic and heterochromatic landscapes are shaped by antagonizing effects of transcription on H2A.Z deposition. *PLoS Genet,* 5**,** e1000687.

HATANO, S. Y., TADA, M., KIMURA, H., YAMAGUCHI, S., KONO, T., NAKANO, T., SUEMORI, H., NAKATSUJI, N. & TADA, T. 2005. Pluripotential competence of cells associated with Nanog activity. *Mech Dev,* 122**,** 67-79.

HATTORI, N., IMAO, Y., NISHINO, K., HATTORI, N., OHGANE, J., YAGI, S., TANAKA, S. & SHIOTA, K. 2007. Epigenetic regulation of Nanog gene in embryonic stem and trophoblast stem cells. *Genes Cells,* 12**,** 387-96.

HAWKINS, R. D., HON, G. C., LEE, L. K., NGO, Q., LISTER, R., PELIZZOLA, M., EDSALL, L. E., KUAN, S., LUU, Y., KLUGMAN, S., ANTOSIEWICZ-BOURGET, J., YE, Z., ESPINOZA, C., AGARWAHL, S., SHEN, L., RUOTTI, V., WANG, W., STEWART, R., THOMSON, J. A., ECKER, J. R. & REN, B. 2010. Distinct epigenomic landscapes of pluripotent and lineage-committed human cells. *Cell Stem Cell,* 6**,** 479-91.

HAWKINS, R. D., HON, G. C., YANG, C., ANTOSIEWICZ-BOURGET, J. E., LEE, L. K., NGO, Q. M., KLUGMAN, S., CHING, K. A., EDSALL, L. E., YE, Z., KUAN, S., YU, P., LIU, H., ZHANG, X., GREEN, R. D., LOBANENKOV, V. V., STEWART, R., THOMSON, J. A. & REN, B. 2011. Dynamic chromatin states in human ES cells reveal potential regulatory sequences and genes involved in pluripotency. *Cell Res,* 21**,** 1393-409.

HE, Y. F., LI, B. Z., LI, Z., LIU, P., WANG, Y., TANG, Q. Y., DING, J. P., JIA, Y. Y., CHEN, Z. C., LI, L., SUN, Y., LI, X. X., DAI, Q., SONG, C. X., ZHANG, K. L., HE, C. & XU, G. L. 2011. Tet-Mediated Formation of 5-Carboxylcytosine and Its Excision by TDG in Mammalian DNA. *Science,* 333**,** 1303-1307.

HEINTZMAN, N. D., HON, G. C., HAWKINS, R. D., KHERADPOUR, P., STARK, A., HARP, L. F., YE, Z., LEE, L. K., STUART, R. K., CHING, C. W., CHING, K. A., ANTOSIEWICZ-BOURGET, J. E., LIU, H., ZHANG, X., GREEN, R. D., LOBANENKOV, V. V., STEWART, R., THOMSON, J. A., CRAWFORD, G. E., KELLIS, M. & REN, B. 2009. Histone modifications at human enhancers reflect global cell-type-specific gene expression. *Nature,* 459**,** 108-12.

HEINTZMAN, N. D., STUART, R. K., HON, G., FU, Y., CHING, C. W., HAWKINS, R. D., BARRERA, L. O., VAN CALCAR, S., QU, C., CHING, K. A., WANG, W., WENG, Z., GREEN, R. D., CRAWFORD, G. E. & REN, B. 2007. Distinct and predictive chromatin signatures of transcriptional promoters and enhancers in the human genome. *Nat Genet,* 39**,** 311-8.

HEITZ, E. 1928. Das heterochromatin der moose. *Jahrb Wiss Botanik*, 69, 762-818.

HELLMAN, A. & CHESS, A. 2007. Gene body-specific methylation on the active X chromosome. *Science,* 315**,** 1141-3.

HELLSTEN, U., HARLAND, R. M., GILCHRIST, M. J., HENDRIX, D., JURKA, J., KAPITONOV, V., OVCHARENKO, I., PUTNAM, N. H., SHU, S., TAHER, L., BLITZ, I. L., BLUMBERG, B., DICHMANN, D. S., DUBCHAK, I., AMAYA, E., DETTER, J. C., FLETCHER, R., GERHARD, D. S., GOODSTEIN, D., GRAVES, T., GRIGORIEV, I. V., GRIMWOOD, J., KAWASHIMA, T., LINDQUIST, E., LUCAS, S. M., MEAD, P. E., MITROS, T., OGINO, H., OHTA, Y., POLIAKOV, A. V., POLLET, N., ROBERT, J., SALAMOV, A., SATER, A. K., SCHMUTZ, J., TERRY, A., VIZE, P. D., WARREN, W. C., WELLS, D., WILLS, A., WILSON, R. K., ZIMMERMAN, L. B., ZORN, A. M., GRAINGER, R., GRAMMER, T., KHOKHA, M. K., RICHARDSON, P. M. & ROKHSAR, D. S. 2010. The genome of the Western clawed frog Xenopus tropicalis. *Science,* 328**,** 633-6.

HOLLIDAY, R. & PUGH, J. E. 1975. DNA modification mechanisms and gene activity during development. *Science,* 187**,** 226-32.

HON, G. C., RAJAGOPAL, N., SHEN, Y., MCCLEARY, D. F., YUE, F., DANG, M. D. & REN, B. 2013. Epigenetic memory at embryonic enhancers identified in DNA methylation maps from adult mouse tissues. *Nature Genetics,* 45**,** 1198-U340.

HOSKINS, R. A., CARLSON, J. W., KENNEDY, C., ACEVEDO, D., EVANS-HOLM, M., FRISE, E., WAN, K. H., PARK, S., MENDEZ-LAGO, M., ROSSI, F., VILLASANTE, A., DIMITRI, P., KARPEN, G. H. & CELNIKER, S. E. 2007. Sequence finishing and mapping of Drosophila melanogaster heterochromatin. *Science,* 316**,** 1625-8.

HOU, P., LI, Y., ZHANG, X., LIU, C., GUAN, J., LI, H., ZHAO, T., YE, J., YANG, W., LIU, K., GE, J., XU, J., ZHANG, Q., ZHAO, Y. & DENG, H. 2013. Pluripotent stem cells induced from mouse somatic cells by small-molecule compounds. *Science,* 341**,** 651-4.

HOUSTON, D. W. & KING, M. L. 2000. A critical role for Xdazl, a germ plasm-localized RNA, in the differentiation of primordial germ cells in Xenopus. *Development,* 127**,** 447-56.

HU, G., CUI, K., NORTHRUP, D., LIU, C., WANG, C., TANG, Q., GE, K., LEVENS, D., CRANE-ROBINSON, C. & ZHAO, K. 2013. H2A.Z facilitates access of active and repressive complexes to chromatin in embryonic stem cell self-renewal and differentiation. *Cell Stem Cell,* 12**,** 180-92.

ICHIDA, J. K., BLANCHARD, J., LAM, K., SON, E. Y., CHUNG, J. E., EGLI, D., LOH, K. M., CARTER, A. C., DI GIORGIO, F. P., KOSZKA, K., HUANGFU, D., AKUTSU, H., LIU, D. R., RUBIN, L. L. & EGGAN, K. 2009. A small-molecule inhibitor of tgf-Beta signaling replaces sox2 in reprogramming by inducing nanog. *Cell Stem Cell,* 5**,** 491-503.

INOUE, A. & ZHANG, Y. 2011. Replication-Dependent Loss of 5-Hydroxymethylcytosine in Mouse Preimplantation Embryos. *Science,* 334**,** 194-194.

IQBAL, K., JIN, S. G., PFEIFER, G. P. & SZABO, P. E. 2011. Reprogramming of the paternal genome upon fertilization involves genome-wide oxidation of 5-methylcytosine. *Proceedings of the National Academy of Sciences of the United States of America,* 108**,** 3642-3647.

ISHIBASHI, T., LI, A., EIRIN-LOPEZ, J. M., ZHAO, M., MISSIAEN, K., ABBOTT, D. W., MEISTRICH, M., HENDZEL, M. J. & AUSIO, J. 2010. H2A.Bbd: an X-chromosome-encoded histone involved in mammalian spermiogenesis. *Nucleic Acids Res,* 38**,** 1780-9.

ITO, S., D'ALESSIO, A. C., TARANOVA, O. V., HONG, K., SOWERS, L. C. & ZHANG, Y. 2010. Role of Tet proteins in 5mC to 5hmC conversion, ES-cell self-renewal and inner cell mass specification. *Nature,* 466**,** 1129-33.

ITO, S., SHEN, L., DAI, Q., WU, S. C., COLLINS, L. B., SWENBERG, J. A., HE, C. & ZHANG, Y. 2011. Tet Proteins Can Convert 5-Methylcytosine to 5-Formylcytosine and 5-Carboxylcytosine. *Science,* 333**,** 1300-1303.

IWASAKI, Y., FUJIO, K., OKAMURA, T., YANAI, A., SUMITOMO, S., SHODA, H., TAMURA, T., YOSHIDA, H., CHARNAY, P. & YAMAMOTO, K. 2013. Egr-2 transcription factor is

required for Blimp-1-mediated IL-10 production in IL-27-stimulated CD4+ T cells. *Eur J Immunol,* 43**,** 1063-73.

JIN, C. & FELSENFELD, G. 2007. Nucleosome stability mediated by histone variants H3.3 and H2A.Z. *Genes Dev,* 21**,** 1519-29.

JOHNSON, A. D., BACHVAROVA, R. F., DRUM, M. & MASI, T. 2001. Expression of axolotl DAZL RNA, a marker of germ plasm: widespread maternal RNA and onset of expression in germ cells approaching the gonad. *Dev Biol,* 234**,** 402-15.

JOHNSON, A. D., CROTHER, B., WHITE, M. E., PATIENT, R., BACHVAROVA, R. F., DRUM, M. & MASI, T. 2003. Regulative germ cell specification in axolotl embryos: a primitive trait conserved in the mammalian lineage. *Philos Trans R Soc Lond B Biol Sci,* 358**,** 1371-9.

JOHNSON, A. D., RICHARDSON, E., BACHVAROVA, R. F. & CROTHER, B. I. 2011. Evolution of the germ line-soma relationship in vertebrate embryos. *Reproduction,* 141**,** 291-300.

JONES, P. A. 1999. The DNA methylation paradox. *Trends Genet,* 15**,** 34-7.

JULLIEN, J., MIYAMOTO, K., PASQUE, V., ALLEN, G. E., BRADSHAW, C. R., GARRETT, N. J., HALLEY-STOTT, R. P., KIMURA, H., OHSUMI, K. & GURDON, J. B. 2014. Hierarchical molecular events driven by oocyte-specific factors lead to rapid and extensive reprogramming. *Mol Cell,* 55**,** 524-36.

KAGEY, M. H., NEWMAN, J. J., BILODEAU, S., ZHAN, Y., ORLANDO, D. A., VAN BERKUM, N. L., EBMEIER, C. C., GOOSSENS, J., RAHL, P. B., LEVINE, S. S., TAATJES, D. J., DEKKER, J. & YOUNG, R. A. 2010. Mediator and cohesin connect gene expression and chromatin architecture. *Nature,* 467**,** 430-435.

KAGEY, M. H., NEWMAN, J. J., BILODEAU, S., ZHAN, Y., ORLANDO, D. A., VAN BERKUM, N. L., EBMEIER, C. C., GOOSSENS, J., RAHL, P. B., LEVINE, S. S., TAATJES, D. J., DEKKER, J. & YOUNG, R. A. 2011. Mediator and cohesin connect gene expression and chromatin architecture (vol 467, pg 430, 2010). *Nature,* 472**,** 247-247.

KAMAKAKA, R. T. & BIGGINS, S. 2005. Histone variants: deviants? *Genes Dev,* 19**,** 295-310.

KASS, S. U., LANDSBERGER, N. & WOLFFE, A. P. 1997. DNA methylation directs a time-dependent repression of transcription initiation. *Curr Biol,* 7**,** 157-65.

KIDDER, B. L., PALMER, S. & KNOTT, J. G. 2009. SWI/SNF-Brg1 regulates self-renewal and occupies core pluripotency-related genes in embryonic stem cells. *Stem Cells,* 27**,** 317-28.

KIM, C. G., CHUNG, I. Y., LIM, Y., LEE, Y. H. & SHIN, S. Y. 2011. A Tcf/Lef element within the enhancer region of the human NANOG gene plays a role in promoter activation. *Biochem Biophys Res Commun,* 410**,** 637-42.

KIM, K., DOI, A., WEN, B., NG, K., ZHAO, R., CAHAN, P., KIM, J., ARYEE, M. J., JI, H., EHRLICH, L. I. R., YABUUCHI, A., TAKEUCHI, A., CUNNIFF, K. C., HONGGUANG, H., MCKINNEY-FREEMAN, S., NAVEIRAS, O., YOON, T. J., IRIZARRY, R. A., JUNG, N., SEITA, J., HANNA, J., MURAKAMI, P., JAENISCH, R., WEISSLEDER, R., ORKIN, S. H., WEISSMAN, I. L., FEINBERG, A. P. & DALEY, G. Q. 2010a. Epigenetic memory in induced pluripotent stem cells. *Nature,* 467**,** 285-U60.

KIM, T. K., HEMBERG, M., GRAY, J. M., COSTA, A. M., BEAR, D. M., WU, J., HARMIN, D. A., LAPTEWICZ, M., BARBARA-HALEY, K., KUERSTEN, S., MARKENSCOFF-PAPADIMITRIOU, E., KUHL, D., BITO, H., WORLEY, P. F., KREIMAN, G. & GREENBERG, M. E. 2010b. Widespread transcription at neuronal activity-regulated enhancers. *Nature,* 465**,** 182-7.

KIMURA, H. 2013. Histone modifications for human epigenome analysis. *J Hum Genet,* 58**,** 439-45.

KORNBERG, R. D. 1974. Chromatin structure: a repeating unit of histones and DNA. *Science,* 184**,** 868-71.

KREJCI, J., UHLIROVA, R., GALIOVA, G., KOZUBEK, S., SMIGOVA, J. & BARTOVA, E. 2009. Genome-wide reduction in H3K9 acetylation during human embryonic stem cell differentiation. *J Cell Physiol,* 219**,** 677-87.

KRIAUCIONIS, S. & HEINTZ, N. 2009. The nuclear DNA base 5-hydroxymethylcytosine is present in Purkinje neurons and the brain. *Science,* 324**,** 929-30.

KU, M., JAFFE, J. D., KOCHE, R. P., RHEINBAY, E., ENDOH, M., KOSEKI, H., CARR, S. A. & BERNSTEIN, B. E. 2012. H2A.Z landscapes and dual modifications in pluripotent and multipotent stem cells underlie complex genome regulatory functions. *Genome Biol,* 13**,** R85.

KURODA, T., TADA, M., KUBOTA, H., KIMURA, H., HATANO, S. Y., SUEMORI, H., NAKATSUJI, N. & TADA, T. 2005. Octamer and Sox elements are required for transcriptional cis regulation of Nanog gene expression. *Mol Cell Biol,* 25**,** 2475-85.

LAI, F. & KING, M. L. 2013. Repressive translational control in germ cells. *Mol Reprod Dev,* 80**,** 665-76.

LALONDE, M. E., CHENG, X. & COTE, J. 2014. Histone target selection within chromatin: an exemplary case of teamwork. *Genes Dev,* 28**,** 1029-41.

LAURENT, L., WONG, E., LI, G., HUYNH, T., TSIRIGOS, A., ONG, C. T., LOW, H. M., KIN SUNG, K. W., RIGOUTSOS, I., LORING, J. & WEI, C. L. 2010. Dynamic changes in the human methylome during differentiation. *Genome Res,* 20**,** 320-31.

LAVIAL, F., ACLOQUE, H., BERTOCCHINI, F., MACLEOD, D. J., BOAST, S., BACHELARD, E., MONTILLET, G., THENOT, S., SANG, H. M., STERN, C. D., SAMARUT, J. & PAIN, B. 2007. The Oct4 homologue PouV and Nanog regulate pluripotency in chicken embryonic stem cells. *Development,* 134**,** 3549-63.

LEE, J. S., SMITH, E. & SHILATIFARD, A. 2010. The language of histone crosstalk. *Cell,* 142**,** 682-5.

LEVASSEUR, D. N., WANG, J., DORSCHNER, M. O., STAMATOYANNOPOULOS, J. A. & ORKIN, S. H. 2008. Oct4 dependence of chromatin structure within the extended Nanog locus in ES cells. *Genes & Development,* 22**,** 575-580.

LI, B., CAREY, M. & WORKMAN, J. L. 2007. The role of chromatin during transcription. *Cell,* 128**,** 707-19.

LI, E., BESTOR, T. H. & JAENISCH, R. 1992. Targeted mutation of the DNA methyltransferase gene results in embryonic lethality. *Cell,* 69**,** 915-26.

LI, R., LIANG, J., NI, S., ZHOU, T., QING, X., LI, H., HE, W., CHEN, J., LI, F., ZHUANG, Q., QIN, B., XU, J., LI, W., YANG, J., GAN, Y., QIN, D., FENG, S., SONG, H., YANG, D., ZHANG, B., ZENG, L., LAI, L., ESTEBAN, M. A. & PEI, D. 2010. A mesenchymal-to-epithelial transition initiates and is required for the nuclear reprogramming of mouse fibroblasts. *Cell Stem Cell,* 7**,** 51-63.

LI, W., SUN, W., ZHANG, Y., WEI, W., AMBASUDHAN, R., XIA, P., TALANTOVA, M., LIN, T., KIM, J., WANG, X., KIM, W. R., LIPTON, S. A., ZHANG, K. & DING, S. 2011. Rapid induction and long-term self-renewal of primitive neural precursors from human embryonic stem cells by small molecule inhibitors. *Proc Natl Acad Sci U S A,* 108**,** 8299-304.

LIANG, J., WAN, M., ZHANG, Y., GU, P., XIN, H., JUNG, S. Y., QIN, J., WONG, J., COONEY, A. J., LIU, D. & SONGYANG, Z. 2008. Nanog and Oct4 associate with unique transcriptional repression complexes in embryonic stem cells. *Nat Cell Biol,* 10**,** 731-9.

LISTER, R., PELIZZOLA, M., DOWEN, R. H., HAWKINS, R. D., HON, G., TONTI-FILIPPINI, J., NERY, J. R., LEE, L., YE, Z., NGO, Q. M., EDSALL, L., ANTOSIEWICZ-BOURGET, J., STEWART, R., RUOTTI, V., MILLAR, A. H., THOMSON, J. A., REN, B. & ECKER, J. R.

2009. Human DNA methylomes at base resolution show widespread epigenomic differences. *Nature,* 462**,** 315-322.

LOH, Y. H., WU, Q., CHEW, J. L., VEGA, V. B., ZHANG, W., CHEN, X., BOURQUE, G., GEORGE, J., LEONG, B., LIU, J., WONG, K. Y., SUNG, K. W., LEE, C. W., ZHAO, X. D., CHIU, K. P., LIPOVICH, L., KUZNETSOV, V. A., ROBSON, P., STANTON, L. W., WEI, C. L., RUAN, Y., LIM, B. & NG, H. H. 2006. The Oct4 and Nanog transcription network regulates pluripotency in mouse embryonic stem cells. *Nat Genet,* 38**,** 431-40.

LORCH, Y., LAPOINTE, J. W. & KORNBERG, R. D. 1987. Nucleosomes Inhibit the Initiation of Transcription but Allow Chain Elongation with the Displacement of Histones. *Cell,* 49**,** 203-210.

LUGER, K., MADER, A. W., RICHMOND, R. K., SARGENT, D. F. & RICHMOND, T. J. 1997. Crystal structure of the nucleosome core particle at 2.8 A resolution. *Nature,* 389**,** 251-60.

MAH, Y. H., HSU, C. S., LIU, C. H., LIU, C. J., LAI, M. Y., CHEN, P. J., CHEN, D. S. & KAO, J. H. 2011. Serum p53 gene polymorphisms and severity of hepatitis B or C-related chronic liver diseases in Taiwan. *Hepatol Int,* 5**,** 814-21.

MALIK, H. S. & HENIKOFF, S. 2003. Phylogenomics of the nucleosome. *Nat Struct Biol,* 10**,** 882-91.

MARTIN, G. R. 1981. Isolation of a pluripotent cell line from early mouse embryos cultured in medium conditioned by teratocarcinoma stem cells. *Proc Natl Acad Sci U S A,* 78**,** 7634-8.

MATTOUT, A. & MESHORER, E. 2010. Chromatin plasticity and genome organization in pluripotent embryonic stem cells. *Curr Opin Cell Biol,* 22**,** 334-41.

MEDVEDEVA, Y. A., KHAMIS, A. M., KULAKOVSKIY, I. V., BA-ALAWI, W., BHUYAN, M. S., KAWAJI, H., LASSMANN, T., HARBERS, M., FORREST, A. R., BAJIC, V. B. & CONSORTIUM, F. 2014. Effects of cytosine methylation on transcription factor binding sites. *BMC Genomics,* 15**,** 119.

MESHORER, E., YELLAJOSHULA, D., GEORGE, E., SCAMBLER, P. J., BROWN, D. T. & MISTELI, T. 2006. Hyperdynamic plasticity of chromatin proteins in pluripotent embryonic stem cells. *Dev Cell,* 10**,** 105-16.

MESSERSCHMIDT, D. M., KNOWLES, B. B. & SOLTER, D. 2014. DNA methylation dynamics during epigenetic reprogramming in the germline and preimplantation embryos. *Genes Dev,* 28**,** 812-28.

MIKKELSEN, T. S., HANNA, J., ZHANG, X., KU, M., WERNIG, M., SCHORDERET, P., BERNSTEIN, B. E., JAENISCH, R., LANDER, E. S. & MEISSNER, A. 2008. Dissecting direct reprogramming through integrative genomic analysis. *Nature,* 454**,** 49-55.

MITO, Y., HENIKOFF, J. G. & HENIKOFF, S. 2007. Histone replacement marks the boundaries of cis-regulatory domains. *Science,* 315**,** 1408-11.

MITSUI, K., TOKUZAWA, Y., ITOH, H., SEGAWA, K., MURAKAMI, M., TAKAHASHI, K., MARUYAMA, M., MAEDA, M. & YAMANAKA, S. 2003. The homeoprotein Nanog is required for maintenance of pluripotency in mouse epiblast and ES cells. *Cell,* 113**,** 631-42.

MIYAMOTO, K., FURUSAWA, T., OHNUKI, M., GOEL, S., TOKUNAGA, T., MINAMI, N., YAMADA, M., OHSUMI, K. & IMAI, H. 2007. Reprogramming events of mammalian somatic cells induced by Xenopus laevis egg extracts. *Mol Reprod Dev,* 74**,** 1268-77.

MOAREFI, A. H. & CHEDIN, F. 2011. ICF syndrome mutations cause a broad spectrum of biochemical defects in DNMT3B-mediated de novo DNA methylation. *J Mol Biol,* 409**,** 758-72.

MORRISON, G. M. & BRICKMAN, J. M. 2006. Conserved roles for Oct4 homologues in maintaining multipotency during early vertebrate development. *Development,* 133**,** 2011-22.

MULLIN, N. P., YATES, A., ROWE, A. J., NIJMEIJER, B., COLBY, D., BARLOW, P. N., WALKINSHAW, M. D. & CHAMBERS, I. 2008. The pluripotency rheostat Nanog functions as a dimer. *Biochem J,* 411**,** 227-31.

MURATA, K., KOUZARIDES, T., BANNISTER, A. J. & GURDON, J. B. 2010. Histone H3 lysine 4 methylation is associated with the transcriptional reprogramming efficiency of somatic nuclei by oocytes. *Epigenetics Chromatin,* 3**,** 4.

NASHUN, B., HILL, P. W. S. & HAJKOVA, P. 2015. Reprogramming of cell fate: epigenetic memory and the erasure of memories past. *Embo Journal,* 34**,** 1296-1308.

NAVARRO, P., FESTUCCIA, N., COLBY, D., GAGLIARDI, A., MULLIN, N. P., ZHANG, W., KARWACKI-NEISIUS, V., OSORNO, R., KELLY, D., ROBERTSON, M. & CHAMBERS, I. 2012. OCT4/SOX2-independent Nanog autorepression modulates heterogeneous Nanog gene expression in mouse ES cells. *EMBO J,* 31**,** 4547-62.

NERI, F., INCARNATO, D., KREPELOVA, A., RAPELLI, S., ANSELMI, F., PARLATO, C., MEDANA, C., DAL BELLO, F. & OLIVIERO, S. 2015. Single-Base Resolution Analysis of 5-Formyl and 5-Carboxyl Cytosine Reveals Promoter DNA Methylation Dynamics. *Cell Rep*.

NG, R. K. & GURDON, J. B. 2005. Epigenetic memory of active gene transcription is inherited through somatic cell nuclear transfer. *Proceedings of the National Academy of Sciences of the United States of America,* 102**,** 1957-1962.

NG, R. K. & GURDON, J. B. 2008a. Epigenetic inheritance of cell differentiation status. *Cell Cycle,* 7**,** 1173-7.

NG, R. K. & GURDON, J. B. 2008b. Epigenetic memory of an active gene state depends on histone H3.3 incorporation into chromatin in the absence of transcription. *Nature Cell Biology,* 10**,** 102-U83.

NICHOLS, J., ZEVNIK, B., ANASTASSIADIS, K., NIWA, H., KLEWE-NEBENIUS, D., CHAMBERS, I., SCHOLER, H. & SMITH, A. 1998. Formation of pluripotent stem cells in the mammalian embryo depends on the POU transcription factor Oct4. *Cell,* 95**,** 379-91.

NIEUWKOOP, P. D. 1996. What are the key advantages and disadvantages of urodele species compared to anurans as a model system for experimental analysis of early development? *Int J Dev Biol,* 40**,** 617-9.

NISHIMOTO, M., FUKUSHIMA, A., OKUDA, A. & MURAMATSU, M. 1999. The gene for the embryonic stem cell coactivator UTF1 carries a regulatory element which selectively interacts with a complex composed of Oct-3/4 and Sox-2. *Mol Cell Biol,* 19**,** 5453-65.

NITZSCHE, A., PASZKOWSKI-ROGACZ, M., MATARESE, F., JANSSEN-MEGENS, E. M., HUBNER, N. C., SCHULZ, H., DE VRIES, I., DING, L., HUEBNER, N., MANN, M., STUNNENBERG, H. G. & BUCHHOLZ, F. 2011. RAD21 Cooperates with Pluripotency Transcription Factors in the Maintenance of Embryonic Stem Cell Identity. *Plos One,* 6.

NIWA, H., MIYAZAKI, J. & SMITH, A. G. 2000. Quantitative expression of Oct-3/4 defines differentiation, dedifferentiation or self-renewal of ES cells. *Nat Genet,* 24**,** 372-6.

OBRI, A., OUARARHNI, K., PAPIN, C., DIEBOLD, M. L., PADMANABHAN, K., MAREK, M., STOLL, I., ROY, L., REILLY, P. T., MAK, T. W., DIMITROV, S., ROMIER, C. & HAMICHE, A. 2014. ANP32E is a histone chaperone that removes H2A.Z from chromatin. *Nature,* 505**,** 648-53.

OKANO, M., BELL, D. W., HABER, D. A. & LI, E. 1999. DNA methyltransferases Dnmt3a and Dnmt3b are essential for de novo methylation and mammalian development. *Cell,* 99**,** 247-257.

OKANO, M., XIE, S. P. & LI, E. 1998. Cloning and characterization of a family of novel mammalian DNA (cytosine-5) methyltransferases. *Nature Genetics,* 19**,** 219-220.

OKUMURA-NAKANISHI, S., SAITO, M., NIWA, H. & ISHIKAWA, F. 2005. Oct-3/4 and Sox2 regulate Oct-3/4 gene in embryonic stem cells. *J Biol Chem,* 280**,** 5307-17.

OKUWAKI, M., KATO, K., SHIMAHARA, H., TATE, S. & NAGATA, K. 2005. Assembly and disassembly of nucleosome core particles containing histone variants by human nucleosome assembly protein I. *Mol Cell Biol,* 25**,** 10639-51.

OLMER, R., HAASE, A., MERKERT, S., CUI, W., PALECEK, J., RAN, C., KIRSCHNING, A., SCHEPER, T., GLAGE, S., MILLER, K., CURNOW, E. C., HAYES, E. S. & MARTIN, U. 2010. Long term expansion of undifferentiated human iPS and ES cells in suspension culture using a defined medium. *Stem Cell Research,* 5**,** 51-64.

PALMIERI, S. L., PETER, W., HESS, H. & SCHOLER, H. R. 1994. Oct-4 transcription factor is differentially expressed in the mouse embryo during establishment of the first two extraembryonic cell lineages involved in implantation. *Dev Biol,* 166**,** 259-67.

PANOPOULOS, A. D., YANES, O., RUIZ, S., KIDA, Y. S., DIEP, D., TAUTENHAHN, R., HERRERIAS, A., BATCHELDER, E. M., PLONGTHONGKUM, N., LUTZ, M., BERGGREN, W. T., ZHANG, K., EVANS, R. M., SIUZDAK, G. & IZPISUA BELMONTE, J. C. 2012. The metabolome of induced pluripotent stem cells reveals metabolic changes occurring in somatic cell reprogramming. *Cell Res,* 22**,** 168-77.

PAPAMICHOS-CHRONAKIS, M., WATANABE, S., RANDO, O. J. & PETERSON, C. L. 2011. Global regulation of H2A.Z localization by the INO80 chromatin-remodeling enzyme is essential for genome integrity. *Cell,* 144**,** 200-13.

PARK, S. H., PARK, S. H., KOOK, M. C., KIM, E. Y., PARK, S. & LIM, J. H. 2004. Ultrastructure of human embryonic stem cells and spontaneous and retinoic acid-induced differentiating cells. *Ultrastruct Pathol,* 28**,** 229-38.

PASQUE, V., GILLICH, A., GARRETT, N. & GURDON, J. B. 2011a. Histone variant macroH2A confers resistance to nuclear reprogramming. *Embo Journal,* 30**,** 2373-2387.

PASQUE, V., HALLEY-STOTT, R. P., GILLICH, A., GARRETT, N. & GURDON, J. B. 2011b. Epigenetic stability of repressed states involving the histone variant macroH2A revealed by nuclear transfer to Xenopus oocytes. *Nucleus-Austin,* 2**,** 533-539.

PASQUE, V., RADZISHEUSKAYA, A., GILLICH, A., HALLEY-STOTT, R. P., PANAMAROVA, M., ZERNICKA-GOETZ, M., SURANI, M. A. & SILVA, J. C. 2012. Histone variant macroH2A marks embryonic differentiation in vivo and acts as an epigenetic barrier to induced pluripotency. *J Cell Sci,* 125**,** 6094-104.

PASTOR, W. A., PAPE, U. J., HUANG, Y., HENDERSON, H. R., LISTER, R., KO, M., MCLOUGHLIN, E. M., BRUDNO, Y., MAHAPATRA, S., KAPRANOV, P., TAHILIANI, M., DALEY, G. Q., LIU, X. S., ECKER, J. R., MILOS, P. M., AGARWAL, S. & RAO, A. 2011. Genome-wide mapping of 5-hydroxymethylcytosine in embryonic stem cells. *Nature,* 473**,** 394-397.

PEKOWSKA, A., BENOUKRAF, T., ZACARIAS-CABEZA, J., BELHOCINE, M., KOCH, F., HOLOTA, H., IMBERT, J., ANDRAU, J. C., FERRIER, P. & SPICUGLIA, S. 2011. H3K4 tri-methylation provides an epigenetic signature of active enhancers. *EMBO J,* 30**,** 4198-210.

PERRY, A. C. & WAKAYAMA, T. 2002. Untimely ends and new beginnings in mouse cloning. *Nat Genet,* 30**,** 243-4.

PESCE, M. & SCHOLER, H. R. 2001. Oct-4: gatekeeper in the beginnings of mammalian development. *Stem Cells,* 19**,** 271-8.

PETERS, T. J., BUCKLEY, M. J., STATHAM, A. L., PIDSLEY, R., SAMARAS, K., R, V. L., CLARK, S. J. & MOLLOY, P. L. 2015. De novo identification of differentially methylated regions in the human genome. *Epigenetics Chromatin,* 8**,** 6.

PFAFFENEDER, T., HACKNER, B., TRUSS, M., MUNZEL, M., MULLER, M., DEIML, C. A., HAGEMEIER, C. & CARELL, T. 2011. The Discovery of 5-Formylcytosine in Embryonic Stem Cell DNA. *Angewandte Chemie-International Edition,* 50**,** 7008-7012.

PFEIFFER, M. J., SIATKOWSKI, M., PAUDEL, Y., BALBACH, S. T., BAEUMER, N., CROSETTO, N., DREXLER, H. C., FUELLEN, G. & BOIANI, M. 2011. Proteomic analysis of mouse oocytes reveals 28 candidate factors of the "reprogrammome". *J Proteome Res,* 10**,** 2140-53.

PHIEL, C. J., ZHANG, F., HUANG, E. Y., GUENTHER, M. G., LAZAR, M. A. & KLEIN, P. S. 2001. Histone deacetylase is a direct target of valproic acid, a potent anticonvulsant, mood stabilizer, and teratogen. *J Biol Chem,* 276**,** 36734-41.

PIYASENA, C., REYNOLDS, R. M., KHULAN, B., SECKL, J. R., MENON, G. & DRAKE, A. J. 2015. Placental 5-methylcytosine and 5-hydroxymethylcytosine patterns associate with size at birth. *Epigenetics,* 10**,** 692-7.

POLO, J. M., ANDERSSEN, E., WALSH, R. M., SCHWARZ, B. A., NEFZGER, C. M., LIM, S. M., BORKENT, M., APOSTOLOU, E., ALAEI, S., CLOUTIER, J., BAR-NUR, O., CHELOUFI, S., STADTFELD, M., FIGUEROA, M. E., ROBINTON, D., NATESAN, S., MELNICK, A., ZHU, J., RAMASWAMY, S. & HOCHEDLINGER, K. 2012. A molecular roadmap of reprogramming somatic cells into iPS cells. *Cell,* 151**,** 1617-32.

POMBO, A. & DILLON, N. 2015. Three-dimensional genome architecture: players and mechanisms. *Nat Rev Mol Cell Biol,* 16**,** 245-57.

RADA-IGLESIAS, A. & WYSOCKA, J. 2011. Epigenomics of human embryonic stem cells and induced pluripotent stem cells: insights into pluripotency and implications for disease. *Genome Med,* 3**,** 36.

RAMSAHOYE, B. H., BINISZKIEWICZ, D., LYKO, F., CLARK, V., BIRD, A. P. & JAENISCH, R. 2000. Non-CpG methylation is prevalent in embryonic stem cells and may be mediated by DNA methyltransferase 3a. *Proceedings of the National Academy of Sciences of the United States of America,* 97**,** 5237-5242.

RANJAN, A., MIZUGUCHI, G., FITZGERALD, P. C., WEI, D., WANG, F., HUANG, Y., LUK, E., WOODCOCK, C. L. & WU, C. 2013. Nucleosome-free region dominates histone acetylation in targeting SWR1 to promoters for H2A.Z replacement. *Cell,* 154**,** 1232-45.

RESNICK, J. L., BIXLER, L. S., CHENG, L. & DONOVAN, P. J. 1992. Long-term proliferation of mouse primordial germ cells in culture. *Nature,* 359**,** 550-1.

RHEE, I., BACHMAN, K. E., PARK, B. H., JAIR, K. W., YEN, R. W. C., SCHUEBEL, K. E., CUI, H. M., FEINBERG, A. P., LENGAUER, C., KINZLER, K. W., BAYLIN, S. B. & VOGELSTEIN, B. 2002. DNMT1 and DNMT3b cooperate to silence genes in human cancer cells. *Nature,* 416**,** 552-556.

RIGGS, A. D. 1975. X inactivation, differentiation, and DNA methylation. *Cytogenet Cell Genet,* 14**,** 9-25.

ROBERTSON, K. D. 2005. DNA methylation and human disease. *Nature Reviews Genetics,* 6**,** 597-610.

RODDA, D. J., CHEW, J. L., LIM, L. H., LOH, Y. H., WANG, B., NG, H. H. & ROBSON, P. 2005. Transcriptional regulation of nanog by OCT4 and SOX2. *J Biol Chem,* 280**,** 24731-7.

ROTHBART, S. B. & STRAHL, B. D. 2014. Interpreting the language of histone and DNA modifications. *Biochim Biophys Acta,* 1839**,** 627-43.

ROUNTREE, M. R. & SELKER, E. U. 1997. DNA methylation inhibits elongation but not initiation of transcription in Neurospora crassa. *Genes Dev,* 11**,** 2383-95.

RUHL, D. D., JIN, J., CAI, Y., SWANSON, S., FLORENS, L., WASHBURN, M. P., CONAWAY, R. C., CONAWAY, J. W. & CHRIVIA, J. C. 2006. Purification of a human SRCAP complex that remodels chromatin by incorporating the histone variant H2A.Z into nucleosomes. *Biochemistry,* 45**,** 5671-7.

RUZOV, A., TSENKINA, Y., SERIO, A., DUDNAKOVA, T., FLETCHER, J., BAI, Y., CHEBOTAREVA, T., PELLS, S., HANNOUN, Z., SULLIVAN, G., CHANDRAN, S., HAY, D. C., BRADLEY, M., WILMUT, I. & DE SOUSA, P. 2011. Lineage-specific distribution of high levels of genomic 5-hydroxymethylcytosine in mammalian development. *Cell Res,* 21**,** 1332-42.

SANCHEZ-SANCHEZ, A. V., CAMP, E. & MULLOR, J. L. 2011. Fishing pluripotency mechanisms in vivo. *Int J Biol Sci,* 7**,** 410-7.

SANCHO-MARTINEZ, I. & IZPISUA BELMONTE, J. C. 2013. Stem cells: Surf the waves of reprogramming. *Nature,* 493**,** 310-1.

SANTOS, F., HENDRICH, B., REIK, W. & DEAN, W. 2002. Dynamic reprogramming of DNA methylation in the early mouse embryo. *Dev Biol,* 241**,** 172-82.

SARCINELLA, E., ZUZARTE, P. C., LAU, P. N., DRAKER, R. & CHEUNG, P. 2007. Monoubiquitylation of H2A.Z distinguishes its association with euchromatin or facultative heterochromatin. *Mol Cell Biol,* 27**,** 6457-68.

SCHAEFER, M. & LYKO, F. 2007. DNA methylation with a sting: an active DNA methylation system in the honeybee. *Bioessays,* 29**,** 208-11.

SCHLAEGER, T. M., DAHERON, L., BRICKLER, T. R., ENTWISLE, S., CHAN, K., CIANCI, A., DEVINE, A., ETTENGER, A., FITZGERALD, K., GODFREY, M., GUPTA, D., MCPHERSON, J., MALWADKAR, P., GUPTA, M., BELL, B., DOI, A., JUNG, N., LI, X., LYNES, M. S., BROOKES, E., CHERRY, A. B. C., DEMIRBAS, D., TSANKOV, A. M., ZON, L. I., RUBIN, L. L., FEINBERG, A. P., MEISSNER, A., COWAN, C. A. & DALEY, G. Q. 2015. A comparison of non-integrating reprogramming methods. *Nature Biotechnology,* 33**,** 58-U230.

SCHNEIDERMAN, J. I., ORSI, G. A., HUGHES, K. T., LOPPIN, B. & AHMAD, K. 2012. Nucleosome-depleted chromatin gaps recruit assembly factors for the H3.3 histone variant. *Proc Natl Acad Sci U S A,* 109**,** 19721-6.

SCHUETTENGRUBER, B., MARTINEZ, A. M., IOVINO, N. & CAVALLI, G. 2011. Trithorax group proteins: switching genes on and keeping them active. *Nat Rev Mol Cell Biol,* 12**,** 799-814.

SCHWEIKHARD, V., MENG, C., MURAKAMI, K., KAPLAN, C. D., KORNBERG, R. D. & BLOCK, S. M. 2014. Transcription factors TFIIF and TFIIS promote transcript elongation by RNA polymerase II by synergistic and independent mechanisms. *Proc Natl Acad Sci U S A,* 111**,** 6642-7.

SENNER, C. E. 2011. The role of DNA methylation in mammalian development. *Reprod Biomed Online,* 22**,** 529-35.

SHIPONY, Z., MUKAMEL, Z., COHEN, N. M., LANDAN, G., CHOMSKY, E., ZELIGER, S. R., FRIED, Y. C., AINBINDER, E., FRIEDMAN, N. & TANAY, A. 2014. Dynamic and static maintenance of epigenetic memory in pluripotent and somatic cells. *Nature,* 513**,** 115-+.

SILVA, J., NICHOLS, J., THEUNISSEN, T. W., GUO, G., VAN OOSTEN, A. L., BARRANDON, O., WRAY, J., YAMANAKA, S., CHAMBERS, I. & SMITH, A. 2009. Nanog is the gateway to the pluripotent ground state. *Cell,* 138**,** 722-37.

SIMONSSON, S. & GURDON, J. 2004. DNA demethylation is necessary for the epigenetic reprogramming of somatic cell nuclei. *Nat Cell Biol,* 6**,** 984-90.

SMALLWOOD, S. A., TOMIZAWA, S., KRUEGER, F., RUF, N., CARLI, N., SEGONDS-PICHON, A., SATO, S., HATA, K., ANDREWS, S. R. & KELSEY, G. 2011. Dynamic CpG island

methylation landscape in oocytes and preimplantation embryos. *Nature Genetics,* 43**,** 811-U126.

SMITH, A. 2005. The battlefield of pluripotency. *Cell,* 123**,** 757-60.

SMITH, Z. D. & MEISSNER, A. 2013. DNA methylation: roles in mammalian development. *Nat Rev Genet,* 14**,** 204-20.

SOBOLEVA, T. A., NEKRASOV, M., PAHWA, A., WILLIAMS, R., HUTTLEY, G. A. & TREMETHICK, D. J. 2012. A unique H2A histone variant occupies the transcriptional start site of active genes. *Nat Struct Mol Biol,* 19**,** 25-30.

SOUFI, A., DONAHUE, G. & ZARET, K. S. 2012. Facilitators and impediments of the pluripotency reprogramming factors' initial engagement with the genome. *Cell,* 151**,** 994-1004.

SRIDHARAN, R., TCHIEU, J., MASON, M. J., YACHECHKO, R., KUOY, E., HORVATH, S., ZHOU, Q. & PLATH, K. 2009. Role of the Murine Reprogramming Factors in the Induction of Pluripotency. *Cell,* 136**,** 364-377.

STADTFELD, M., NAGAYA, M., UTIKAL, J., WEIR, G. & HOCHEDLINGER, K. 2008. Induced pluripotent stem cells generated without viral integration. *Science,* 322**,** 945-9.

STANCHEVA, I., HENSEY, C. & MEEHAN, R. R. 2001. Loss of the maintenance methyltransferase, xDnmt1, induces apoptosis in Xenopus embryos. *Embo Journal,* 20**,** 1963-1973.

STRAHL, B. D. & ALLIS, C. D. 2000. The language of covalent histone modifications. *Nature,* 403**,** 41-5.

STRAHL, B. D., OHBA, R., COOK, R. G. & ALLIS, C. D. 1999. Methylation of histone H3 at lysine 4 is highly conserved and correlates with transcriptionally active nuclei in Tetrahymena. *Proc Natl Acad Sci U S A,* 96**,** 14967-72.

STROUD, H., FENG, S., MOREY KINNEY, S., PRADHAN, S. & JACOBSEN, S. E. 2011. 5-Hydroxymethylcytosine is associated with enhancers and gene bodies in human embryonic stem cells. *Genome Biol,* 12**,** R54.

STRUHL, G. & ADACHI, A. 1998. Nuclear access and action of notch in vivo. *Cell,* 93**,** 649-60.

SUBRAMANIAN, V., FIELDS, P. A. & BOYER, L. A. 2015. H2A.Z: a molecular rheostat for transcriptional control. *F1000Prime Rep,* 7**,** 01.

SUBRAMANIAN, V., MAZUMDER, A., SURFACE, L. E., BUTTY, V. L., FIELDS, P. A., ALWAN, A., TORREY, L., THAI, K. K., LEVINE, S. S., BATHE, M. & BOYER, L. A. 2013. H2A.Z acidic patch couples chromatin dynamics to regulation of gene expression programs during ESC differentiation. *PLoS Genet,* 9**,** e1003725.

SUTCLIFFE, E. L., PARISH, I. A., HE, Y. Q., JUELICH, T., TIERNEY, M. L., RANGASAMY, D., MILBURN, P. J., PARISH, C. R., TREMETHICK, D. J. & RAO, S. 2009. Dynamic histone variant exchange accompanies gene induction in T cells. *Mol Cell Biol,* 29**,** 1972-86.

SUTO, R. K., CLARKSON, M. J., TREMETHICK, D. J. & LUGER, K. 2000. Crystal structure of a nucleosome core particle containing the variant histone H2A.Z. *Nat Struct Biol,* 7**,** 1121-4.

SZWAGIERCZAK, A., BULTMANN, S., SCHMIDT, C. S., SPADA, F. & LEONHARDT, H. 2010. Sensitive enzymatic quantification of 5-hydroxymethylcytosine in genomic DNA. *Nucleic Acids Res,* 38**,** e181.

TABERLAY, P. C., KELLY, T. K., LIU, C. C., YOU, J. S., DE CARVALHO, D. D., MIRANDA, T. B., ZHOU, X. J., LIANG, G. & JONES, P. A. 2011. Polycomb-repressed genes have permissive enhancers that initiate reprogramming. *Cell,* 147**,** 1283-94.

TACHIBANA, M., AMATO, P., SPARMAN, M., GUTIERREZ, N. M., TIPPNER-HEDGES, R., MA, H., KANG, E., FULATI, A., LEE, H. S., SRITANAUDOMCHAI, H., MASTERSON, K., LARSON, J., EATON, D., SADLER-FREDD, K., BATTAGLIA, D., LEE, D., WU, D.,

JENSEN, J., PATTON, P., GOKHALE, S., STOUFFER, R. L., WOLF, D. & MITALIPOV, S. 2013. Human embryonic stem cells derived by somatic cell nuclear transfer. *Cell,* 153**,** 1228-38.

TAGUCHI, A., TAKII, M., MOTOISHI, M., ORII, H., MOCHII, M. & WATANABE, K. 2012. Analysis of localization and reorganization of germ plasm in Xenopus transgenic line with fluorescence-labeled mitochondria. *Dev Growth Differ,* 54**,** 767-76.

TAHILIANI, M., KOH, K. P., SHEN, Y. H., PASTOR, W. A., BANDUKWALA, H., BRUDNO, Y., AGARWAL, S., IYER, L. M., LIU, D. R., ARAVIND, L. & RAO, A. 2009. Conversion of 5-Methylcytosine to 5-Hydroxymethylcytosine in Mammalian DNA by MLL Partner TET1. *Science,* 324**,** 930-935.

TAKAHASHI, K. & YAMANAKA, S. 2006. Induction of pluripotent stem cells from mouse embryonic and adult fibroblast cultures by defined factors. *Cell,* 126**,** 663-76.

TAKAI, D. & JONES, P. A. 2002. Comprehensive analysis of CpG islands in human chromosomes 21 and 22. *Proceedings of the National Academy of Sciences of the United States of America,* 99**,** 3740-3745.

TALBERT, P. B., BRYSON, T. D. & HENIKOFF, S. 2004. Adaptive evolution of centromere proteins in plants and animals. *J Biol,* 3**,** 18.

TANAKA, A., FURUYA, A., YAMASAKI, M., HANAI, N., KURIKI, K., KAMIAKITO, T., KOBAYASHI, Y., YOSHIDA, H., KOIKE, M. & FUKAYAMA, M. 1998. High frequency of fibroblast growth factor (FGF) 8 expression in clinical prostate cancers and breast tissues, immunohistochemically demonstrated by a newly established neutralizing monoclonal antibody against FGF 8. *Cancer Res,* 58**,** 2053-6.

THEUNISSEN, T. W., COSTA, Y., RADZISHEUSKAYA, A., VAN OOSTEN, A. L., LAVIAL, F., PAIN, B., CASTRO, L. F. & SILVA, J. C. 2011a. Reprogramming capacity of Nanog is functionally conserved in vertebrates and resides in a unique homeodomain. *Development,* 138**,** 4853-65.

THEUNISSEN, T. W. & SILVA, J. C. 2011. Switching on pluripotency: a perspective on the biological requirement of Nanog. *Philos Trans R Soc Lond B Biol Sci,* 366**,** 2222-9.

THEUNISSEN, T. W., VAN OOSTEN, A. L., CASTELO-BRANCO, G., HALL, J., SMITH, A. & SILVA, J. C. 2011b. Nanog overcomes reprogramming barriers and induces pluripotency in minimal conditions. *Curr Biol,* 21**,** 65-71.

THOMSON, J. A., ITSKOVITZ-ELDOR, J., SHAPIRO, S. S., WAKNITZ, M. A., SWIERGIEL, J. J., MARSHALL, V. S. & JONES, J. M. 1998. Embryonic stem cell lines derived from human blastocysts. *Science,* 282**,** 1145-7.

TOKUZAWA, Y., KAIHO, E., MARUYAMA, M., TAKAHASHI, K., MITSUI, K., MAEDA, M., NIWA, H. & YAMANAKA, S. 2003. Fbx15 is a novel target of Oct3/4 but is dispensable for embryonic stem cell self-renewal and mouse development. *Mol Cell Biol,* 23**,** 2699-708.

TOMIOKA, M., NISHIMOTO, M., MIYAGI, S., KATAYANAGI, T., FUKUI, N., NIWA, H., MURAMATSU, M. & OKUDA, A. 2002. Identification of Sox-2 regulatory region which is under the control of Oct-3/4-Sox-2 complex. *Nucleic Acids Res,* 30**,** 3202-13.

TSUMURA, A., HAYAKAWA, T., KUMAKI, Y., TAKEBAYASHI, S., SAKAUE, M., MATSUOKA, C., SHIMOTOHNO, K., ISHIKAWA, F., LI, E., UEDA, H. R., NAKAYAMA, J. & OKANO, M. 2006. Maintenance of self-renewal ability of mouse embryonic stem cells in the absence of DNA methyltransferases Dnmt1, Dnmt3a and Dnmt3b. *Genes to Cells,* 11**,** 805-814.

TUTTER, A. V., KOWALSKI, M. P., BALTUS, G. A., IOURGENKO, V., LABOW, M., LI, E. & KADAM, S. 2009. Role for Med12 in regulation of Nanog and Nanog target genes. *J Biol Chem,* 284**,** 3709-18.

VALDES-MORA, F., SONG, J. Z., STATHAM, A. L., STRBENAC, D., ROBINSON, M. D., NAIR, S. S., PATTERSON, K. I., TREMETHICK, D. J., STIRZAKER, C. & CLARK, S. J. 2012. Acetylation of H2A.Z is a key epigenetic modification associated with gene deregulation and epigenetic remodeling in cancer. *Genome Res,* 22**,** 307-21.

VAN DER HEIJDEN, G. W., DERIJCK, A. A., POSFAI, E., GIELE, M., PELCZAR, P., RAMOS, L., WANSINK, D. G., VAN DER VLAG, J., PETERS, A. H. & DE BOER, P. 2007. Chromosome-wide nucleosome replacement and H3.3 incorporation during mammalian meiotic sex chromosome inactivation. *Nat Genet,* 39**,** 251-8.

VISEL, A., BLOW, M. J., LI, Z., ZHANG, T., AKIYAMA, J. A., HOLT, A., PLAJZER-FRICK, I., SHOUKRY, M., WRIGHT, C., CHEN, F., AFZAL, V., REN, B., RUBIN, E. M. & PENNACCHIO, L. A. 2009. ChIP-seq accurately predicts tissue-specific activity of enhancers. *Nature,* 457**,** 854-8.

WAKAYAMA, T., TABAR, V., RODRIGUEZ, I., PERRY, A. C., STUDER, L. & MOMBAERTS, P. 2001. Differentiation of embryonic stem cell lines generated from adult somatic cells by nuclear transfer. *Science,* 292**,** 740-3.

WANG, J., LEVASSEUR, D. N. & ORKIN, S. H. 2008. Requirement of Nanog dimerization for stem cell self-renewal and pluripotency. *Proc Natl Acad Sci U S A,* 105**,** 6326-31.

WANG, J., QIAO, M., HE, Q., SHI, R., LOH, S. J., STANTON, L. W. & WU, M. 2015. Pluripotency Activity of Nanog Requires Biochemical Stabilization by Variant Histone Protein H2A.Z. *Stem Cells,* 33**,** 2126-34.

WANG, J., RAO, S., CHU, J., SHEN, X., LEVASSEUR, D. N., THEUNISSEN, T. W. & ORKIN, S. H. 2006. A protein interaction network for pluripotency of embryonic stem cells. *Nature,* 444**,** 364-8.

WANG, S.-H., TSAI, M.-S., CHIANG, M.-F. & LI, H. 2003. A novel NK-type homeobox gene, ENK (early embryo specific NK), preferentially expressed in embryonic stem cells. *Gene Expression Patterns,* 3**,** 99-103.

WANG, Z. X., KUEH, J. L., TEH, C. H., ROSSBACH, M., LIM, L., LI, P., WONG, K. Y., LUFKIN, T., ROBSON, P. & STANTON, L. W. 2007. Zfp206 is a transcription factor that controls pluripotency of embryonic stem cells. *Stem Cells,* 25**,** 2173-82.

WATANABE, A., YAMADA, Y. & YAMANAKA, S. 2013. Epigenetic regulation in pluripotent stem cells: a key to breaking the epigenetic barrier. *Philos Trans R Soc Lond B Biol Sci,* 368**,** 20120292.

WEBER, C. M. & HENIKOFF, S. 2014. Histone variants: dynamic punctuation in transcription. *Genes Dev,* 28**,** 672-82.

WEI, Z., YANG, Y., ZHANG, P., ANDRIANAKOS, R., HASEGAWA, K., LYU, J., CHEN, X., BAI, G., LIU, C., PERA, M. & LU, W. 2009. Klf4 interacts directly with Oct4 and Sox2 to promote reprogramming. *Stem Cells,* 27**,** 2969-78.

WHYTE, W. A., ORLANDO, D. A., HNISZ, D., ABRAHAM, B. J., LIN, C. Y., KAGEY, M. H., RAHL, P. B., LEE, T. I. & YOUNG, R. A. 2013. Master transcription factors and mediator establish super-enhancers at key cell identity genes. *Cell,* 153**,** 307-19.

WILMUT, I., SCHNIEKE, A. E., MCWHIR, J., KIND, A. J. & CAMPBELL, K. H. 1997. Viable offspring derived from fetal and adult mammalian cells. *Nature,* 385**,** 810-3.

WOLFFE, A. P. & HAYES, J. J. 1999. Chromatin disruption and modification. *Nucleic Acids Res,* 27**,** 711-20.

WU, H., D'ALESSIO, A. C., ITO, S., XIA, K., WANG, Z., CUI, K., ZHAO, K., SUN, Y. E. & ZHANG, Y. 2011a. Dual functions of Tet1 in transcriptional regulation in mouse embryonic stem cells. *Nature,* 473**,** 389-93.

WU, H. & ZHANG, Y. 2011. Mechanisms and functions of Tet protein-mediated 5-methylcytosine oxidation. *Genes Dev,* 25**,** 2436-52.

WU, T., WANG, H., HE, J., KANG, L., JIANG, Y., LIU, J., ZHANG, Y., KOU, Z., LIU, L., ZHANG, X. & GAO, S. 2011b. Reprogramming of trophoblast stem cells into pluripotent stem cells by Oct4. *Stem Cells,* 29**,** 755-63.

XIE, W., SCHULTZ, M. D., LISTER, R., HOU, Z. G., RAJAGOPAL, N., RAY, P., WHITAKER, J. W., TIAN, S., HAWKINS, R. D., LEUNG, D., YANG, H. B., WANG, T., LEE, A. Y., SWANSON, S. A., ZHANG, J. C., ZHU, Y., KIM, A., NERY, J. R., URICH, M. A., KUAN, S., YEN, C. A., KLUGMAN, S., YU, P. Z., SUKNUNTHA, K., PROPSON, N. E., CHEN, H. M., EDSALL, L. E., WAGNER, U., LI, Y., YE, Z., KULKARNI, A., XUAN, Z. Y., CHUNG, W. Y., CHI, N. C., ANTOSIEWICZ-BOURGET, J. E., SLUKVIN, I., STEWART, R., ZHANG, M. Q., WANG, W., THOMSON, J. A., ECKER, J. R. & REN, B. 2013. Epigenomic Analysis of Multilineage Differentiation of Human Embryonic Stem Cells. *Cell,* 153**,** 1134-1148.

XU, C., FAN, Z. P., MULLER, P., FOGLEY, R., DIBIASE, A., TROMPOUKI, E., UNTERNAEHRER, J., XIONG, F., TORREGROZA, I., EVANS, T., MEGASON, S. G., DALEY, G. Q., SCHIER, A. F., YOUNG, R. A. & ZON, L. I. 2012. Nanog-like regulates endoderm formation through the Mxtx2-Nodal pathway. *Dev Cell,* 22**,** 625-38.

XU, G. L., BESTOR, T. H., BOURC'HIS, D., HSIEH, C. L., TOMMERUP, N., BUGGE, M., HULTEN, M., QU, X. Y., RUSSO, J. J. & VIEGAS-PEQUIGNOT, E. 1999. Chromosome instability and immunodeficiency syndrome caused by mutations in a DNA methyltransferase gene. *Nature,* 402**,** 187-191.

XU, N., PAPAGIANNAKOPOULOS, T., PAN, G., THOMSON, J. A. & KOSIK, K. S. 2009. MicroRNA-145 regulates OCT4, SOX2, and KLF4 and represses pluripotency in human embryonic stem cells. *Cell,* 137**,** 647-58.

YAMAGUCHI, S., KIMURA, H., TADA, M., NAKATSUJI, N. & TADA, T. 2005. Nanog expression in mouse germ cell development. *Gene Expr Patterns,* 5**,** 639-46.

YANG, X., NOUSHMEHR, H., HAN, H., ANDREU-VIEYRA, C., LIANG, G. & JONES, P. A. 2012. Gene reactivation by 5-aza-2'-deoxycytidine-induced demethylation requires SRCAP-mediated H2A.Z insertion to establish nucleosome depleted regions. *PLoS Genet,* 8**,** e1002604.

YING, Q. L., WRAY, J., NICHOLS, J., BATLLE-MORERA, L., DOBLE, B., WOODGETT, J., COHEN, P. & SMITH, A. 2008. The ground state of embryonic stem cell self-renewal. *Nature,* 453**,** 519-23.

YU, J., VODYANIK, M. A., SMUGA-OTTO, K., ANTOSIEWICZ-BOURGET, J., FRANE, J. L., TIAN, S., NIE, J., JONSDOTTIR, G. A., RUOTTI, V., STEWART, R., SLUKVIN, II & THOMSON, J. A. 2007. Induced pluripotent stem cell lines derived from human somatic cells. *Science,* 318**,** 1917-20.

ZEMACH, A., MCDANIEL, I. E., SILVA, P. & ZILBERMAN, D. 2010. Genome-wide evolutionary analysis of eukaryotic DNA methylation. *Science,* 328**,** 916-9.

ZENTNER, G. E., TESAR, P. J. & SCACHERI, P. C. 2011. Epigenetic signatures distinguish multiple classes of enhancers with distinct cellular functions. *Genome Res,* 21**,** 1273-83.

ZHANG, M., WANG, F. C., KOU, Z. H., ZHANG, Y. & GAO, S. R. 2009. Defective Chromatin Structure in Somatic Cell Cloned Mouse Embryos. *Journal of Biological Chemistry,* 284**,** 24981-24987.

ZHANG, R., POUSTOVOITOV, M. V., YE, X., SANTOS, H. A., CHEN, W., DAGANZO, S. M., ERZBERGER, J. P., SEREBRIISKII, I. G., CANUTESCU, A. A., DUNBRACK, R. L., PEHRSON, J. R., BERGER, J. M., KAUFMAN, P. D. & ADAMS, P. D. 2005. Formation of MacroH2A-containing senescence-associated heterochromatin foci and senescence driven by ASF1a and HIRA. *Dev Cell,* 8**,** 19-30.

ZLATANOVA, J. & THAKAR, A. 2008. H2A.Z: view from the top. *Structure,* 16**,** 166-79.

APPENDIX A

Supplementary data 1: Trimethylation of H3K9 level on the mouse Oct4 and Nanog promoters after axolotl and Xenopus oocyte extract treatment

It was previously shown in our lab that extracts from the oocytes of both axolotl and Xenopus can remove the repressive marks trimethylation of H3K9 (H3K9me3) and H3K27 (H3K27me3) located on regulatory regions of the pluripotency genes Nanog and Oct4. In order to confirm the previous results and to test the activity of Xenopus and axolotl oocyte extracts, ChIP assay were carried out by using a specific antibody for H3K9me3 (Active Motif, 39161). Oct4 promoter and Nanog promoter regions were then amplified with quantitative PCR. IgG pull-down was tested to show the specificity of H3K9me3 antibody.

As the graph shows, the levels of H3K9me3 on both the Oct4 and Nanog promoters were reduced by about 5 fold after 6 hours of axolotl and Xenopus oocyte extract treatment. Immunoprecipitation with IgG antibody resulted similar to the level of untreated (control) cells, showing that the reductions on Oct4 and Nanog promoters are specific for the histone mark. These data indicate that XOE were active, and differences in the remodelling activities of XOE and AOE can then be attributed to the makeup of factors expressed in the respective oocytes.

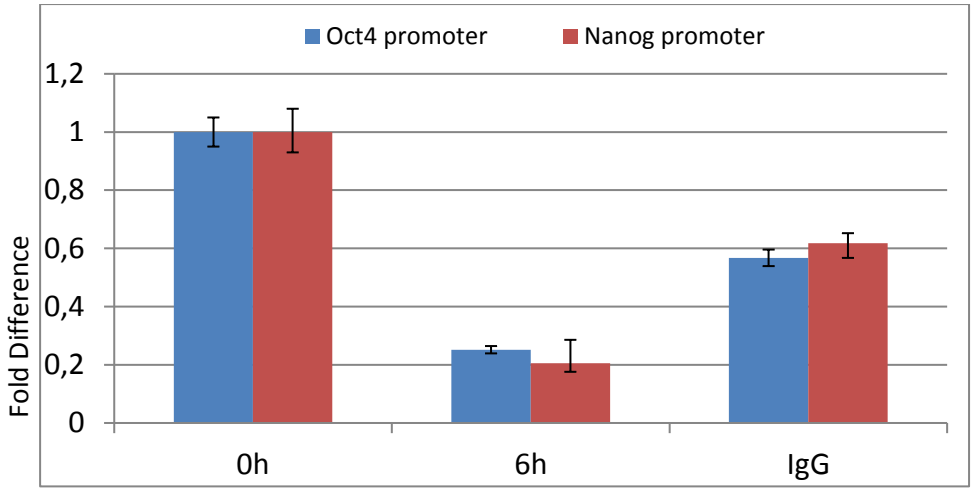

Figure S1a Levels of H3K9me3 on the mouse Nanog and Oct4 promoters in NIH3T3 cells after AOE treatment

Sheared chromatin from 2 x 10^6 cells was immunoprecipitated with 5µg H3K9me3 antibody and the levels of specific DNA sequences (as indicated) were quantified by qPCR. The graph shows the changes in fold differences of H3K9me3 levels on the Oct4 promoter (blue) and the Nanog promoter in control NIH3T3 cells (0h) and NIH3T3 cells treated with AOE. Immunoprecipitation with IgG is a negative control. Biological repeat number= 3 and error bars indicate standard deviations in technical replicates.

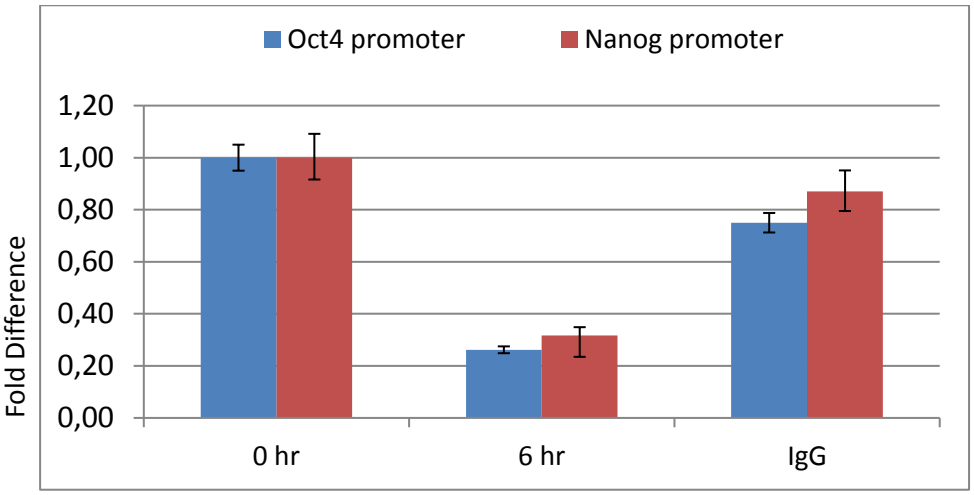

Figure S1b Levels of H3K9me3 on the mouse Nanog and Oct4 promoters in NIH3T3 cells after XOE treatment

Sheared chromatin from 2 x 10^6 cells was immunoprecipitated with 5µg H3K9me3 antibody and the levels of specific DNA sequences (as indicated) were quantified by qPCR. The graph shows the changes in fold differences of H3K9me3 levels on the Oct4 promoter (blue) and the Nanog promoter in control NIH3T3 cells (0h) and NIH3T3 cells treated with XOE. Immunoprecipitation with IgG is a negative control. Biological repeat number= 3 and error bars indicate standard deviations in technical replicates.

Supplementary data 2: Nanog antibody specificity

To show the Nanog antibody specificity, immunocytochemistry experiments were carried out using pre-iPS cells which overexpress axNanog. Mouse pre-iPS cells derived from neural stem cells were null for the endogenous mouse Nanog and have been transduced by lentivirus to express axolotl Nanog driven by EF1-alpha promoter constitutively. In this experiment, IgG was used as a negative control. The result showed that Nanog antibody specifically binds to axNanog.

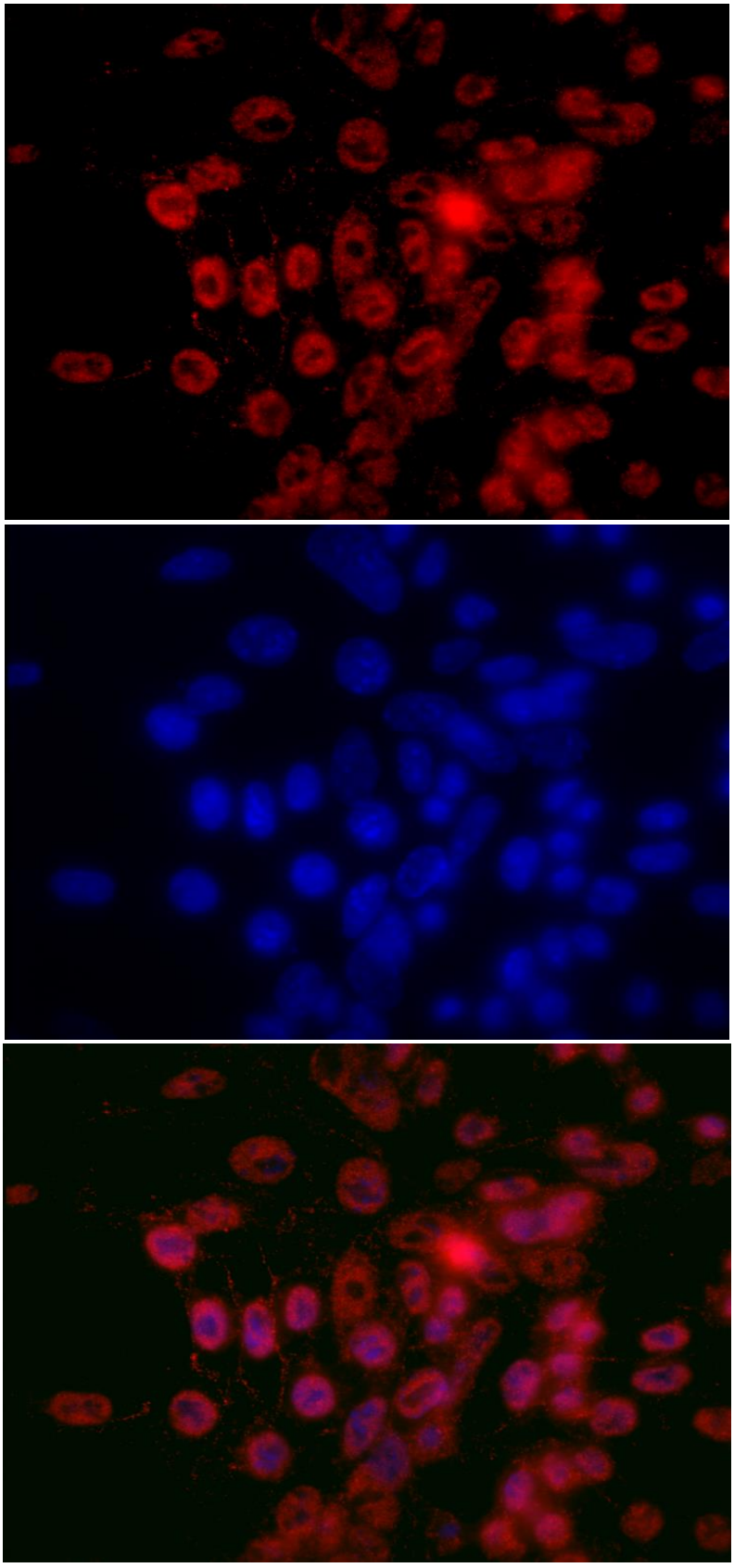

Figure S2 Immunocytochemistry showing the specificity of the Nanog antibody.

AxNanog-overexpressing pre-iPS cells were immunostained by Nanog antibody (red) merged with DAPI (blue). Antibody concentration was 0.7 µg/ml.

Supplementary data 3: Extraction of Histone H2A.Z

Histone extraction was carried out on NIH3T3 cells accompanied with the mouse ES cells as positive control. Figure S3 refers to the western blot assay shown in Figure 4.11.

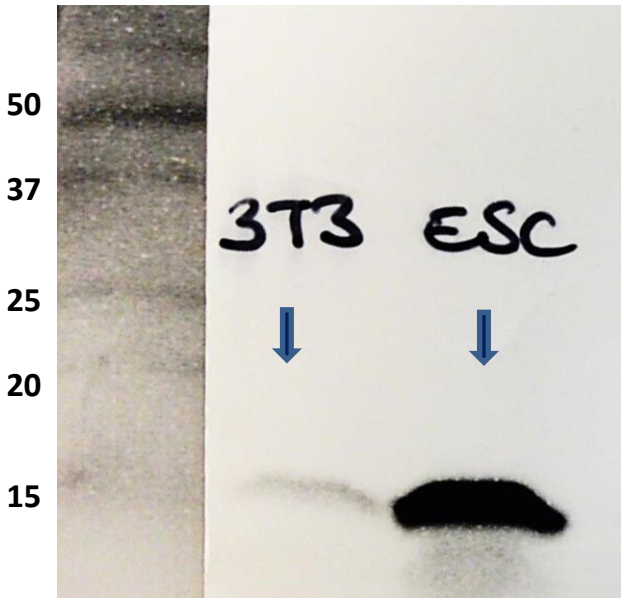

Figure S3 Western blotting indicating H2A.Z was detected at the molecular weight of approximately 15 kDa. Histones were extracted from 2 x 10^5 of NIH3T3 or mouse ES cells and analysed by Western blotting using 1:2000 diluted H2A.Z antibody. Signals were visualized in the Bio-ChemiDoc System after 20 minutes exposure.

APPENDIX B

MEDIA AND STOCK SOLUTIONS

I. Media and Stock Solutions for Cell Culture

Culture Media for NIH3T3 cells and MEFs

DMEM

2mM non-essential amino acids (Invitrogen)

0.1 mM β-mercaptoethanol (β-MG, Invitrogen)

100 IU/ml penicillin and 100 μg/ml streptomycin

10% FBS

Low serum media

DMEM

2mM non-essential amino acids (Invitrogen)

100 IU/ml penicillin and 100 μg/ml streptomycin

0.5% FBS

Culture Media for mouse ES cells

DMEM

15% Hyclone foetal bovine serum

1000 U/ml of leukaemia inhibitory factor (ESGRO, Chemicon, CA)

1 mM L-glutamine (Invitrogen)

0.1 mM β-MG (Invitrogen)

2 mM non-essential

1 mM sodium pyruvate (Invitrogen)

100 IU/ml penicillin and 100 μg/ml streptomycin

II. Buffer for Cell Permeabilization

Digitonin transport buffer

170 mM Potassium Gluconate

5 mM KCl

2 mM $MgCl_2$

1 mM KH_2PO_4

1 mM EGTA

20 mM Hepes (pH 7.3)

Protease Inhibitor Coctail (Sigma-Aldrich)

Energy regenerating system

60 mM Phosphocreatine

150 µg/ml Creatine phosphokinase

ATP

III. Buffers for Immunostaining

Washing solution (PBST-BSA)

1% BSA

0.05% Tween20

In 1xPBS

Blocking solution

5% BSA

0.05% Tween20

In 1xPBS

IV. Reagents and Gel Preparation for SDS-PAGE Slab Gels

TGS Buffer

0.025 M TRIS

0.192 M Glycine

0.1% Sodium Dodecyl Sulfate

Lysis Buffer

980 µl TGS Buffer

With protease inhibitors:

200 mM Sodium Orthovanadate

250 mM AEBSF

10 mg/ml Leupeptin

BIO-RAD Preweighed Acrylamide/bis:

Acrylamide/bis 37.5:1 mixture (Catalog number: 161-0106, 200 g) or

Acrylamide/bis 90 g (30 g/ 100 ml)

ddH_2O 300 ml

1.5 M Tris-HCl, pH 8.8:

Tris base 27.23 g

ddH_2O ~80 ml

Adjust to pH 8.8 with 1 N HCl, and make up to 150 ml with ddH_2O and store at 4˚C.

0.5 M Tris-HCl, pH 8.8:

Tris base 6 g

ddH_2O ~60 ml

Adjust to pH 6.8 with 1 N HCl, and make up to 150 ml with ddH_2O and store at 4˚C.

10 % SDS:

Dissolve 10 g SDS in water with gentle stirring and bring to 100 ml with ddH_2O.

2X SDS Sample Buffer:

5 ml 0.5 M Tris-HCl, pH 6.8

4 ml Glycerol

0.8 g SDS

617 mg DTT

1mg 1 % (w/v) bromophenol blue

8 ml ddH_2O

Then make up tp 20 ml with ddH_2O and store at -70˚C.

Sample Buffer:

50 µl β-mercaptoethanol

950 µl Laemmli buffer

5X Electrode (Running) Buffer:

9 g Tris base

43.2 g Glycine

3 g SDS

Make up to 600 ml with ddH_2O and store at 4˚C.

Warm to 37˚C before use if precipitation occurs. Dilute 60 ml 5X stock with 240 ml ddH_2O for one electrophoretic run.

Separating gel (15%) preparation – 0.375 M Tris, pH 8.8:

4.7 ml ddH_2O

5 ml 4X Tris-HCl (1.5 M, pH 8.8)

10 ml 30% stock acrylamide/bis

200 µl 10% SDS

100 µl 10% (w/v) Ammonium Persulfate (APS)

14 µl TEMED

A total of 10 ml is sufficient for 2 mini gels.

Stacking gel (4%) preparation – 0.125 M Tris, pH 6.8:

6 ml ddH_2O

2.5 ml 4X Tris-HCl (0.5 M, pH 6.8)

1.4 ml 30% stock acrylamide/bis

100 µl 10% SDS

50 µl 10% (w/v) Ammonium Persulfate (APS)

10 µl TEMED

A total of 10 ml is sufficient for 2 mini gels.

Antibodies stripping buffer:

0.2 M Glycine pH 2.8